Demethylation of Sulfobutylated Kraft Lignin and its Application as Phenol-Formaldehyde Adhesives

Juan Paez

B.Eng Chemical Engineering, Lakehead University

Supervisor: Pedram Fatehi

Thesis

Presented to the Faculty of Graduate Studies

Lakehead University

Thunder Bay, Ontario, Canada

in Partial Fulfillment of the Requirements for the Degree of Master of Science in Chemical Engineering

March 2025

Dedication

To my parents, for your unwavering support, sacrifices, and constant encouragement throughout every stage of my academic and personal journey.

Acknowledgments

I would like to express my deepest gratitude to my supervisor, Dr. Pedram Fatehi, for his invaluable guidance, support, and mentorship throughout my research. His expertise and encouragement have been instrumental in the completion of this work.

I would also like to sincerely thank Dr. Weijue Gao, Dr. Ayyoub Salaghi, Dr. Jonathan Diaz-Baca, and Dr. Banchamlak Bemerw Kassaun for their guidance, insightful discussions, and support throughout my research. Their expertise and willingness to share their knowledge have contributed significantly to my research development.

My heartfelt appreciation extends to the Green Process Research Center at Lakehead University, not just for providing the facilities and resources crucial for my research but also for fostering an environment filled with collaboration and support. I am deeply grateful to all the members of the center who have helped me along the way, whether through technical assistance, valuable advice, or simply making the lab a place of learning and growth. Your camaraderie and generosity made this journey more meaningful.

I would also like to thank my colleagues and friends, both inside and outside the lab, for their encouragement, collaboration, and unwavering support. Your advice, patience, and friendship have been instrumental throughout this journey, and I am truly grateful for each and every one of you.

Finally, my deepest gratitude goes to my family for their unconditional love and support. Your belief in me has been my greatest source of strength, and I could not have done this without you.

Table of Contents

List of Tables

List of Figures

Abstract

The shift toward sustainable and eco-friendly adhesives has led to increased research into renewable alternatives for petroleum-derived components in phenol-formaldehyde (PF) resins. Lignin, a natural phenolic polymer, presents a promising option due to its structural similarity to phenol. However, its high molecular weight, structural heterogeneity, and low reactivity hinder its direct incorporation into adhesive formulations. To overcome these limitations, this study investigates a two-step chemical modification—sulfobutylation followed by demethylation—to improve lignin's solubility and performance in PF resins.

The sulfobutylation (SB) step resulted in a decrease in methoxy and hydroxyl groups while increasing molecular weight, sulfur content, solubility, and charge density, significantly improving lignin's aqueous compatibility. Demethylation of sulfobutylated lignin (DSB) further decreased methoxy content, with a slight increase in hydroxyl groups compared to SB lignin. Additionally, demethylation led to higher molecular weight and a reduction in sulfur content back to levels observed in kraft lignin (KL) while maintaining solubility. These changes were attributed to an increase in β-O-4 interunit linkages, which contributed to improved reactivity. The demethylated sulfobutylated lignin-PF (DSBPF) resins retained the PF resin's molecular structure but exhibited more reactive formaldehyde adducts. Increasing the lignin content led to higher MW and viscosity, which enhanced bonding strength but reduced thermal stability. The β-O-4 linkages in DSB contributed to improved adhesive properties, increasing bonding strength by 19% in DSBPF20 and 25% in DSBPF60. However, the resins also exhibited higher free formaldehyde emissions, exceeding safety limits. Additionally, while pH and non-volatile content remained stable, water absorption increased, potentially impacting long-term durability. Despite these challenges, the modified resins showed enhanced fire resistance and adhesion performance compared to conventional PF resins.

Future research should focus on optimizing resin synthesis parameters, including NaOH catalyst amount, reaction time and temperature, and curing conditions, to improve performance while reducing emissions. Furthermore, incorporating enhancers such as melamine, urea, or furfural could help maintain or improve adhesive properties while minimizing formaldehyde content. This study provides valuable insights into lignin-based PF resins, contributing to the development of more sustainable, high-performance adhesives and reducing reliance on petroleum-based materials.

Chapter 1: Introduction

Adhesives play a crucial role in various industries, serving as essential materials for bonding and structural integrity. Among the diverse range of adhesives available, phenol-formaldehyde (PF) resins stand out for their exceptional mechanical strength, thermal stability, and water resistance, making them the preferred choice for exterior applications, such as plywood, particleboard, and laminated veneer lumber. However, the production and use of PF resins present significant environmental and health challenges due to their reliance on petroleum-derived phenol and the emission of formaldehyde, a known carcinogen. Consequently, the search for sustainable and eco-friendly alternatives has driven extensive research into incorporating renewable resources, such as lignin, into adhesive formulations.

Lignin, the second most abundant biopolymer after cellulose, is an attractive candidate for partially replacing phenol in PF resins due to its phenolic structure. However, its high molecular weight, structural heterogeneity, and low reactivity hinder its direct incorporation into adhesive formulations without compromising performance. Various chemical modifications have been explored to enhance lignin's reactivity and compatibility with PF resins, including demethylation, phenolation, hydroxymethylation, and depolymerization. Among these, demethylation has been extensively studied as it directly increases the number of reactive hydroxyl groups available for crosslinking, thereby improving the adhesive properties of lignin-based PF resins.

This thesis consists of four chapters. **Chapter 1**, i.e., the current chapter, is the introduction of this thesis, along with the research motivations, objectives, and novelty statement.

Chapter 2 provides a comprehensive literature review on the application of lignin in adhesives, covering a range of adhesive types, including PF, urea-formaldehyde (UF), melamine-formaldehyde (MF), epoxy, polyurethane, lignin-tannin, lignin-soy protein, lignin-polyethyleneimine (PEI), and lignin-furfural resins. Each adhesive type is defined, its structure, uses, properties, strengths, and shortcomings are discussed, and relevant studies are reviewed to highlight trends and challenges in lignin incorporation. The review critically examines the modifications applied to lignin to improve its adhesive performance and the remaining limitations despite these modifications.

Chapter 3 presents an experimental investigation into the demethylation of kraft lignin in an aqueous medium via sulfobutylation, followed by its application as a PF resin for plywood production. The sulfobutylation step was introduced to enhance lignin's solubility, facilitating the demethylation reaction in water rather than organic solvents. The modified lignin was characterized using Fourier-transform infrared spectroscopy (FTIR), nuclear magnetic resonance (NMR) spectroscopy (^{1}H, ^{31}P, and HSQC), and static light scattering (SLS) to evaluate the effectiveness of the chemical modifications. The performance of the demethylated sulfobutylated lignin-PF resin was assessed through various tests, including thermal stability (TGA and DTG), viscosity, molecular weight analysis, bonding strength, water absorption, and fire resistance. The results were compared against conventional PF resins and existing lignin-based PF resins in the literature to determine the efficacy of the proposed modification.

Chapter four discusses the conclusion and future work of this thesis.

By addressing the limitations of lignin incorporation in PF adhesives, this research aims to contribute to the development of more sustainable and high-performance adhesive systems, reducing dependence on petroleum-based chemicals while maintaining or enhancing adhesive properties.

1.1 Objectives

The objectives of this thesis are to:

1. To perform demethylation in an aqueous media via Sulfobutylation
2. To observe the effect that sulfobutylation has on demethylation
3. To produce LPF adhesive from modified lignin
4. To investigate the impact of sulfonate group on flame retardancy of product

1.2 Novelty

The novelty of this thesis work is 1) the development of a comprehensive literature review of the use of lignin in adhesive with compressive tables and mechanisms, 2) the demethylation of lignin using water as solvent via sulfobutylation, and 3) the double modification of lignin. Although others have performed a double modification of lignin, most methods involve demethylation, oxidation, or reduction, followed by a grafting modification. The double modification performed in this case consisted of grafting sulfobutyl functional groups followed by demethylation. This approach aimed to improve the solubility of lignin via sulfobutylation to enable demethylation using an aqueous medium

Commented [PF1]: Read preivous thesis and write the same way

Chapter 2: Literature Review- Use of Lignin in Adhesives: Review

Abstract

Adhesives are essential in various industries, but petroleum-based resins pose environmental and health concerns. Lignin, a renewable biopolymer, offers a sustainable alternative due to its functional groups that enable integration into adhesives. Lignin-based resins reduce dependence on fossil resources, lower costs, and improve sustainability. However, challenges such as low reactivity, structural heterogeneity, and performance limitations hinder its commercialization. In this review, the fabrication of lignin derived adhesives is comprehensively discussed. Modification strategies, such as, hydroxymethylation, depolymerization, and phenolation improve lignin's reactivity, with the best performance observed when using enhancers, such as urea, melamine, polyethyleneimine (PEI), and furfural. Lignin-phenol formaldehyde (LPF), lignin-polyurethane (LPU) are closest to commercialization due to lower production costs, increased water resistance while maintaining bonding strength. Lignin-epoxy (LEP) and lignin-tannin adhesives exhibit strong mechanical properties but require further optimization. Lignin-phenol-formaldehyde (LPF) adhesives are among the most commercially available, with companies, such as, Latvijas Finieris, incorporating bio-based lignin in plywood production, while maintaining performance. Similarly, lignin-polyurethane (LPU) adhesives are advancing toward broader commercialization with efforts focused on replacing 80-100% of phenol, improving sustainability and performance. Research on lignin-melamine, lignin-PEI, and lignin-furfural adhesives remains limited due to lack of research, though they hold potential for improving durability and processing. The most promising approach in adhesive performance is to utilize urea, melamine, PEI, and furfural as enhancers to improve adhesion and curing efficiency of lignin-based adhesives. Despite advancements, lignin-based adhesives face challenges in strength, durability, water resistance, and processing efficiency. Many require costly enhancers to achieve good performance, increasing production costs. Issues such as, brittleness, and high modification costs limit widespread adoption. Market reluctance and the lack of standardized formulations further complicate commercialization. Future research should focus on cost-effective processing, performance enhancement, and formaldehyde-free formulations. Standardizing lignin modification techniques and expanding applications in construction, automotive, and packaging industries will be crucial to making lignin-based adhesives a viable commercial alternative.

2.1 Introduction

Adhesives play a vital role as auxiliary materials in various industries. The main function of an adhesive is to join two surfaces and resist separation under shears [1]. Adhesion of surfaces can be carried out through physical, chemical, and/or mechanical bonding processes. Typically, physical bonds are weak as they rely on intermolecular forces, whereas mechanical bonds occur when the adhesive penetrates surface pores, cracks, or rough areas, creating an effective mechanical interlock. Chemical bonds are also strong but can be difficult to achieve due to the need for specific chemical interactions [2]. Chemical bonds are used widespread for many applications in packaging, transportation, construction, manufacturing, healthcare, and renewable energy sectors [3]. In 2020, the global adhesive market was reported to be around 58 billion USD [3].

Historically, adhesives were obtained form natural resources, such as animal bones, plants, and minerals [4]. In the early 1900's, synthetic adhesives were first developed and implemented industrially [4]. These synthetic adhesives permitted for significantly stronger adhesive bonds, leading to extended service life and increased water and heat resistance [4-5]. Some of the first synthetic adhesives were made from formaldehyde, such as, phenol-formaldehyde, urea-formaldehyde, and melamine-formaldehyde adhesives, which are primarily used to bond plywood. The first truly synthetic adhesive was phenol formaldehyde used in extreme environments, such as waterproofing plywood on boats [4]. As research progressed, acrylates were introduced, which paved the way for the subsequent emergence of polyurethanes. This option significantly broadened the spectrum of adhesive applications [4]. The creation of epoxy adhesives soon followed the path, which has been merited for the most significant milestone in adhesive development [4].

However, these synthetic adhesives use petroleum derivatives as the feedstock for their synthetizes, such as phenol, formaldehyde, and polyether polyols [5-6]. Thus, with a growing demand for petroleum, increase in prices, foreseen supply shortages, and environmental and health concerns, more environmentally friendly alternatives have been investigated. Biobased adhesives have attracted significant attention over the years in order to lessen our dependency on petroleum. Biobased adhesives have been synthesized using tannin, furfural, soy proteins and polyethylenimine [7-10]. Despite their popularity, the biobased adhesives possess inferior mechanical strength and water resistance to synthetic adhesives. Therefore, the incentives for generating biobased adhesive with improved characteristics are high.

The objective of this literature review is to provide a comprehensive analysis of lignin-based adhesives, compiling all known methods of incorporating lignin into adhesive formulations. The novelty of this review lies in its comprehensive analysis of both synthetic and bio-based resin adhesives, consolidating key findings into a single resource. Unlike previous studies that focused solely on synthetic resins [11], phenolic-based adhesives [5], or formaldehyde-based systems [12], this paper provides a broader perspective, covering various adhesive formulations. While some prior work includes both synthetic and bio-based resins [3], they lack extensive quantitative comparisons, detailed property assessments, and mechanistic explanations. This review identifies research trends, highlights promising studies, and examines emerging patterns in lignin-based adhesives.

2.2 Lignin derivatization

Lignin is the second largest renewable source, following cellulose and stands as the primary source of aromatic compounds on earth [13]. Lignin is a three-dimensional, amorphous, highly branched, high-molecular weight macromolecule. It is currently produced as a by-product of the pulp and paper industry where it is burned as fuel for energy recovery [14]. Its structure primarily depends on its delignification process and its source (e.g. softwood, hardwood, or non-wood) [14-15]. Although its chemical structure is complex and undefined, lignin polymer primarily consists of three phenylpropanoids monomeric building blocks of the syringyl (S), guaiacyl (G) and para-hydroxyphenyl (H) monomers [14]. Softwood species are predominately composed of G monomers, while hardwoods mainly consist of S [14]. Lignin also contains various functional groups, i.e., aliphatic and phenolic hydroxyls, carboxyl, methoxyl groups and some terminal aldehyde groups, as well as aryl, alkyl, ester, and ether linkages [14-15]. The most common linkages include C-O (ether) (e.g., β–O–4, α–O–4, and 4–O–5) and C-C (e.g., β–β, β–5, and β–1). The most common linkage in lignin is the ether (β–O–4) linkage, which represents approximately 50% and 60% of the total linkages in softwood and hardwood, respectively [3]. Lignin can be classified as native or technical. Native referring to lignin that exists in plants with its original structure, and technical referring to lignin that has been extracted and isolated from biomass (delignified) [3]. Most studies focus primarily on technical lignin, which include kraft, hydrolysis, soda, organosolv, lignosulfonate and pyrolytic lignin [3], [14]. The composition, molecular weight and functionality of lignin depends on the delignification process [3]. The physical and chemical properties of technical lignin may significantly vary within the same species [14]. However, the main issues with lignin are its low reactivity, its large intrinsic steric hindrance and complex heterogenous structure [5, 16-17]. The low reactivity of lignin is due to the polyphenols having fewer ortho- and para- reactive sites [18]. The ortho positions of lignin can be occupied by one or two methoxy groups, inherently contributing to its steric hinderance. If these methoxy groups were to be removed, the amount of free reactive phenolic hydroxyl groups would increase, naturally increasing the reactivity of lignin [18].

The reactivity of lignin can be improved through various modification. The most common modifications for improving the reactivity of lignin are demethylation, depolymerization, phenolation, hydroxymethylation, and glyoxalation [19-25]. The mechanism for the modifications can be seen Figure 2-1. Demethylation is the removal of the methoxy group from the aromatic structure of lignin. The demethylation is usually conducted using hydroiodic acid, iodocyclohexane, 1-dodecanethiol or sodium sulfite at a relatively high temperature (130°C) [22], [26]. Depolymerization consists of the degradation of the complex lignin compound into value added products made of smaller molecules [27-28]. The depolymerization of lignin has been conducted using a variety of methods, such as hydrothermal conversion, pyrolysis, enzymatic degradation, photocatalytic degradation, electrochemical degradation, ionic liquid degradation and microwave irradiation oxidation [27-28]. Typically, depolymerization is conducted at elevated pressures and temperatures. Phenolation involves the grafting of a phenol group to the aliphatic chain of lignin [29]. It is typically conducted by reacting lignin with phenol under acidic conditions [29]. Generally, it is seen that the amount of phenol incorporated into the lignin structure is dependent on the amount of aliphatic hydroxyl [30]. Hydroxymethylation consist of grafting a hydroxymethyl group onto the lignin structure using formaldehyde [25]. It allows for condensation and crosslinking to occur between lignin and phenol. Glyoxalation involves the grafting a glyoxal group on the lignin using glyoxal under a nitrogen atmosphere [31]. Glyoxal is a natural aldehyde and therefore can replace formaldehyde in adhesive systems [32]. The impact of lignin types on its modifications was studied for adhesive applications [33-34] . Hydroxymethylation was conducted on sodium lignosulfonate, kraft lignin, and organosol lignin [33]. It was observed that sodium lignosulfonate demonstrated the most promising potential for PF resins despite containing the most impurities while the purest, organosolv lignin,

exhibited the lowest compatibility [33]. This difference in performance is associated with the increased number for reactive hydroxyl sites in sodium lignosulfonate compared to organosolv lignin [33]. Phenolation was performed on corncob lignin, poplar lignin, hydrothermally treated poplar lignin, kraft lignin, and wheat straw alkali lignin, where it was seen that corncob demonstrated the highest conversion, which was associated with its increased reactivity compared the other lignin types [34]. It was observed that the lignin with the highest number of reactive sites resulted in the highest reaction conversion.

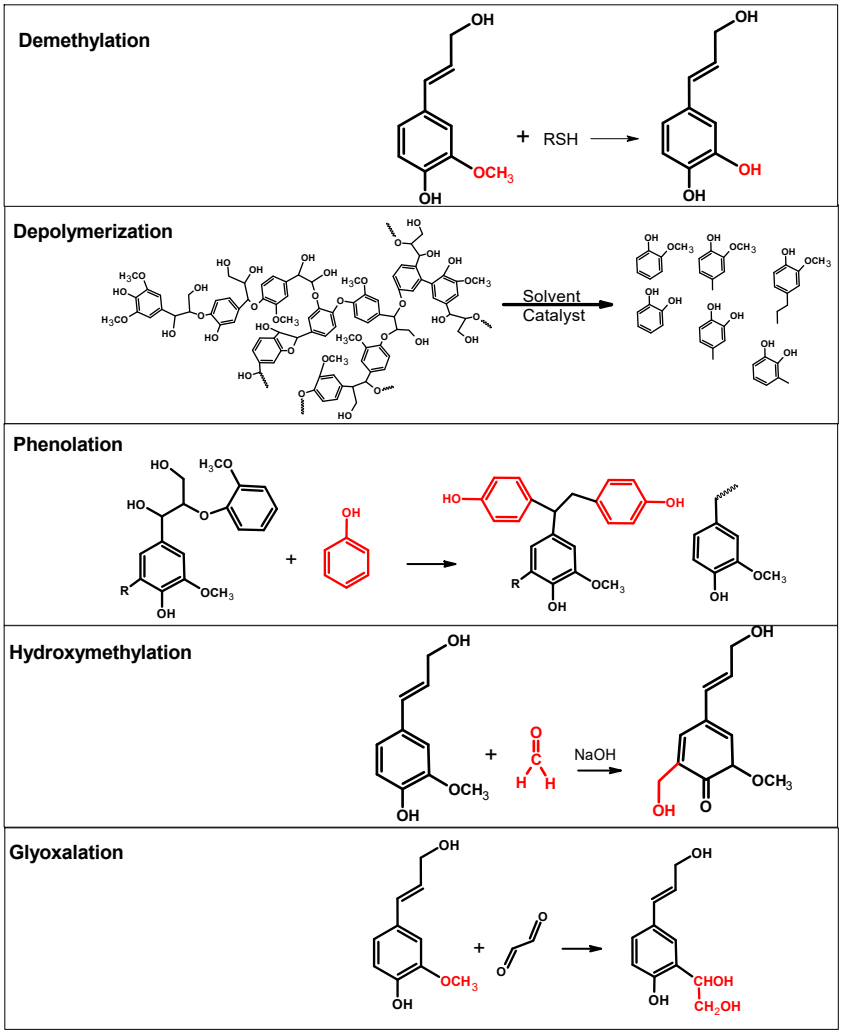

Figure 2-1: Mechanism of lignin modifications.

Commented [PF2]: Remove CH20 from phenolation product

Commented [PF3R2]: Not done yet

2.3 Synthetic Adhesive

2.3.1 Lignin-Phenol-Formaldehyde Adhesive (LPFA)

Phenol-formaldehyde (PF) adhesives are thermosetting polymers produced when phenol reacts with formaldehyde in the presence of a basic catalyst [17]. With the total worldwide consumption of PF adhesives is estimated to be approximately 3.5-4 million tones per year, PF adhesives play an important role in several industry applications [17]. PF adhesives are widely used for engineering wood products, such as particle board, plywood, oriented strand boards, waferboard, headboard, laminated veneer lumber, etc [17], [35]. Additionally, PF resins can be used for other applications such as moldings, electrical insulators, brake linings and brake pads. Due to the unique network-crosslinked structure of this polymer, it has excellent heating resistance and bond strength, good aging and weather resistance, and satisfactory chemical stability [17]. The properties of PF resins can be seen in Table 1.

PF resins have several shortcomings, they can be brittle, limiting their use in flexible applications [36]. As a feedstock, phenol and formaldehyde are highly toxic and non-renewable petrochemical derivatives [17], [37]. As a result, research has leaned toward finding more sustainable and healthy alternatives [37]. During production and curing, they release formaldehyde, posing health and environmental risks [36]. It should be mentioned that the maximum allowable free formaldehyde content is 0.3% according to GB/T-14074 [37]. The synthesis and curing processes require precise control, complicating manufacturing. As thermosetting plastics, PF resins do not melt or degrade easily, making recycling challenging and impacting the environment [36]. Additionally, they require high pressing pressures for applications like wood impregnation, which can limit their commercial use. [36].

To generate sustainable PF resin, the incorporation of lignin in PF resin was studied in the past. The mechanism of lignin-PF resin fabrication can be seen in Figure 2-2. Generally, hydroxymethylation occurs as the first step in the reaction, with phenol undergoing this process at a faster rate compared to lignin [5]. Initially, phenol reacts with formaldehyde at its more reactive para position, forming para-hydroxymethyl phenol (a) in Figure 2-2. As the reaction progresses and additional formaldehyde is introduced in stages, hydroxymethylation occurs at the ortho position, also leading to the formation of ortho and ortho-para-hydroxymethyl phenol (c & d, respectively in Figure 2-2) [5]. Following this step, lignin undergoes hydroxymethylation, though at a slower rate than phenol (b in Figure 2-2). In the next stage, ortho-para-hydroxymethyl phenol undergoes condensation, forming a dimer linked by a methylene bond (e in Figure 2-2). Additionally, condensation occurs at unsubstituted active sites on the benzene rings of hydroxymethylated phenol and phenol (f & g), hydroxymethylated lignin and phenol (h), and hydroxymethylated lignin and lignin (i & j), producing prepolymers (Figure 2-2) [5]. As polycondensation progresses, particularly in the later stages, methylol groups from different prepolymers begin to react, forming a crosslinked network structure. This ultimately results in a lignin-based phenol-formaldehyde (PF) adhesive, which is interconnected by both methylene and methylene ether bonds (not shown in Figure 2-2) [5]. Lignin-PF adhesives have demonstrated a bonding strength ranging from 0.6 to 15.2 MPa, with free formaldehyde content from 0.089 to 1%.

Due to its similarity of molecular structure to phenol, lignin is a promising alternative that has been investigated as early as the 1990's [38-39]. However, this has proved challenging due to the heterogenous molecular weight, complex structure, and low reactivity, which result in lignin-PF adhesives with lower performance when compared to PF adhesives [17]. This low reactivity is a result of the methoxy groups that occupy the meta position of lignin and prevents it from crosslinking in the PF adhesive reaction. This lower reactivity is why the addition of lignin generally decreases the bonding strength of the adhesive and

results in higher free formaldehyde and phenol emissions [3]. Due to the decrease in bonding strength and the increase in toxic emission, the amount of lignin that can be substituted in the adhesives has been limited.

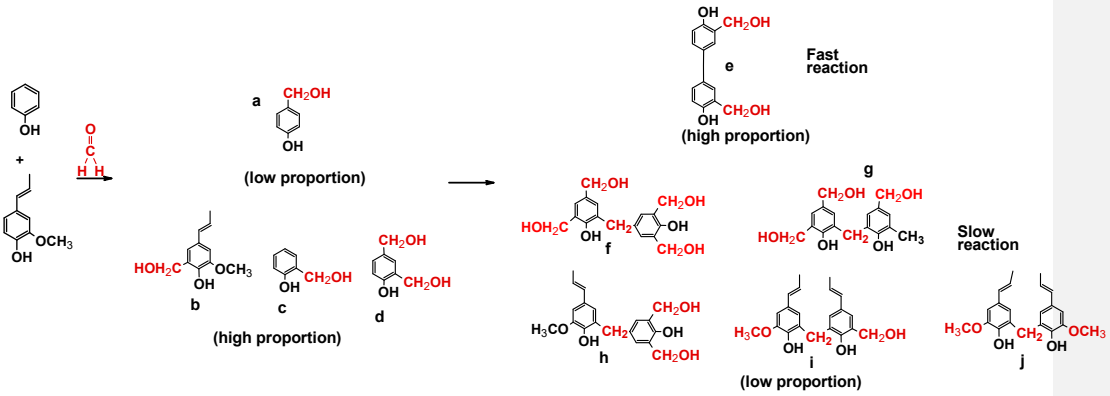

Figure 2-2: Mechanism for lignin-phenol-formaldehyde resin [5].

Commented [KK4]: This Figure may need modification. It may not print properly later.

Commented [JP5R4]: Made figure smaller. Prints fine

Some modifications have been conducted to improve the reactivity of lignin, such as hydroxymethylation, phenolation, demethylation and depolymerization, with demethylation and depolymerization being the most intensively researched, as can be seen in Table 2. Generally, it is seen that the bonding strength of lignin PF (LPF) adhesives increase with modification of lignin [40-41]. However, the modified LPFAs is not as strong as the PF adhesives due to the fact that the reactivity of lignin is inherently weaker than phenol [41].

The effect of temperature on the modification of lignin was examined (A4, A5, A6, A9, A16). For depolymerization, it is seen that the amount of phenolic content/bio-oil decreased with temperature elevation (A4, A5). This is because as the temperature is elevated, the bio-oil is further broken down into gasses. There is no clear trend for the effect of temperature on lignin demethylation. At optimum temperature of 170 °C, Di et al., saw an increase in bonding strength of 58% with 40 wt% lignin (A5). The demethylation of wheat straw alkali lignin using iodocyclohexane (ICH) reported an increase then decrease in conversion when the temperature was elevated from 130-155 °C. At the optimum temperature of 145 °C, a decrease in bonding strength of 10% with 40 wt% lignin was observed (A6). Meanwhile, the demethylation of alkali lignin using sodium sulfite and NaOH was reported a decrease in conversion when temperature was increased from 80 to 100 °C (A9**)**. At 80°C, the bonding strength decreased by 14% with 50 wt% lignin (A9). The variation in the optimum reaction temperature required by each modification for resin production is attributed to the different reagents used and their underlying mechanisms. The demethylation of ICH is generally conducted through nucleophilic attack, while demethylation using sodium sulfite and NaOH is carried out through nucleophilic attack and hydrolysis. The presence of hydrolysis allows for a reduced reaction temperature [42].

The effect of lignin fractionation on modification efficiency has also been examined (A3, A13). For example, Kraft lignin was separated into 3 fractions: ethyl acetate, acetate/petroleum ether, and ether soluble fractions, then phenolated via phenol. Interestingly, the ether soluble fraction, which contained the highest number of carboxylic hydroxyl, aromatic hydroxyl, and aliphatic hydroxyl reactive sites, made resin with the highest bonding strength and lowest free formaldehyde emissions comparable to that of PF adhesive (A13). In the same vein, the bio-oil and oligomer products of the base catalytic depolymerization of lignin

were incorporated into produce LPFAs. It was seen that not only did the LPFA using the oligomers outperformed the LPFA using oil, but it also performed better than the commercial PF adhesive (A3). Li et al. conducted the demethylation of soda lignin using a variety of sulfur containing reagents. It was found that Na_2SO_3 was the best sulfur containing reagent for the demethylation of lignin for PF resin application (A10). Lignin nanoparticles have also been recently explored for PF adhesives and showed promising results in improving its bonding strength (A18, A19, A20).

The main shortcomings of LPFA's are 1) increased formaldehyde emissions and typically decreased bonding strength that is resultant of the addition of lignin with a low reactivity when compared to phenol [43], 2) increased viscosity of resin, which is due to the larger molecular weight of lignin compared to phenol [43], and 3) the inconsistent quality of lignin incorporated in LPFAs due to the varied quality and properties of lignin [13].

Table 2-1: Properties of synthetic adhesives.

Properties	PF [44]	UF [45]	MF [46]	Epoxy [47]	Polyurethane [48]
Density, kg/m^3	1360	147 – 1520	1500	860-2600	1050-1250
Water Absorption, wt%/day	0.2	0.5	0.1	0.03-1.20	1.0
Ultimate tensile strength, MPa	–	30	36-90	5-97	29-49
Young's Modulus, GPa	–	9	7.6-10	0.0207-215	–
Rockwell Hardness	–	–	115-125	–	–
Elongation at break, %	–	–	–	–	10-21
Thermal Conductivity, W/m·K	0.25	0.30 – 0.42	0.167	0.1-1.20	0.21
Specific Heat Capacity, J/kg·K	–	1200	1674	–	1800
Coefficient of Thermal Expansion, 1/°C	1.6×10^{-5}	2.2×10^{-5} – 9.6×10^{-5}	2.2×10^{-5}	1.6×10^{-5} – 1.75×10^{-4}	10^{-4} – 2×10^{-4}
Relative Permittivity (@1 MHz)	5.0 - 6.5	–	–	–	–
Electrical Resistivity, Ω·cm	1012	–	–	–	–
Dielectric Field Strength, kV/cm	120 - 160	120 – 160	110-160	3.20-6.60	
Electrical resistance, Ω·cm	–	–	–	–	10^{12}
Refractive Index (589 nm)	–	1.55	–	1.48-1.54	–

Table 2-2: Studies on lignin-PF adhesives.

Modification	Lignin Type	Reagent	Conditions	Lignin Substitution, %	Resin synthesis, F/P [d] (mol/mol) NaOH/P [f] (mol/mol)	Hot press Conditions	Bonding Strength, MPa	Bonding strength Percent Difference, %	Free Formaldehyde Content, %	Symbol	References
Unmodified	White birch bark, white spruce bark	----	----	25, 50	F/P [e]: 1.8 NaOH/P: 0.35 • 84°C, 180min	250g/m^2 150°C, 3MPa, 4min	WBB-LPF-50: 1.33 WSB-LPF-50: 1.78	-39 -46	0.54[a] 0.45[a]	A1	[49]
	Bagasse	ClO_2, acetic acid	55°C	15	F/P [e]: 1.37 KOH/P: 0.06 • 70°C, 60 min+KOH	250-300g/m^2 130°C, 1MPa, 7min	LPF: 0.13[b]	-43 7	----	A2	[50]
Depolymerization	Kraft	Base-catalysed, catalytic	320°C, 25MPa, 10min	50, 60, 70	Prefere resin method (Commercial)	200g/m^2 120°C, 0.8MPa, 20min	DLPF-olig-70: 15.2 DLPF-oil-70: 11.6	11 -15	N/A 0.9	A3	[51]
	Organosolv	Base-catalysed, catalytic hydrothermal	340°C, 5MPa, 2hr	50, 75	F/P [e]: 1.3 NaOH/P [f]: 0.54 • 80°C, 120min+NaOH • 80°C, 120min, + F (dropwise)	250g/m^2 140°C, 17MPa, 4min	LPF-50: 2.3 DLPF-50: 2.0	28 11	1.0 0.5	A4	[52]
	Wheat straw	microwave alkali catalysis	130-170°C, 10-40min	20-100	F/P [e]: 1.5 NaOH/P [f]: 0.26 • 90°C, 90min+NaOH • 60°C, 60min+80%F • 80°C, 90min+20%F	140g/m^2 150°C, 1MPa, 5min	LPF-40: 1.3 DLPF-40: 1.9	8 58	1.0 0.9	A5	[53]
Demethylation	Wheat straw Akali	Iodocyclo-hexane	145°C, 3hr	40	F/P [e]: 5.28 NaOH/P: 0.43 • 50°C, 15min+ NaOH • 90°C, 120/210min+ F (dropwise)	125g/m^2 150°C, 1MPa, 6min	LPF: 1.13 DLPF: 2.28	-56 -10	0.65 0.22	A6	[43]
	Wheat straw soda	Sulfur	225°C, 10min	50, 60, 65	F/P [e]: 3.6 NaOH/P [f]: 0.35 • 60°C, 15min+NaOH • 95°C, 45min+80%F • 70°C +20%F • 95°C, 90min	125g/m^2 145°C, 1MPa, 3.5min	DLPF-50: 1.52 DLPF-60: 1.35 DLPF-65: 1.09	----	----	A7	[38]
	Alkali	HI or HBr	135°C, 12hr	50	F/P [e]: 2.2 NaOH/P [e]: 0.79 • 60°C, 30min+67% • 70°C, 30min+17%F • 90°C, 60min+16%F (NaOH added each step)	150g/m^2 130°C, 1.2MPa, 7min	DLPF-HI: 0.9 DLPF-Br: 0.6	-40 -60	0.47[a] 0.49[a]	A8	[41]

	Alkali	Na_2SO_3 with NaOH	80°C, 1hr	50	F/P [e]: 2.2 • 85°C, 50min • 85°C, 60min+33%F • 85°C, 50min+66%F (NaOH added each step)	125-150g/m^2 130°C, 1.2MPa, 5min	DLPF: 1.07	-14	0.31[a]	A9	[54]
Demethylation	Soda	S, NaSH, Na_2SO_3, or mercaptan	90°C, 1hr	30	F/P [e]: 2.2 NaOH/P: 0.58 • 87°C, 50min+38%F • 87°C, 60min+31%F • 87°C, 50min+31%F • 87°C, 30min + urea (NaOH added each step)	250-300g/m^2 130°C, 1MPa, 7min	DLPF-Na_2SO_3: 1.14 Na_2SO_3 was the most effective sulfur containing reagent.	-9%	0.56	A10	[16]
	Alkali	Urea, NaOH	Room temp, 16hrs	10-60	F/P [e]: 2 NaOH/P: 0.2 • 85°C, 60min+66%F • 85°C, 50min+33%F (NaOH added each step)	180g/m^2 180°C, 1.2MPa, 4.5min	DLPF-20: 1.6 DLPF-60: 1.2	33 0	0.12 0.28	A11	[37]
	Kraft	Na_2SO_3 with NaOH	80°C, 2hr	10-70	F/P [e]: 0.5 • NaOH/P: 0.35 90°C, 90min+F+NaOH	250-280g/m^2 130°C, 1.2MPa, 15min	DLPF-30: 2.43 DLPF-50: 2.18 DLPF-70: 1.34	70 52 -6	0.09 0.19 0.27	A12	[55]
Phenolation	Organosolv	phenol	110°C, 2.5hr	40	F/P [e]: 5.49 • NaOH/P: 0.24 • 80°C, 60min+50%F • 80°C, 90min+50%F • 60°C, 30min (NaOH added each step)	50g/m^2 150°C, 1.5MPa, 6min	PLFP:1.36[c]	-9	0.31	A13	[56]
	Kraft, hydrolysis, wheat straw alkali	Phenol	90°C, 1hr	----	----	----	----	----	----	A14	[34]
Hydroxymethylation	Softwood Kraft	Para-formaldehyde	80-120°C, 15-240min	----	----	----	----	----	----	A15	[57]
	Kraft, sodium lignosulfonate organosolv	Para-formaldehyde	50°C, 45min	----	----	----	----	----	----	A16	[33]
	Cornstalk	H2O and NaOH	60-80°C, 210min	----	----	----	----	----	----	A17	[58]
Nanoparticles/ macroparticles	Alkali	HCl	pH 2	10-60	F/P [e]: 1.8 NaOH/P: 0.37 • 65°C, 40min+67% (F + NaOH) 85°C, 240min+ 33% (F+NaOH) + Urea	----	LPF-40:1.11 NLPF-30: 1.59 NLPF-40: 1.30 NLPF-50: 1.10	14 64 34 13	3.20 0.12 0.28 0.53	A18	[59]
	Hydrolysis	HCl	35°C, 240min	5, 10	----	80°C, 72 hr 100°C, 1 hr	NLPF-5: 9.58 MLPF-5: 10.92 NLPF-10: 8.10	10 26 -7	----	A19	[60]

Commented [JP6]: Add abbreviation

					MLFP-10: 5.90	-32				
Alkali	50-95°C, 240min	----	----	----	----	----	----	A20	[61]	

a: mg/L, b: molding, c: wet strength, d: F/P – formaldehyde/phenol (mol/mol)

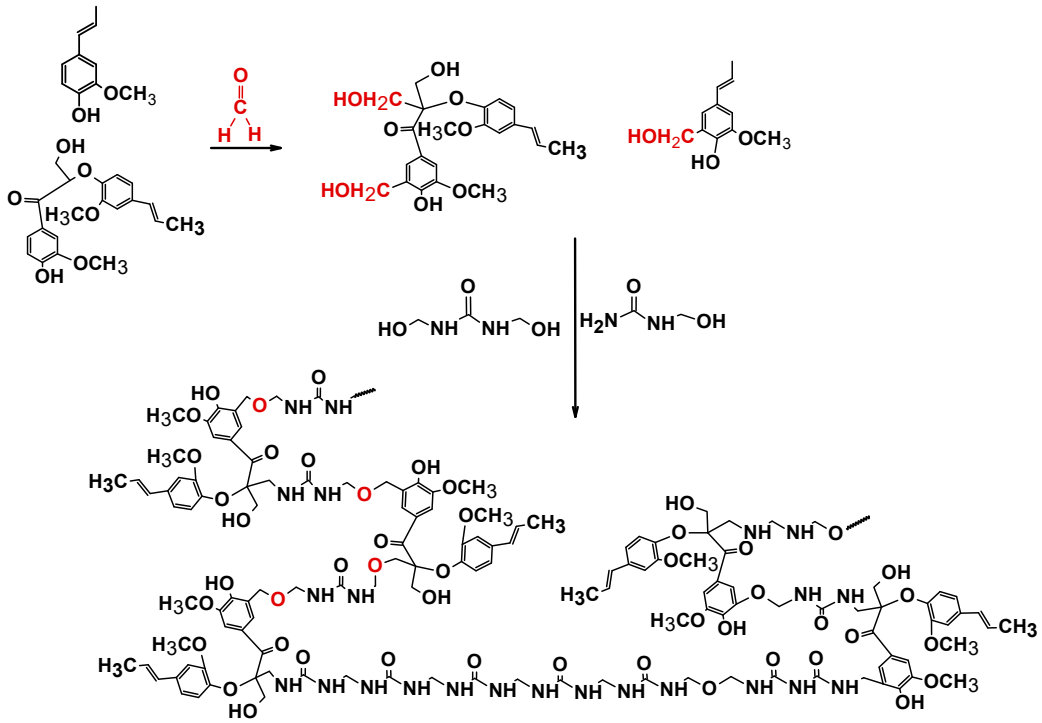

Figure 2-3: Mechanism for lignin-urea-formaldehyde resin [12].

2.3.2 Lignin-Urea-Formaldehyde Adhesive (LUFA)

The most common type of thermoset adhesive is urea formaldehyde adhesive (UFA) [62]. UF resins is synthesized through the polycondensation of urea formaldehyde and other modifiers [63]. The mechanism for lignin-UF resins can be seen in Figure 2-3. The synthesis of lignin-UF resin mainly consists of two stages. First, in the hydroxymethylation stage, an addition reaction occurs where both urea and lignin react with formaldehyde, leading to the formation of hydroxymethyl urea and hydroxymethylated lignin [12]. Second, in the condensation stage, linear or branched oligomers are formed through the condensation of hydroxymethyl urea under acidic conditions [12].

UF adhesives are most commonly used in manufacturing wood-based composites, such as medium density fiberboard (MDF), particleboard and plywood [64]. Additionally, UF resins can be used in a variety of applications such as abrasives, foams, impregnated paper laminates, textiles, molded compounds, coating, and slow-release fertilizer [62], [63], [65]. Approximately, 11 million tons of UFAs are produced annually [66]. In 2022, UF adhesives accounted for nearly 80% of the total world demand for thermoset adhesives [62].

UF resins have been widely utilized in the industry due to their low-cost raw materials, excellent thermal stability, resistance to microorganisms and abrasion, high hardness, strong mechanical properties, superior adhesion to wood, low curing temperature, aqueous solubility, and colorless glue line [63-64, 66-67]. The properties of UF resins can be seen in Table 2-1. The literature reports bonding strength values ranging from 0.03 MPa to 4.84 MPa, with free formaldehyde levels in cured wood products ranging from 0.0017% to 0.0093% [62], [66], [68]. This is slightly higher than the internation standard (EN ISO 12460–5:2015) of 0.008%.

However, UFAs have their own limitations, such as high formaldehyde emissions and poor water resistance [69]. Additionally, the modifiers, e.g., glycerol diglycidyl ether (GDE), PMDI and melamine, that are used to enhance their performance are expensive [67]. To address these limitations, researchers have studied the incorporation of lignin in UFA adhesives to improve their environmental impacts. Lignin can be used to improve UFA's water resistance, formaldehyde emission, and thermal stability while maintaining its mechanical properties when compared to UFA [70-75]. However, the low reactivity of lignin limits it direct utilization. Some modifications used for improving the reactivity of lignin in LUFA's are glyoxalation, depolymerization, phenolation, sulfonation and ionic-liquid treatment (Table 2-3).

The use of different modifiers, such as epoxy (B5), glycerol diglycidyl ether (GDE) (B7), pMDI (B8), and maleated lignin-based polyacids (B9) have shown to improve LUFA performance. For example, a maleated lignin-based polyacid catalyst (MA-HL) was synthesized to enhance the water resistance and bonding strength of UFA (B9). The lignin-based catalyst was compared against commercial catalyst, like ammonium chloride (NH_4Cl) and isophthalic acid (IPA). When a catalyst of 1% MA-HL was used, the lignin-based polyacid resin exhibited the lowest shear strength and longest curing time [63]. It should be noted that the formaldehyde emission decreased with the use of the lignin-based polyacid catalyst, suggesting that the remaining active sites of lignin were potentially reacted with formaldehyde [63]. When the catalyst dosage was increased to 5% MA-HL, the bonding strength of 1.74 MPa was achieved, which was higher than the LUFA using commercial catalyst at 1%. Additionally, its water resistance increased when compared to commercial catalyst NH_4Cl (B9) [63]. In another work, glyoxalation and ionic liquid treatment of lignin were compared to observe how such modifications would affect the performance of LUFAs (B3). The ionic liquid treated LUFA exhibited an extended gel time and increased shear strength when compared to glyoxalated LUFA [69]. This is because lignin contained more acetate anion and imidazolium cation reactive sites than glyoxalation after ionic liquid treatment [69]. Both modified LUFA had a slightly lower

shear strength than UFA. Also, the phenolation of kraft lignin has been conducted to investigate the effect on the formaldehyde emissions and the bonding strength of particleboard (B11). Interestingly, the bonding strength of LUFA using 20% phenolated lignin was comparable to raw UFA. There was no observable change in performance when the lignin substitution increased from 10 % to 20 %, while the bonding strength of LUFA made from unmodified KL decreased with the increased substitution [21]. Regardless, the formaldehyde emissions decreased with addition of both modified and unmodified lignin [21]. In the same vein, the incorporation of modified lignin nanoparticles into LUFA has been investigated (B14, B15). Interestingly, demethylated lignin-based nanoparticles improved the bonding strength and but reduced free formaldehyde content of LUFA (B14). In contrast, when maleated lignin nanoparticles substitution increased from 10% to 30%, the bonding strength increased, and free formaldehyde decreased, surpassing the performance of the UFA (B15). Additionally, urea can be used to improve PF resin performance by creating PF-UF resin mixture (B10, B13). The incorporation of urea resulted in a bonding strength and free formaldehyde content comparable to raw PF resin. Demethylated lignin was used to produce a lignin-PF adhesive with 60% demethylated lignin (B13). The modified lignin-PF adhesive (LPFA) had bonding strength and free formaldehyde content comparable with those of commercial adhesive [37]. The low free formaldehyde content at high substitutions was associated with the addition of urea which was used to make urea-formaldehyde adhesive, improving bonding strength and consuming free formaldehyde [37]. It should also be noted that, as the substitution of lignin increased so did its viscosity. In this case, a large volume of water was needed to reduce viscosity to improve the spread ability and allow for more lignin to be substituted.

Modified lignin urea-formaldehyde (UF) adhesives, while beneficial in certain aspects, have several shortcomings compared to UF adhesives. These include lower bonding strength due to lignin's less reactive nature, longer curing times, and reduced water resistance, which can limit their application in moisture-prone environments. Additionally, the variability in lignin's chemical structure can lead to inconsistencies in adhesive performance. Although lignin can help reduce formaldehyde content, modified lignin UF adhesives may still emit formaldehyde, albeit at lower levels.

Table 2-3: Studies on lignin-UF adhesives.

Modification	Lignin Type	Reagent	Conditions	Lignin Substitution, %	Application	Resin synthesis,	Hot press Conditions	Bonding Strength, MPa	Bonding strength percent difference, %	Free formaldehyde content [a], mg/100g	Symbol	References
Unmodified	Magnesium, sodium Lignosulfonates	----	----	10, 20, 30, 50, 75, 100	Resin-particleboard	Purchased UF resin	200°C, 2.5MPa, 10min	Mg-LUF-10: 0.16 Na-LUF-10:0.14 Mg-LUF-100: 0.06 Na-LUF-100: 0.03	-7 -15 -65 -83	2.4 2.0 0.8 1.7	B1	[66]
	Alkali bagasse and molasse	----	----	5, 10, 13, 15	Resin-particleboard	Purchased UF resin	190°C, 2.26MPa, 7min	B-LUF-10: 4.84 M-LU-10: 4.20 B-LUF-13: 4.23 M-LU-13: 4.52	7 -7 -6 0	3.1 - - 3.3	B2	[68]
	sodium Lignosulfonates	----	-----	20	Resin-plywood	F/U [e]: 2.0 >1.5 >1.1 • 80°C, 30min, (F/U=2) • pH 4-4.5 (H_3PO_4), then 85-90°C • pH 6-6.5 (NaOH) + Urea (F/U= 1.5) • Urea (F/U=1.1), pH>7	180g/m^2 120-125°C, 1.2MPa, 60s/mm	0.88 [d]	-2	0.12 [b]	B3	[63]
Glyoxalation	Bagasse soda black liquor	Glyoxal, NaOH (30%)	58°C, 8hr	10, 15, 20	Resin-plywood	Purchased UF resin	250g/m^2 120°C, 1MPa, 5min	GLUF-10: 1.89 GLUF-15: 1.56 GLUF-20: 1.32	-2 -19 -32	3.4 3.2 3.2	B4	[69]
	Bagasse soda black liquor	Glyoxal, NaOH (30%)	58°C, 8hr	15 + epoxy	Resin-plywood	• 40°C, 30min+ Urea • 75°C, 120min • GL+ CH_2O_2 (pH 4-4.5), 75°C, 60min	310g/m^2 180°C, 6MPa, 5min	GLUF+5% epoxy: 1.7	295	No formaldehyde used	B5	[76]
	Bagasse soda black liquor	Glyoxal, NaOH (30%)	58°C, 8hr	10, 15, 20	Resin-plywood	F/U [e]: 1.3 • 90°C, 60min, F+NaOH+Urea (65 wt%) • 90°C, 90min, +lignin (20wt% of Urea) • 40°C + remained of Urea	250g/m^2 120°C, 1MPa, 5min	GLUF-10: 1.78 GLUF-15: 1.51 GLUF-20: 1.29	-7 -21 -33	3.4 3.2 3.2	B6	[64]
	Kraft	Glyoxal, NaOH (33%)	60°C, 3hr	62+ Glycerol diglycidyl ether (GDE) extender	Resin-particleboard	• GL+ Urea+ dialdehyde, 25°C, 90-120min • 5 wt% GDE	220°C, • 2.8MPa, 3min • 1.2 MPa, 4min • 0.58MPa, 3min	0.81	----	No formaldehyde used	B7	[77]
Ionic liquid	Bagasse soda black liquor	1-ethyl-3-methylimid	120°C, 30min	15 + 6% pMDI isocyanate	Resin-plywood	F/U: 1.3 • Urea +F+ NaOH 40°C, 30min	250g/m^2 120°C, 1MPa,	ILUF-6PMDI: 2.2	40	2.9	B8	[78]

		azolium acetate				• 90°C over 30min, hold 60min • pH 5-5.5 with CH_2O_2 • add IL, 90°C, 90min • add final urea, 40°C • + pMDI	5min					
	Bagasse soda black liquor	1-ethyl-3-methylimid azolium acetate	120°C, 30min	10, 15, 20	Resin-plywood	F/U [e]: 1.3 • Urea +F+ NaOH 40°C, 30min • 90°C over 30min, hold 60min • pH 5-5.5 with CH_2O_2 • add IL, 90°C, 90min • add final urea, 40°C	250g/m^2 120°C, 1MPa, 5min	ILUF-10: 1.89 ILUF-15: 1.56 ILUF-20: 1.32	-2 -19 -32	3.7 3.5 3.0	B4	[67]
Hydroxymethylation	3-methoxy-4-hydroxyphenyl-propane	Form-aldehyde	90°C, 1hr	1, 3, 5 Used as polyacid catalyst	Resin-Medium density fiberboards, Plywood	F/(Urea+melamine): 1 • F + 33% (U+M) • 33% (U+M) • 33% (U+M)) •	280g/m^2 • 0.8MPa, 1hr • 125°C, 0.2MPa, 60s/mm	HLUF-1: 1.33 HLUF-3: 1.42 HLUF-5: 1.72	29 37 67	0.42[b] 0.21[b] 0.19[b]	B9	[25]
Depolymerization	Alkali	NaOH/Urea	-16°C, 24hr	50	Resin-plywood	F/P [f]: 1.2 • P + lignin + NaOH +33% F, 85°C, 50min • +33% F, 85°C, 60min • +33% F, 85°C, 50min • U + NaOH 80°C, 15min	125-150g/m^2 • 25°C, 0.8MPa, 30min • 130°C, 1.2MPa, 5min	1.06	-14	0.38[b]	B10	[79]
Phenolation	Kraft	Phenol with oxalic acid catalyst	130°C, 50 min	10, 15, 20	Resin-Particleboard	F/U [e]: 1.3 • Urea + lignin + NaOH + F, 40°C, 30min • Increase 90°C, 30min ramp + 60min • pH 5-5.5 with CH_2O_2 then neutralize NaOH • add lignin, 90°C, 90min • add final urea, 40°C	• 180°C, 2.5MPa, 5min • 25°C, 2.5MPa, 5min	PLUF-10: 1.88 PLUF-15: 1.84 PLUF-20: 1.76	-2 -4 -8	3.2 2.9 2.7	B11	[21]
Sulfonation	Kraft	Purchased modified lignin	----	5, 10, 15, 20, 30	----	• Purchased UF resin	----	----	----	----	B12	[65]
Demethylation	Alkali	Urea, NaOH	Room temp, 16hrs	10-60	Resin-plywood	F/P [f]: 2 NaOH/P: 0.2 • 85°C, 60min+66%F • 85°C, 50min+33%F	180g/m^2 180°C, 1.2MPa, 4.5min	DLPF-20: 1.6 DLPF-60: 1.2	33 0	0.95[c] 0.62[c]	B13	[37]

						• (NaOH added each step)						
Nanoparticles	Softwood kraft (demethylated)	Sodium sulfite, NaOH	95°C, 3hrs	1, 3, 7	Resin-Medium density fiberboards	F/U [e]: 1.12 • F + NaOH, 45°C • Add urea 89°C,50min • pH 5-5.5 with CH_2O_2 • add 2nd urea, 50°C • add lignin nanoparticles	185°C, 3.4MPa, 5min	NLUF-1: 0.55 NLUF-3: 0.53 NLUF-7: 0.48	-2 -5 -14	9.3 6.9 2.9	B14	[62]
	Kraft (maleated)	1-ethyl-3-methylimidazolium acetate	80°C, 3hr	10, 20, 30	Resin-plywood	F/U [e]: 1.3 • F + NaOH, • Add Urea. 40°C, 30min • Increase 90°C, 30min ramp + 60min • pH 5-5.5 with CH_2O_2 then neutralize NaOH • add NL, 90°C, 90min add final urea, 40°C	300 g/m^2 120°C, 1MPa, 5min	NLUF-10: 1.43 NLUF-20: 1.59 NLUF-30: 1.72 MNLUF-10: 1.74 MNLUF-20: 1.86 MNLUF-30: 2.14	-26 -18 -11 -10 -4 10	2.9 2.8 2.8 2.7 2.5 2.4	B15	[80]

a: free formaldehyde content of cured plywood, b: mg/L, c: mg/m^3, d: wet strength, e: F/U – formaldehyde/urea (mol/mol), f: F/P – formaldehyde/phenol (mol/mol)

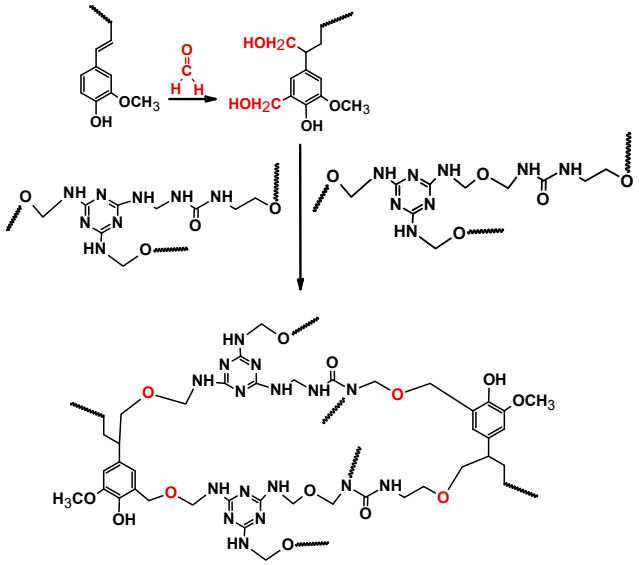

Figure 2-4: Mechanism for lignin-melamine-formaldehyde resin [81].

2.3.3 Lignin-Melamine-Formaldehyde Adhesive (LMFA)

Another type of formaldehyde-based adhesive is a melamine-formaldehyde adhesive, which is synthesized by reacting melamine with formaldehyde. Melamine formaldehyde (MF) resins are used in a variety of applications, such as laminates, tableware, automotive coatings, insulation foam, textile finishings, paper treatment, and adhesives for wood products like plywood, particleboard and fiberboards [3, 82-87]. Melamine-formaldehyde resins are valued for their durability, thermal and flame resistance, water resistance, and excellent electrical insulation. Their adhesives offer strong bonding, easy curing, and high resistance to heat, water, abrasion, and aging, making them superior to urea-formaldehyde adhesives in strength and stability for demanding applications [3], [88]. Compared to urea-formaldehyde adhesives, melamine-formaldehyde adhesives contain higher strength and heat stability properties. The properties of MF resins can be seen in Table 2-1. The main shortcomings of MF resin include high brittleness and poor flexibility, which make it prone to cracking under stress, limiting its use in applications requiring elasticity. Additionally, it has low storage stability and formaldehyde emissions, which raise health and environmental concerns.

Similar to other resin, lignin incorporation in the resin has benefits. The mechanisms for lignin-melamine formaldehyde resin reaction can be seen in Figure 2-4. Lignin is first activated through hydroxymethylation with formaldehyde present in the system. The source of formaldehyde is primarily free formaldehyde. Next, due to the abundance of active sites in lignin, the resulting structures of the product would be relatively complex, ultimately leading to the formation of a three-dimensional crosslinked network of resin [81]. It should be noted that lignin units that would not participate in the reaction could act as fillers, integrating into the MUF structure through electrostatic absorption [81]. Although is still a lot to be explored, in the literature, lignin-MF adhesives (LMFA) have demonstrated a bonding strength of 1.34 MPa, with free formaldehyde content of 0.06%. LMFAs have a high production cost due to the high cost of melamine [89], because the price of melamine is about 70-50% more expensive than phenol [89].

Although it has not been researched as extensively as the LPFA's and LUFA's, lignin has been used to make lignin-melamine-formaldehyde (LMFA) (C1) and lignin-melamine-urea-formaldehyde (LMUFA) (C2) adhesives, as seen in Table 2-4. For example, tosylated lignin was reacted with formaldehyde to develop a LMFA (C1). The LMFA demonstrated good thermal stability; however, the elevated curing temperature of the resin (around 200°C) is a drawback [90]. In another work, hydroxymethylated alkali lignin was mixed with urea and formaldehyde producing a LMUFA (C2). In this work, the gel time and bonding strength increased while decreasing the free formaldehyde emissions [81]. This decrease in formaldehyde emissions suggested that hydroxymethylated lignin could potentially be used as a formaldehyde catching agent. When substitution of lignin was too high (e.g., 8 wt%), it deteriorated the resin's performance. This could be a result of unreacted active sights of lignin's benzene ring reacting with formaldehyde, which affected the urea-formaldehyde and melamine-formaldehyde reactions. It is also a result of steric hindrance created by lignin's complicated structure [81].

Table 2-4: Studies on lignin-MF adhesives.

Modification	Lignin Type	Reagent	Conditions	Lignin Substitution, %	Application	Resin synthesis, F/U [a] (mol/mol) NaOH/P [b] (mol/mol)	Hot press Conditions	Bonding Strength, MPa	Bonding strength percent difference, %	Free formaldehyde content, %	Symbol	References
Tosylation	Kraft	Tosyl chloride with triethylamine catalyst	25°C, 24hr	100	Resin	Copolymer • Lignin + Melamine in DMSO, 100°C, 6hr Resin • Copolymer + THF, 65°C • Add F, pH 9.0, 1h • Cool down solution	----	----	----	----	C1	[90]
Hydroxymethylation	Alkali	Formaldehyde + Urea	90°C, 1hr	2, 4, 6, 8	Resin-plywood	F/U [a]: 1.12 • F+ NaOH, 50°C, pH 9.0 • Add U, M, lignin, 90°C pH 5.0–5.2, 60min • pH 8.7–8.9, add M • pH to 9.0, 45°C Add U, 10min • pH 8.0–8.5, 25°C	160g/m^2 130°C, 1.5MPa, 5min	HLMF-2: 1.01 HLMF-4: 1.25 HLMF-6: 1.34 HLMF-8: 1.16	18 37 47 27	0.08 0.06 0.06 0.07	C2	[81]

a: F/U – formaldehyde/urea (mol/mol), b: NaOH/P – sodium hydroxide/phenol (mol/mol)

2.3.4 Lignin-Epoxy Adhesive (LEA)

Epoxy adhesives consist of a three-dimensional network of a thermoset polymer, which is produced by reacting an epoxide resin with a curing agent through means of self-homo-polymerization [20]. Furthermore, its epoxide terminal groups can be easily modified using a variety of reagents (such as amines, anhydrides and other acids, alcohols, esters) to obtain different properties [91].

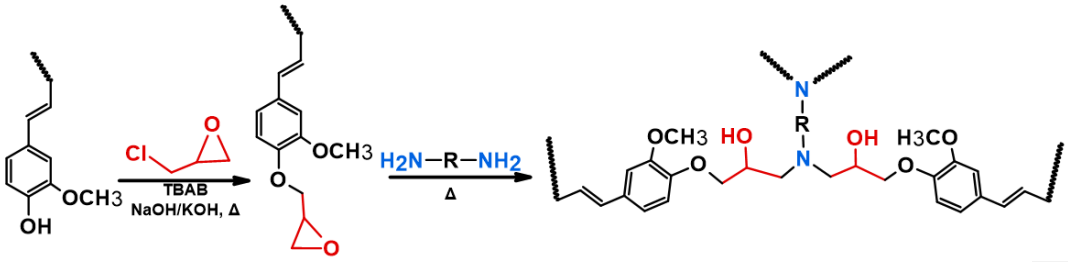

Figure 2-5: Mechanism for lignin-epoxy resins [91].

In 2022 the worldwide consumption of epoxy resins was estimated to be approximately 3.6 million tons, and it was estimated to grow up to 5 million by 2030 [92]. Epoxies are incredibly versatile resulting in a variety of applications, such as adhesives, plywood, furniture manufacturing, sealants, high performance composites, electronic component packaging, electronic laminates, electric insulators, flooring [20, 93-96]. This wide range in applications is a result of their excellent strength, adhesion ability, thermal and dimensional stability, and chemical, solvent, and corrosion resistance [20], [94], [97]. The properties of epoxy resin can be seen in Table 2-1

Epoxies contain high degree of crosslinking that can lead to increased brittleness [95]. Additionally, Bisphenol-A (BPA) and epichlorohydrin (ECH) are the raw material for epoxy synthesis. BPA has been proved to an environmental hormone and an endocrine disruptor that negatively effect human health [98]. Prolonged longed exposure to BPA may induce reproduce, developmental and metabolic disorders [98]. Currently, the most common commercial epoxy adhesive is diglycidyl ether of bisphenol A (DGEBA), which is synthesised by mixing bisphenol-A (BPA) and epichlorohydrin (ECH), and it consists of about 90% of the worldwide epoxy adhesive market [91], [98].

The mechanism for lignin-epoxy resins can be seen in Figure 2-5**.** First, lignin undergoes epoxidation using epichlorohydrin under alkaline conditions (NaOH/KOH) with Tetrabutylammonium bromide (TBAB) as a catalyst, forming a reactive epoxy resin. In the second step, the epoxy groups react with a diamine hardener, leading to crosslinking via amine-epoxide reactions. This curing process results in a stable, three-dimensional network, producing a lignin-based epoxy cured material with enhanced structural properties [91]. In the literature lignin-epoxy adhesives have demonstrated a bonding strength ranging from 2.7 MPa to 99.4 MPa.

Despite its use in pristine form, lignin modifications, such as depolymerization, demethylation, phenolation and amination, have proven to improve its molecular weight and reactive site for epoxy resin, (Table 2-5). For example, the impact of demethylated, phenolated and demethylated-phenolated lignin have been compared on LEA performance (D4). The demethylated LEA had a lower flexural and impact strength of about 19%, while phenolate LEA had an increase of 5% in such properties [97]. With the demethylated-phenolated lignin, the flexural and impact strength increased by 10%, surpassing demethylated and phenolated LEAs [97]. Demethylated lignin was used to produce lignin epoxy adhesive (LEA) at various lignin substitutions (10-35 wt%) (D5). The LEA with 30 wt% lignin substitution exhibited an increase in bonding strength of 148%, when compared to commercial epoxy adhesives. In another work, depolymerized lignin was separated into water soluble, ammonia water-ethanol soluble, and ethylenediamine-ethanol soluble fractions (D10). Bonding strength increased by 49% for the use of water-soluble fraction in resin, 49% for the ammonia water-ethanol soluble fraction, and 42% for the ethylenediamine-ethanol soluble fraction at 2 wt% dosage [99]. Depolymerized lignin was also used to make 100% lignin substituted LEA using oligomer products with and without epoxied cardanol glycidyl ether (ECGE), (D7). Without the ECGE, the bonding strength of the depolymerized LEA decreased by 19%, while the addition of the ECGE increased bonding strength by 4% compared to a commercial epoxy [100].

Lignin has also been investigated as a curing agent for epoxy adhesives (D3, D13). Demethylated and esterified organosolv lignin has been used as a curing agent for commercial epoxy adhesive, E-51 (D3)[101]. Aminated lignin has also been used as curing agent for a commercial epoxy (D13). The synthesized lignin-based curing agent exhibited good overall performance, with no clear relationship between thermal and mechanical properties as its lignin content increased [102]. Lignin nanoparticles have also been explored in epoxy resins (D14, D15, D16). The incorporation of nanoparticles shows promising performance with up to 50 wt% lignin substitution [103], [104]. As its shortcoming, the mechanical properties of lignin incorporated lignin resins may still not match those of the fully synthetic adhesives, and depending on the type of modification, the water resistance could be affected. Additionally, some LEAs still require the use of BPA, which is harmful to human life [105], [106].

Table 2-5: Studies on lignin-epoxy adhesives.

Modification	Lignin Type	Reagent	Conditions	Lignin Substitution, %	Application	Resin synthesis,	Curing conditions	Bonding Strength, MPa	Bonding strength percent difference, %	Symbol	References
Raw	13 commercial lignin	----	-----	9	Resin-mold	• Lignin + DMF, 25°C, 10min • TBAB + ECH, 60°C, 3hr • TBAB + NaOH (dropwise), 25°C, 8hr	• Add GX-3090, 130°C, 2hr • 150°C, 1hr	-----	----	D1	[107]
	Kraft	----	----			• Lignin, ECH, NaOH, 50°C, 5hr	• Add Jeffamine D2000, 50°C, 1hr • 100°C, 2hr • 150°C, 2hr	LEP: 66	14	D2	[108]
Demethylation	Organosolv + esterification	HBr	110°C, 24hr	5, 10, 20, 30 + 1% DMAP	Resin-mold	• Purchased E51	• Add lignin curing agent + DMAP, 80°C, 1hr • 150°C, 3hr • 190°C, 2hr	DLEP-5: 39.19 DLEP-10: 71.54 DLEP-20: 55.43 DLEP-30: 35.26	----	D3	[101]
	Alkali	HI	120°C, 20hr	10	Resin-mold	• Lignin + phenol + H_2SO_3 + Formaldehyde, 65°C, 2hr • TBAB + ECH, 65°C, 3hr • NaOH, 65°C, 3hr	• Add MNA, 85°C, 10min • 85°C, 4hr • 120°C, 4hr • 160°C, 4hr	DLEP: 98.38[a] DPLEP: 134.12[a]	-19 10	D4	[97]
	Unspecified	HBr	120°C, 3hr	10, 20, 30, 35	Resin-mold	• Lignin + DMF, 25°C, 1hr • NaOH + ECH (E-44), 80°C, 3hr	• Add E-44 + T-31, 80°C, 4hr	DLEP-10: 36.78 DLEP-20: 55.43 DLEP-30: 62.50 DLEP-35: 39.96	46 105 148 59	D5	[20]
	Enzymatic hydrolysis	1-dodecanethiol	----	2, 5, 10, 15 + E-51	Resin-mold	• Lignin+ ECH, 25°C • NaOH, 80°C, 30min	• Add polyamine 593, 60°C, 2hr • 80°C, 3hr • 120°C, 1hr	DLEP-2: 52.20 DLEP-5: 55.52 DLEP-10: 41.19 DLEP-15: 29.94	19 27 -6 -32	D6	[94]
Depolymerization	Alkali	Partial-reductive	275°C, 4.5 MPa, 4/8/12hr	8	Resin-mold	• Lignin+ ECH + TEBCA, 110°C, 5hr • Cooled to 50°C • Add NaOH, 60°C, 5hr	• Add MeTHPA + DMBA, 90°C • 120°C, 4hr • 160°C, 1hr • 180°C, 4hr	DLEP: 60 DLEP+ECGE: 77	-19 4	D7	[109]
	Organosolv	Reductive	350°C, 1hr	33	Resin	• Lignin+ ECH + TBAB, 80°C, 1hr • Add NaOH, 55°C, 8hr	-----	-----	----	D8	[110]
	Alkali	Hydrolysis	250°C, 1.5hr	-----	Resin-mold	• BPA + ECH, 50°C • Add Lignin, 30min • 90°C, 1hr	• Add EDA, 100°C, 4hr	DLEP: 2.66	----	D9	[93]

	Dealkalized	Hot compressed ethanol-H_2O	260°C, 30min	.5, 1, 1.5, 2	Resin-mold	• E44, 120°C, 1hr • Add Lignin, 30min • 80°C, 2hr • Cooled 50°C	• Add polyamide 651, 25°C	WDLEP-1.5: 91.25 ADLEP-1.5: 96.88 EDLEP-1.5: 99.37 WDLEP-2: 88.13 ADLEP-2: 92.50 EDLEP-2: 92.50	47 57 61 42 49 49	D10	[99]
	Rice husks+ silica	Hydrothermal	250°C, 1.5hr	15, 20, 25, 30, 35, 40	Resin-mold	• BPA + ECH, 50°C • Add Lignin, 90°C 30min • 90°C, 1hr	• Add EDA, 100°C, 4hr	DLEP-35+S: 3.98 DLEP-40+S: 2.52	83 16	D11	[95]
	Reed magnesium bisulfite	Hydrolysis	160°C, 3hr	17	Resin-mold	• Lignin + ECH + NaOH, 90°C 30min	• Add E-57 + T-31	DPLEP-17: 10.42	228	D12	[98]
phenolation	Alkali	Phenol	110°C, 1hr	10	Resin-mold	• Lignin + phenol + H_2SO_3 + Formaldehyde, 65°C, 2hr • TBAB + ECH, 65°C, 3hr • NaOH, 65°C, 3hr	• Add MNA, 85°C, 10min • 85°C, 4hr • 120°C, 4hr • 160°C, 4hr	PLEP: 127.5[a]	5	D4	[97]
Amination	Kraft	Nano-alumina, $CO(NO_3)_2{\cdot}6H_2O$, $Cu(NO_3)_2{\cdot}6H_2O$, Hydrazine hydrate	140°C, 4hr	10, 13, 16	Resin-mold	• Purchased	• Add lignin curing agent + DMF • 125°C, 2hr • 150°C, 1hr	ALEP-13: 86.91	----	D13	[90]
Nanoparticles	Kraft	Ethanol, THF, deionized water	25°C, 15min	33, 50, 67, 100	Resin-plywood	• ECH, 43°C • Add Lignin, 1ml/min, 11min •	• 300 gm/m^2, 145°C, 5min, 1.1MPa	LNEP-33: 10.28 LNEP-50: 11.26 LNEP-67: 8.97 LNEP-100: 3.96	9 19 -5 -58	D14	[104]
	Dealkalized	Glycerol triglycidyl ether (GTE), NaOH	100°C, 30min	40, 50, 60	Resin-plywood	• Mix GTE, lignin and NaOH, 100°C, 30min	• 140°C, 3min, 0.3MPa • 140°C, 7min, 0.5MPa	LNEP-40: 12.18 LNEP-50: 14.62 LNEP-60: 12.93	43 71 52	D15	[103]
	Alkali	Ethylene glycol (EG)	35°C, 1hr pH 3 (3 drops/min) HCl, H_2SO_3	15	Resin-mold	• Lignin + EPI, 25°C, 30 min • Add BPA, 80°C, 2hr • Add NaOH, 80°C, 3hr • Add NaOH, 80°C, 2hr • 25°C, 2hr	----	LNEP-15: 44.80	----	D16	[111]

a: Flexural strength

2.3.5 Lignin-Polyurethane Adhesive (LPUA)

Polyurethanes are commonly used plastics synthesized by reacting petroleum-derived polyols with di- or tri-isocyanates [3], [11]. The worldwide consumption of PU resins was estimated to be nearly 25.8 million tons in 2022 with forecasted growth to 31.3 million tons by 2030 [112]. PU resins are used in a wide variety of applications such as insulation materials, automotive parts, coatings, adhesives, elastomers, foams, fibers, appliances, biocompatible material for medical devices and construction industry [113-118]. Its wide range of applications is accredited its excellent tensile and compressive strength, thermal stability, insulation properties, fatigue durability and abrasion, and chemical and water resistance [3], [106]. Additionally, PU can be formulated to be rigid or flexible. The mechanical properties of traditional polyurethane adhesives can be controlled by the degree of crosslinking [11]. The properties of PU resins can be seen in Table 2-1. Some of the drawbacks of PU resins are its sensitivity to moisture, which can lead to incomplete curing, susceptibility to UV degradation, limited extreme-temperature resistance, resistance to strong acids or bases [119-120]. Additionally, the high production costs, poor biodegradability and environmental pollutions are associated with polyurethane production [119-123]. Alternatively, a safer and more environmentally friendly alternative, such as lignin, should be investigated.

Lignin contains phenolic and aliphatic hydroxyl groups and can act as polyols, which can potentially react with isocyanate to produce a LPUA [122]. The mechanism for lignin-PU resins can be seen in Figure 2-6. In the first step, lignin's hydroxyl (-OH) groups react with the isocyanate (-N=C=O) groups of toluene dissocyanate (TDI), forming urethane (-NH-COO-) linkages and a lignin-TDI intermediate [124]. In the second step, additional TDI reacts with remaining hydroxyl (-OH) or newly formed amine (-NH) groups, creating more urethane (-NH-COO-) and urea (-NH-CO-NH-) bonds [124]. This results in a highly crosslinked, three-dimensional polyurethane network with lignin as a bio-based structural component. In literature, lignin-PU (LPU) resins have exhibited a bonding strength and compressive strength ranging from 4.4 MPa to 91.2 MPa and 0.09 MPa to 0.92 MPa (E2, E4, E5, E10).

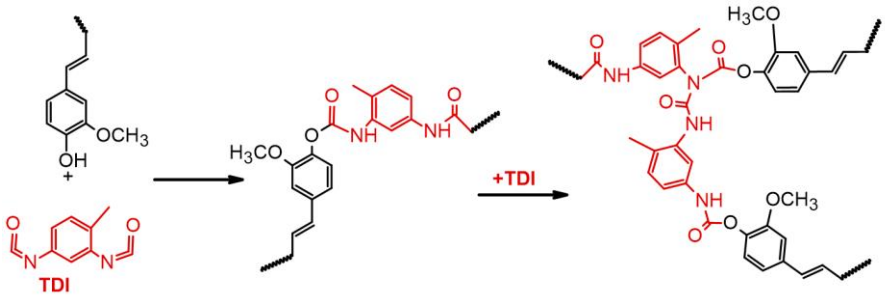

Figure 2-6: Mechanism for lignin-polyurethane resins [124].

The properties of the LPUA can be altered by adjusting the molecular weight of lignin [122]. However, the substitution of lignin is currently limited due to lignin's poor solubility in polyol systems, high molecular weight and low hydroxyl group content that can decrease LPUA's strength [123]. Additionally, the lower nucleophilicity of phenols with respect to aliphatic alcohols diminish its reactivity with isocyanate monomers [121].

Similar to the incorporation lignin in formaldehyde containing resins, modifications have been conducted to improve lignin's performance in polyurethane, such as demethylation, depolymerization, and oxypropylation (Table 2-6). Demethylation and depolymerization were performed to decrease the

molecular weight of lignin along with increasing its solubility and the hydroxy content, while oxypropylation increased aliphatic hydroxyl content. For example, the demethylation of lignin was conducted to produce a lignin-PU adhesive (LPUA) (E10). It was observed that the LPUA contained an increase in glass transition temperature, bonding strength, young's modulus, and elongation at break compared to PU [124]. The bonding strength increased by 66% and 39% with a lignin substitution of 20% and 25%, respectively [124]. This improvement is attributed to the following reasons: (1) demethylation converts unreactive methoxy into hydroxy; (2) demethylation would produce more reactive sites in ortho position, which could react with TDI; (3) more reactive sites would result in an increased crosslink density and rigidity in polyurethane adhesives; and (4) lignin copolymerizing with PU, forming a large number of covalent bonds, rather than acting as a filler [124].

In a similar work, Xu et al. produced a heat resistant, UV-curing polyurethane/polysiloxane pressure sensitive adhesive by grafting 6-bromo-1-hexene onto demethylated bamboo lignin (E7). LPUAs were produced with the modified lignin at different lignin substitutions. It was seen that the lap shear strength increased with the substitution of lignin. With a 40% lignin substitution, the bonding strength increased by 321% [125]. A bio-based PUA was developed using depolymerized lignin via solvolysis reaction in acid catalysis in the presence of diethylene glycol (DEG) (E2). All of depolymerized lignin incorporated resins exhibited lower bonding strength than their unmodified lignin counter parts. This decrease in performance was explained due to the unreacted DEG from the glycolysis product, which induced plasticizing effect on the resulting crosslinked polymeric structure of the LPUA adhesive [126]. Also, a lignin-PU foam adhesive was developed using depolymerized lignin or a combination of both depolymerized and oxypropylated (50/50) kraft lignin (E6). It was observed that, with 50% depolymerized lignin substitution, the compression strength increased by 113%. However, when a combination of 50% depolymerized lignin and 50% oxypropylated lignin was used, an increase of 409% was seen in the compression strength [115]. The significant improvement in performance with oxypropylation was attributed to the fact that oxypropylation would convert all phenolic hydroxy to aliphatic hydroxy, which would transform lignin into a highly branched and functional polyol [115]. Lignin nanoparticles have also been investigated for PU resins (E12, E13, E14). No clear trend was identified. Typically, the optimum amount of lignin nanoparticles is seen to be 5 wt% in this application. Wu et al. produced a LPU film with an increase in tensile strength of 222% when 5 wt% of lignin was substituted (E12).

While modified lignin-based polyurethane (LPU) resins would offer several environmental and performance benefits, they have some shortcomings. For example, the quality of lignin can vary, leading to inconsistencies in the final resin properties [127]. Lignin's lower reactivity compared to traditional polyols can affect resin's curing and mechanical properties [128]. The modification process to improve reactivity and compatibility with isocyanates can be complex and costly [128]. Limited solubility in common solvents poses formulation challenges. Additionally, these resins can sometimes exhibit brittleness, limiting their use in flexible applications [129].

Table 2-6: Studies on lignin-polyurethane adhesives.

Modification	Lignin Type	Reagent	Conditions	Lignin Substitution, %	Application	Resin synthesis,	Curing Conditions	Bonding Strength, MPa	Bonding strength percent difference, %	Symbol	References
Depolymerization	Pinus radiata	Hydrogenolysis, enzymatic mild acidolysis	3.45 MPa, 195°C, 2-24hr	----	Resin	-----	----	-----	----	E1	[130]
	Broadleaf sawdust	Solvolysis	160°C, 4hr	20	Resin	A: lignin + PETOL 46-3MB B: PETOL 250-2 + MDI • Mix A +B	----	4.4	-31	E2	[131]
	Corncob	Hydrolysis	280°C, 15min	----	Resin	-----	----	-----	----	E3	[113]
	Sodium lignosulfonate	Hydrolysis	170°C, 2hr	20, 30	Foam	• Mix lignin, polyols, water, catalyst, surfactant • Add PMDI curing agent, 10-15 sec	• 25°C, 24hr • 80°C, 72hr	DLPU-20: 0.90[a] DLPU-30: 0.84[a]	-44 -48	E4	[129]
	Hydrolysis	Hydrothermal	250°C, 1hr, 2-3Mpa	30, 50	Foam	• Mix polyols, lignin, glycerol, acetone, catalyst, surfactant, and water, 60sec	• Add pMDI, 25°C, 24-48hr	DLPU-30: 0.16[a] DLPU-50: 0.09[a]	-69 -83	E5	[114]
	Kraft	Hydrolysis	250°C, 2hr	50	Foam	• Mix polyols, lignin, glycerol, acetone, catalyst, surfactant, and water, 12sec	• Add pMDI, 25°C, 24-48hr	0.216[a]	113	E6	[114]
Demethylation	Bamboo	HBr	115°C, 20hr	10, 20, 30, 40	Resin	• Mix PGG, PDMS, DBTDL and IPDI, 50°C, 1hr • Add HEMA, 50°C, 2hr • Add lignin + photoinitiator, 25°C, 30min	• 70°C, 10min • UV (108 mJ/cm^2), 60sec	DLPU-40: 0.082	321	E7	[132]
	softwood	HBr	115°C, 20hr	34	Foam	• Mix lignin with TDI, 75°C, 5min • Add PEG 200, 75°C, mix 5min	• 75°C, 2hr	0.34[a]	942	E8	[116]
	Organosolv	Indium triflate + microwave radiation	275°C, 4hr	----	Resin	-----	----	-----	----	E9	[133]
	Acetic acid	HBr	125°C, 20hr	10, 15, 20, 25	Resin	• Mix lignin with TDI, 25°C, 5min	• Add PEG, 25°C, 2hr	DLPU-20: 91.21 DLPU-25: 76.35	66 39	E10	[124]
Oxypropylation	Demethylated kraft	Propylene oxide	150°C, until pressure stabilizes	50, 100	Foam	• Mix polyols, lignin, glycerol, acetone, catalyst, surfactant, and water, 12sec	• Add pMDI, 25°C, 24-48hr	DLPU-50: 0.22[a] ODLPU-50: 0.52[a]	113 409	E6	[114]
	Kraft	Propylene oxide	150°C, until pressure stabilizes	10, 30, 60, 100	Resin	• Mix polyols, lignin, catalyst, and surfactant, 1min	• Add MDI and blowing agent, 25°C, 48hr	OLPU-30: 0.11[a] OLPU-60: 0.10[a] OLPU-100: 0.14[a]	10 0 40	E11	[118]

Nanoparticles	Kraft	γ-valerolactone (GVL)	Ultrasonic, 30min	0.5, 1, 3, 5, 10	Film	• Polyol+ IPDI, 85°C, 1hr • Add 1,4-butanediol, 3hr • Add triethylamine, 60°C, 30min	• Add lignin, mix 2hr • 120°C, 2hr	NLPU-0.5: 19.87 NLPU-1: 29.30 NLPU-3: 48.80 NLPU-5: 59.67 NLPU-10: 53.42	7 58 163 222 188	E12	[134]
	Bamboo acetic acid	DMF	Ultrasonic, 1hr	5, 10, 15	Film	• Polyol, DMF, DBTDL, DMF, 60°C, 4hr • Add lignin + DMF, 80°C, 8hr	• Air dry 60°C, 8hrs • Vacuum oven, 80°C, 8hr	NLPU-5: 55.24 NLPU-10: 50.58 NLPU-15: 47.35	13 3 -3	E13	[135]
	Enzymatic hydrolysis	DMF/H_2O	5hr	0.5, 1, 2, 5	Films	• Polyol, DMPA, 80°C, • Add IPDI + catalyst + acetone, 3hrs • Add 1,4-butanediol, 40min • 40°C, add neutralizing agent	• 25°C until dry	NLPU-0.5: 14.33 NLPU-1: 14.83 NLPU-2: 22.84 NLPU-5: 29.65	-33 -31 7 38	E14	[136]

a: Compression strength

2.3.6 Lignin-Polyethyleneimine Adhesive (LPEIA)

Marine adhesive proteins (MAPs) are strong and water-resistant adhesive produced by marine mussels to stick to rocks and other substances in the seawater in order to withstand the impact of turbulent tides and waves [137]. MAPs are a prime example of formaldehyde-free and renewable adhesives. MAPs are composed of two key functional groups: an amino and catechol group [3]. Various reactions between the amino and catechol groups solidify and crosslink MAP forming a very strong and highly water-resistant adhesive [137]. However, MAP is not readily available for the market.

Polyethyleneimine (PEI) is a synthetic version of MAP, which is created through the acid-catalyzed polymerization of aziridine [138]. PEI is a water-soluble polyamine whose molecular chain possesses a great quantity of primary, secondary, and tertiary amines, which have strong protophilic properties and can form strong hydrogen bonds with proton donor [139]. Polyethyleneimine (PEI) resin is used as an adhesive for polyvinyl chloride (PVC) solution and epoxy resin crosslinker [140]. It also functions as a laminate anchor coating agent for paper, cloth, oriented polypropylene (OPP) film, and polyethylene terephthalate (PET) film, as well as a heavy metal chelating agent, metal plating additive, foam retainer in fire extinguishers, ink adhesion enhancer, and coagulant in water treatment [140]. Polyethyleneimine (PEI) has high reactivity with cellulose, making it useful in paper and textile applications [139]. Its molecular weight variability allows control over ductility, rigidity, and thermal stability, while also enabling formaldehyde-free formulations [141]. The cationic nature enhances adhesion to negatively charged surfaces, and its water solubility ensures easy processing [137]. Once cured, PEI resin exhibits good strength and excellent water resistance for durable applications [142]. PEI resin has limitations, including sensitivity to hydrolysis, leading to reduced durability in humid conditions [137]. It has limited thermal stability, brittleness after curing, and high chemical reactivity, which can cause unwanted side reactions [137], [141]. Its high viscosity complicates processing, while its relatively high cost may limit widespread use [137], [141]. Aesthetic concerns, like yellowing, and health risks, such as skin and respiratory irritation, require careful handling [137], [141]. Environmental concerns arise from production and disposal, and compatibility issues may restrict adhesion to certain surfaces [137], [141]. Additionally, PEI may degrade over time in storage and has limited long-term water resistance compared to synthetic resin adhesives [141].

Lignin, which contains phenolic hydroxyl groups, can be expected to produce an environmentally friendly adhesive, which mimics MAP when blended with PEI [3]. The mechanism for lignin-PEI adhesive can be seen in Figure 2-7. It should be noted that the mechanism between lignin and PEI is not completely understood. Initially, lignin undergoes demethylation, exposing catechol moieties that are prone to oxidation at elevated temperatures (140°C) [143]. This oxidation leads to the formation of quinones, which then react with PEI's amino groups to form Schiff bases [143]. Additionally, Michael addition reactions between quinones and PEI further contribute to crosslinking [143]. Strong hydrogen bonding also occurs between PEI, lignin, and wood hydroxyl groups, enhancing adhesion [143]. These reactions collectively lead to a highly crosslinked, water-resistant adhesive network.

In order to improve the reactivity of lignin, several modifications have been incorporated when producing lignin-PEI adhesive (LPEIA), such as, demethylation, oxidation, and reduction [23], [137], [142], [144]. A summary of LPEI adhesives can be found in Table 2-7. A lignin-PEI adhesive (LPEIA) was developed using poplar wood lignocellulose with a glutaraldehyde enhancer, achieving 95 wt% lignin (F1). The enhancer significantly improved bonding strength by 2,957%, compared to a 986% increase with neat lignin-PEI adhesive [139]. Demethylated brown-rot-fungus lignin was used to develop a LPEIA (F4). The reduction of demethylated lignin increased the bonding strength of the adhesive by 180% [144]. The optimum $NaBH_4$ dosage was found to be 1% (wt%). The reduction time was found to affect the bonding strength significantly with extended reactions being preferred.

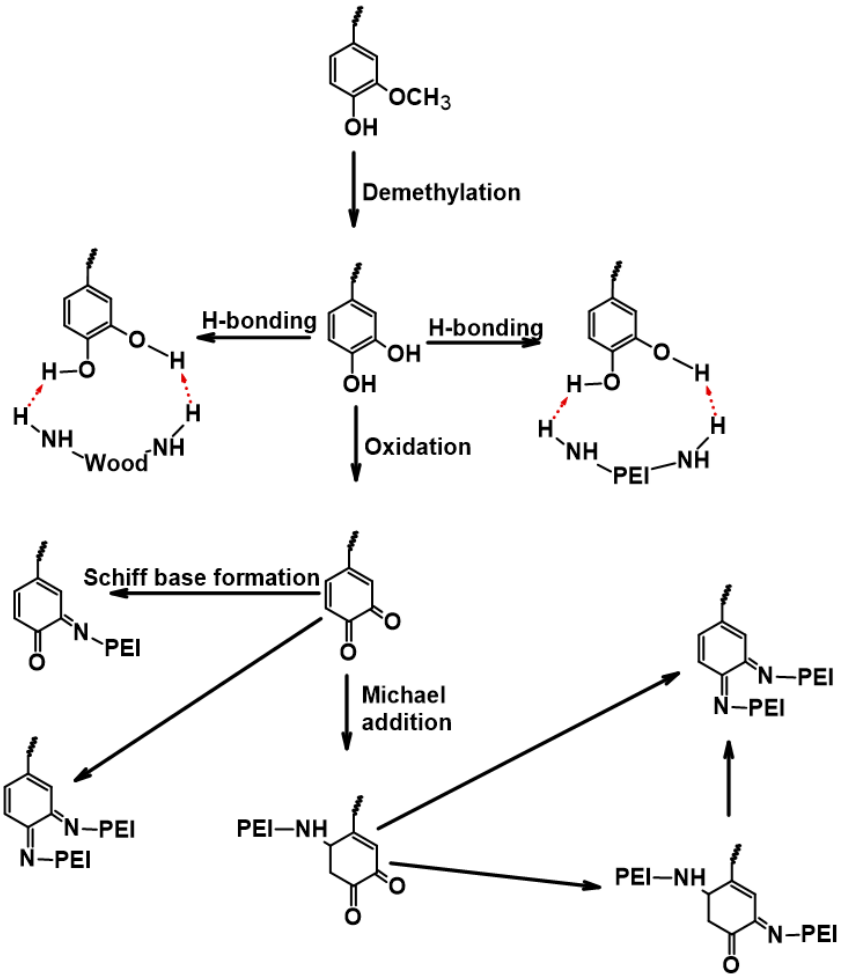

Figure 2-7: Mechanism for lignin-polyethyleneimine resins [143].

Table 2-7:Studies on lignin-PEI adhesives.

Modification	Lignin Type	Reagent	Conditions	Lignin Substitution, %	Application	Resin synthesis, F/P, mol/mol	Hot press Conditions	Bonding Strength, MPa	Bonding strength percent difference, %	Symbol	References
Raw	Poplar wood lignocellulose	----	----	95 + glutaraldehyde	Resin- adhesive	• Mix PEI + water • Add lignin • Add glutaraldehyde	180°C, 2.5MPa, 10min	LPEI: 0.76 LPEI-Glu: 2.14	986 2,957	F1	[139]
	Kraft	----	----	33, 50, 67, 75, 80	Resin- plywood	Mix PEI + lignin, 10-180min	100°C, 120°C, **140°C**, 160°C, 1.91MPa, 2, 4 ,6, 8, **9** ,12min	LPEI-33: 3.41 LPEI-50: 3.39 LPEI-67: 4.85 LPEI-75: 3.50 LPEI-80: 3.28	209 208 340 217 197	F2	[141]
Demethylation	Demethylated kraft (purchased)	----	----	20, 33, 50, 67, 80	Resin- plywood	• Mix lignin + water+ NaOH (pH 10) • Add PEI + water, 10min	41.6 g/m^2 100°C, **120°C**, 140°C, 1.91MPa, 3, **5**, 12min	LPEI-20: 3.84 LPEI-33: 4.55 LPEI-50: 7.06 LPEI-67: 5.59 LPEI-80: 2.45	36 61 150 98 -13	F3	[137]
	Brown rot fungus	Brown rot fungus, NaBH4	70°C, 2hr 25°C, 1hr	17	Resin- plywood	Mix lignin+ PEI, 25°C, 60min	120°C, 1.9MPa, 5min	4.98 + PEI	-11	F4	[144]
Oxidization	Wheat straw soda	Sodium periodate	25°C, 1hr	20, 25, 33, 50, 67, 75, 80 100	Resin- particleboard	Mix lignin + NaOH + PEI, 1hr	130°C, 140°C, 150°C, 160°C, 170°C, **180°C**, 190°C 4, 7, 10, **13**, 16min 5MPa	LPEI-20: 0.82 LPEI-25: 0.99 LPEI-33: 1.20 LPEI-100: 0.80	371 468 587 361	F5	[142]
	lignosulfonate	Sodium periodate	60°C, 0.5hr	50, 75, 83, 87.5, 90	Resin- Fiberboard	Mix lignin + water + PEI, 30min	150°C, 160°C, **170°C**, 180°C, 190°C 3, 5, **7**, 11min 4-10MPa (until thickness is 5mm)	LPEI-50: 0.83 LPEI-75: 0.72 LPEI-83: 1.02 LPEI-87.5: 1.19 LPEI-90: 0.59	----	F6	[23]
nanoparticles	Hardwood soda (hydrolyzed and ammoxidized)	----	----	50	Resin- wood plastic composite (polypropylene)	Mix lignin, water, NaOH and PEI, 15min	Extrusion, 175°C, 5min Mold cure 120°C, 60MPa	NLPEI-H: 38.5 NLPEI-A: 39.8	47 52	F7	[145]

This increase of bonding strength is most likely due to the reduction of ortho-quinones into catechol moieties, which then further react with the amino groups of the PEI in the same way as MAP [144]. Peng et al. developed a lignin-PEI adhesive using oxidized wheat straw lignin (F5). When the PEI content exceeded the lignin content, bonding strength and modulus of elasticity were higher, but water resistance was lower compared to ratios with more lignin than PEI [142]. Optimum was found to be 50 wt% lignin, in which the bonding strength and water-resistance both increased when compared to only lignin and only PEI systems. This suggests that oxidized lignin and PEI were able to create a tight crosslinking between wood shavings, forming a three-dimensional network polymer with a physicochemical reaction [142]. Effect of temperature and time in the curing process has been examined in the literature (F2, F3, F5, F6). The strength of lignin-PEI adhesives increased with temperature, but the optimal range varied depending on the material and adhesive type. While higher temperatures enhanced bonding, excessive heat led to adhesive degradation and reduced strength. Similarly, longer curing durations improved the strength, but over-curing offered no additional benefits and might even cause degradation [23], [137], [141], [142]. Identifying the right balance of temperature and curing time is crucial for maximizing adhesive performance. In another work, LPEI was developed with incorporating 33-80 wt% kraft lignin, and the optimal performance observed at 67 wt% lignin, where bonding strength increased by 340% (F2). In this case, increasing curing temperature and time improved performance, but excessive conditions led to adhesive degradation. In another work, oxidized ammonium lignosulfonate and PEI used to produce a binder for fiberboards (F6). In this case, a 7:1 lignin:PEI mol ratio produced the adhesive with the highest bonding strength [23]. The bonding strength and water resistance increased by 200% and 34%, respectively, with incorporation of oxidized lignin [23]. Increasing the hot-pressing temperature to 170 °C and extending the time to 7 minutes enhanced mechanical performance but further increases led to degradation. Hydrolyzed and ammoxidized lignin was used to formulate a LPEIA, which saw an increase in bonding strength of 51%, as well as a decrease in its wettability[145]. Lignin nanoparticles have also been incorporated into LPEIAs (F7).

Lignin-PEI adhesives face several challenges, including a slow reaction rate at room temperature, requiring prolonged mixing times, and high curing demands of 140°C for up to 9 minutes, increasing energy costs [137]. Their performance depends on lignin quality, with variations in source and purity affecting adhesion [137]. Limited long-term data raises concerns about stability, while high-quality lignin extraction remains costly [137], [141]. Processing complexities include precise pH control, potential odor issues, and scalability challenges [137], [141]. Adhesive properties vary based on formulation, with potential limitations in thermal resistance, elasticity, and durability [141]. Additionally, limited shelf life and aesthetic concerns, such as odor and cured color, may affect the usability of lignin incorporated LPEIA [137], [141].

2.4 Bio-based Adhesive

2.4.1 Lignin-Tannin Adhesive (LTA)

Tannins are naturally occurring polyphenols, which are extracted from the bark, roots, fruits, and leaves of several plants. Up until the mid 2000's, tannins were used to replace phenol in PF adhesives due to their polyphenolic structures. Tannins have demonstrated higher reactivity with formaldehyde compared to phenol [146]. Tannin adhesives are usually synthesized using various hardeners, such as paraformaldehyde, glyoxal and hexamine [146]. The world-wide consumption of tannin was 1.4 million tons in 2020, with an estimated growth to 2 million by 2027 [147].

Tannin resins are widely used in plywood, particle board, wood composites, and laminating veneer, as well as for wood preservation and impregnated resins [148-149]. They also play a role in finger joints and have

applications beyond wood, including use on steel, fiber, and paper [148-149]. Additionally, they are utilized for mercury (II) absorption and uranium recovery, demonstrating their versatility in both industrial and environmental applications [150-151]. These resins are environmentally friendly and offer antibacterial, antiviral, and UV-resistant properties. They also exhibit high tensile strength, excellent deformation properties, good thermal stability, with strong adhesion, making them highly durable and versatile [152], [153]. Additionally, condensed tannins or proanthocyanidines, are repeating units of flavan-3-ol, consisting of A and B type rings, which attributes its adhesive and antioxidant properties [146]. In literature tannin resins have been reported to have a bonding strength ranging from 0.31 MPa to 63.16 MPa (F3, F7).

While tannin resins offer several environmental and performance benefits, they have some shortcomings. Tannin resins do not posses the bonding strength and water resistance that is demonstrated by synthetic adhesives [143]. The quality of tannin can vary, leading to inconsistencies in the final resin properties. Tannins have lower reactivity compared to synthetic resins, affecting curing and mechanical properties [152]. The modification processes to improve reactivity and compatibility can be complex and costly. Additionally, tannins have limited solubility in common solvents and can sometimes exhibit brittleness, limiting their use in flexible applications [152]. Despite being renewable, the chemical processes used to modify tannins can involve hazardous substances and generate waste [152].

In the literature, lignin was used in tannin-based resins. The mechanism for lignin-tannin resins can seen in Figure 2-8. In the first step, tannin reacts with hexamine, forming a tannin-hexamine complex where amine (-NH) groups are introduced (Figure 2-8a), enhancing its reactivity. In the second step, lignin is modified using glyoxal, introducing hydroxyl (-OH) groups to increase its reactivity (Figure 2-8b). Finally, the tannin-hexamine complex reacts with glyoxal-modified lignin through amine (-NH) linkages, forming a highly crosslinked tannin-lignin network. This structure improves adhesive strength and durability through covalent and hydrogen bonding.

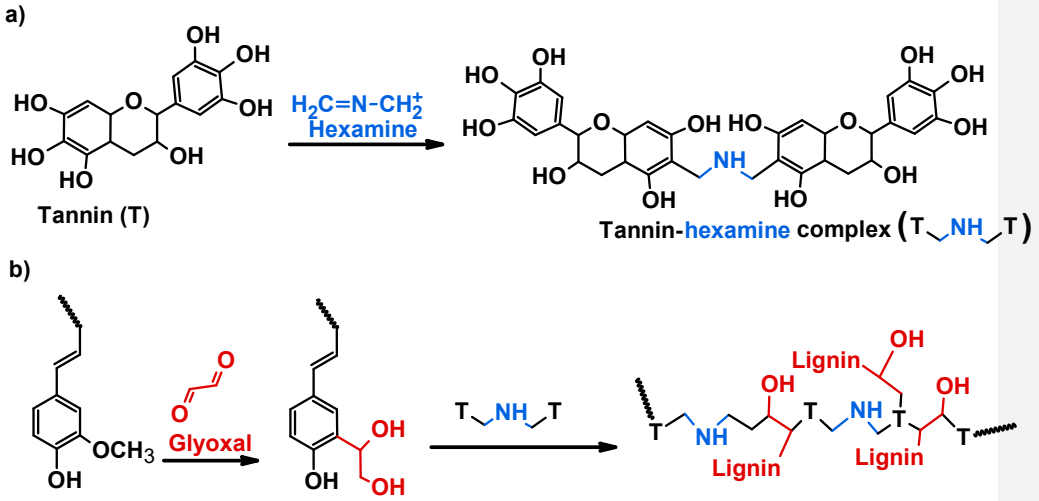

Figure 2-8: Mechanism for lignin-tannin resins [146].

Many efforts have been made to prepare lignin-tannin adhesives in order to improve its performance. A summary of all the LTAs can be found in Table 2-8. Typically, lignin is activated through glyoxalation before being mixed with tannin and a hardener (G1, G2 G3, G4, G5, G6, G7, G8 in Table 2-8). Glyoxal is used because it is a natural resource-based aldehyde that is obtained as a by-product from biological processes and lipid oxidation [24], [146]. In one study, a formaldehyde free adhesive was synthesized using glyoxalated lignin, glyoxalated tannin or a combination of both (G6). It was seen that the adhesive prepared with both glyoxalated tannin and glyoxalated lignin had improved thermal stability when compared to the control samples (raw lignin, raw tannin) [146]. This was attributed to an extended crosslinking as a result of the improved reactivity of modified lignin and tannin. In one study, Faris et al. developed a lignin-tannin adhesive modified with polyethylenimine (PEI) (G7), observing that increasing PEI content (0-12% w/w) led to a rise in solid content and tensile strength from 31% and 32 MPa to 57% and 62 MPa, respectively [143]. Water resistance was also improved with higher PEI levels, likely due to enhanced reactions between the amino groups in PEI and the catechol moieties in lignin and tannin, resulting in increased crosslinking and, consequently, greater tensile strength and water resistance [143]. Sarazin et al. produced lignin-tannin adhesive (LTA) using oxypropylated, glycidolated or unmodified, kraft and organosolv lignin (G9). The bonding strength of oxypropylated, unmodified, and water-soluble kraft lignin samples were all very similar and significantly higher than that of glycidolated kraft lignin and all of the organosolv samples [154]. Various LTAs were produced using unmodified lignin at various substitutions. No change in bonding strength was observed with lignin substitution beyond 10%. For samples with more than 10% lignin, the bonding strength threshold of 10 N/m^2 was not reached [154]. However, all samples, including those exceeding 10% lignin, remained within 10% of this threshold, suggesting that optimization could potentially achieve the required threshold.

Modified lignin tannin resins, while offering environmental benefits and potential cost savings, face several challenges. They often exhibit low reactivity, leading to longer curing times and reduced efficiency [154]. High viscosity can complicate processing and handling [24]. The mechanical properties of these resins may not always match those of traditional resins [155]. Variability in lignin sources and extraction processes can also result in inconsistencies in resin quality and performance. Additionally, if formaldehyde is used in resin synthesis, there can be concerns about formaldehyde emissions.

Table 2-8: Studies on lignin-tannin adhesives.

Modification	Lignin Type	Reagent	Conditions	Lignin Substitution, %	Application	Resin synthesis,	Curing conditions	Bonding Strength, MPa	Bonding strength percent difference, %	Symbol	References
Glyoxalation	Organosolv	Glyoxal	65°C, 8hr	10, 20, 30, 40, 50	Resin-particleboard	• Lignin, water, NaOH, pH 12-12.5, 65°C, 30min • Add glyoxal, 65°C, 8hr • Mix with tannin/hexamine solution (pH 10)	195°C, 0.36kPa	GLT-10: 0.81 GLT-20: 0.77 GLT-30: 0.75 GLT-40: 0.72 GLT-50: 0.45	16 10 7 3 -36	G1	[155]
	Hardwood & softwood kraft	Glyoxal	----	40	Resin-particleboard	• Tannin, water, NaOH, pH 10.4 • Add hexamine and lignin	195°C, 2.75MPa, 7.5min	3436 [a]	----	G2	[156]
	Wood, acetic-acid wheat straw	Glyoxal	58°C, 8hr	55, 60	Resin-particleboard	• Lignin, tannin, pH 11.5-12 • Add pMDI	195°C, 2.5MPa, 7.5min	GLT-55: 0.36 GLT-60: 0.	----	G3	[157]
	Organosolv	Glyoxal	58°C, 8hr	40, 50	Resin-particleboard	• Tannin + NaOH, pH 10 • Add hexamine and lignin	195°C, 3.5MPa, 7.5min	GLT-40: 0.33 GLT-50: 0.41	----	G4	[158]
	Organosolv	Glyoxal	58°C, 8hr	40, 50	Resin-particleboard	• Tannin + hexamine, ligin	195°C, 7.5min total • 3.43MPa • 1.18MPa • 0.69MPa	GLT-40: 0.43 GLT-50: 0.39	----	G5	[24]
	Organosolv	Glyoxal	75°C, 8hr	40, 100	Resin	Tannin + hexamine, ligin	100°C, 150°C, 200°C	----	----	G6	[146]
	Oil palm empty fruit bunch	Glyoxal	60°C, 8hr	40 + 10-20% PEI	Resin-plywood	• Tannin + NaOH, pH 10 • Add hexamine, lignin • Add PEI	250 g/m^2 140°C, 17.2MPa, 7min	GLT: 31.06 GLT-PEI-10: 35.63 GLT-PEI-16: 47.43 GLT-PEI-20: 63.16	----	G7	[143]
	Sodium lignosulfonate, aluminum lignosulfonate	Glyoxal	58°C, 8hr	40, 50, 60, 80	Resin – wood joints	• Tannin + NaOH, pH 10 • Add hexamine, lignin	----	GLT-40: 2,497[a] GLT-50: 2,294[a] GLT-60: 2,264[a] GLT-80: 1,905[a]	----	G8	[8]
Glycidolated	Kraft, organosolv	Glycidol	----	20, 40, 50, 60, 80, 100	Resin-plywood	• Lignin + Tannin + NaOH, pH 11-12 • Add hexamine	150°C, 1.2MPa, 15min	GLT-KL-50: 8.49 GLT-OL-50: 5.35	-31 -56	G9	[154]
Oxypropylated	Kraft, organosolv	Propylene oxide	----	20, 40, 50, 60, 80, 100	Resin-plywood	• Lignin + Tannin + NaOH, pH 11-12 • Add hexamine	150°C, 1.2MPa, 15min	OLT-KL-50: 4.46 OLT-OL-50: 5.43	-64 -56	G9	[154]

a: Modulus of elasticity (MOE)

2.4.2 Lignin-Soy Protein Adhesive (LSPA)

Soy protein adhesives are another interesting alternative adhesives investigated for the industry. Typically, it is formulated using soy protein isolate and a crosslinking resin. During the period spanning from 1930 to 1960s, soy proteins were used widespread in the wood product industry [159]. Soy protein (SP) is an agricultural biomass resource consisting of complex macromolecules composed of 20 different amino acids with different side chains [3]. These side chains contain functional groups that dictate the amino acid's hydrophobic and hydrophilic nature and offer reactions sites for interactions with wood or crosslinking agents [3]. The world-wide soy production was estimated to be 350 million metric tons in 2022 [160].

Soy protein adhesives are widely used in interior decorative plywood, engineered wood flooring, particleboard, fiberboards, and laminates, offering a sustainable alternative to synthetic adhesives. Beyond wood products, they are also applied in heat-resistant paper coatings, packaging, soundproof flooring, and fiberglass insulation [161-162]. Soy protein isolate (SPI) is a by-product of the soybean oil industry making it an ideal feedstock as it is renewable, inexpensive, highly abundant, with good biodegradability, heat resistance and ease of modification [163-164].

However, its high viscosity, poor mechanical properties and water resistance are the primary obstacle that hinder the use of soy protein-based materials [3, 159, 163-165]. This is attributed to the weak intermolecular interactions, numerous hydrophilic groups (such as -COOH, -NH_2, -OH) and molecular entanglement in the polymer chain [164, 165]. Furthermore, the presence of soy protein, and polysaccharides make it susceptible to the attack of mold, bacteria and fungi, which causes mildew and affect its shelf life and performance [165].

One method of modification of soy protein adhesive systems involves the incorporation of lignin due to its hydrophobic nature. Additionally, the modification of lignin can improve its reactivity by increasing its phenolic and aliphatic hydroxyl content. These hydroxyl groups interact with the amine of the soy proteins to form a dense network structure, which improves the bonding strength, water resistance, and bio-durability of the adhesives [3], [164]. The mechanism for lignin-soy protein resins can be seen in Figure 2-9. First, lignin undergoes carboxymethylation via reaction with sodium chloroacetate in the presence of NaOH, introducing carboxyl (-COOH) groups to enhance its reactivity. The modified lignin then interacts with soy protein through covalent bonding between carboxyl (-COOH) and amine (-NH_2) groups, as well as hydrogen bonding [165]. This crosslinked structure enhances the mechanical properties and water resistance of the resulting lignin-soy protein resin. In the literature, the bonding strength of lignin-soy protein adhesives (LSPA) ranges from 0.41 MPa to 12.7 MPa (G10, G13).

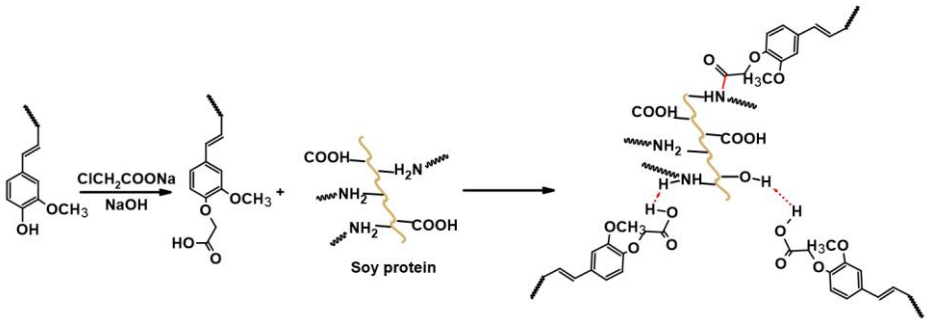

Figure 2-9: Mechanism for lignin-soy protein resin [165].

Various modification methods have been conducted to improve the reactivity of lignin, such as, demethylation, depolymerization, depolymerization by laccase, amination and carboxymethylation (Table 2-9). In one study, soy protein adhesive was produced using kraft lignin (KL) that was first enzymatically demethylated and then reduced with $NaBH_4$ (H10). The demethylated lignin-soy protein adhesive (LSPA) showed no improvement over unmodified lignin, but when reduced demethylated lignin was used, bonding strength increased by 500% [166]. Another type of soy protein adhesive was produced using aminated, and aminated depolymerized lignin (H13). While amination significantly improved bonding strength (by 31%), further depolymerization pretreatment prior to amination reaction led to only a slight 2% increase [9]. After three water-soaking and drying cycles, the shear stress of the lignin-amine adhesive reached 5.0 MPa, surpassing that of phenol-formaldehyde adhesive [9]. A lignin-soy protein adhesive (LSPA) using depolymerized lignin (H7) showed varying bonding performance based on depolymerization conditions. For example, bonding strength increased by 13% at 170°C with 50 wt% lignin substitution, whereas using raw lignin at the same substitution level led to a decrease of 14% [159]. This is because bonding strength increased as depolymerization temperature rose from 140°C to 170°C but declined at higher temperatures due to decomposition of oligomers. The use of enhancers has also been reported in lignin-soybean systems in the literature (H1, H4, H5, H10, H11, H15, H16). Typically, the incorporation of enhancers improves the performance of LSPAs. For example, a LSPA was developed using kraft lignin and various coadjutant polymers (H5). A 47% increase in bonding strength was observed with a 20 wt% lignin substitution and cellulose nanofiber (CNF) [165]. Cao et al. developed a soy protein adhesive modified using dopamine-functionalized hexagonal boron nitride (PDA-BN) and carboxymethylated lignin (CML) (H16). With a 10 wt% lignin substitution, the bonding strength increased by 64%. Additionally, the incorporation of CML and PDA-BN increased water, flame and mildew resistance [165].

The incorporation of SP adhesives with PF resins has been reported in the literature (H3, H4), where an increase in bonding strength was observed. For example, J. Luo et al. formulated an LPF resin with soy protein and corncob lignin, achieving a 200% boost in bonding strength relative to SPA [167]. The incorporation of SP adhesives with epoxy resins has also been observed in the literature (H14, H15). The bonding strength is seen to increase with the incorporation of epoxy. For example, S. Chen, et al. observed an increase in bonding strength of 364% compared to SPA with the incorporation of epoxy (H14).

Modified lignin soy protein adhesives offer several benefits, but they also have some shortcomings that can limit their applications. These adhesives often exhibit weaker bond strength and lower water resistance compared to synthetic adhesives, making them less suitable for high-strength and moisture-prone environments [168]. Additionally, they can be susceptible to mildew in humid conditions, affecting their durability and longevity [168]. The modification process to enhance their properties can be complex and costly, which may not be feasible for all manufacturers. Furthermore, their thermal stability is generally lower than that of some synthetic adhesives, limiting their use in high-temperature applications [168]. These shortcomings highlight the need for ongoing research and development to improve the performance of bio-based adhesives and expand their range of applications.

Table 2-9: Studies on lignin-soy protein adhesives.

Modification	Lignin Type	Reagent	Conditions	Lignin Substitution, %	Application	Resin synthesis	Hot press Conditions	Bonding Strength, MPa	Bonding strength percent difference, %	Symbol	References
Raw	Kraft	----	----	1, 2 + 0.5, 1 PAE	Resin – plywood	SP + lignin + PAE + water, mix 30min	150°C, 2MPa, 10min	LSP-1: 5.7 LSP-2: 4.9 LSP-2-PAE-0.5: 5.8 LSP-2-PAE-1: 5.0	8 -8 9 -6	H1	[169]
	Kraft	----	----	20, 40, 50	Resin – plywood	SP + lignin + water, pH 4.5, mix 2hr	170°C, 2MPa, 10min	LSP-20: 6.4 LSP-40: 5.5 LSP-50: 5.6	19 2 4	H2	[170]
	Corncob	----	----	5, 10, 15, 20, 25 + PF resin (5-25)	Resin – plywood	LPF • Lignin + phenol + F + NaOH, 80°C, 1 hr • F + NaOH, 80°C, 1hr • F + NaOH, 80°C, 1hr SP • Mix SP + water + LPF	180 g/m^2 135°C, 1.2MPa, 70sec/mm	LSP-5: 0.78[a] LSP-10: 1.05[a] LSP-15: 0.91[a]	123 200 160	H3	[167]
	Softwood	----	----	10 + PEA	Resin – plywood	LPF • Lignin + phenol + F + NaOH, 80°C, 1 hr • F + NaOH, 80°C, 1hr SP • Mix SP + water + LPF + PAE	200 g/m^2 130°C, 0.8MPa, 90sec/mm	LSP: 1.32 LSP-PAE: 1.63	35 66	H4	[171]
	Kraft	----	----	20 + coadjutant polymer	Resin – plywood	• Mix NaOH + acetonitrile, 21°C • Add coadjutant polymer then SP, then lignin	155 g/m^2 171°C, 2.4MPa, 10min	LSP: 7.64 LSP-CNF: 12.27	-9 47	H5	[172]
	Sorghum	----	----	10, 20, 30, 40, 50	Resin – plywood	SP + lignin, 25°C, 2hr	170°C, 2MPa, 10min	LSP-10: 5.70 LSP-20: 6.40 LSP-30: 6.12 LSP-50: 5.84	-8 4 -1 -6	H6	[173]
Depolymerization	Kraft	Base-catalyzed	140-200°C, 100-150psi, 3hr	33	Resin – plywood	SP + lignin, 50°C, 1hr	• 25°C, 0.235MPa, 2min • 120°C, 0.101MPa, 30min	1.46	13	H7	[159]
	Alkali	Ultrasound-induced oxidation	50°C, 16hr 20kHz, 480W. 1hr	20	Resin – plywood	• Mix SP + water + lignin, pH 7.2, 1hr • Ad PEGDE, 85°C, 30min	215-237g/m^2, 150°C, 1.03MPa, 10min	DLSP-O: 2.39 DLSP-UO: 2.45	42 46	H8	[174]
Demethylation	Kraft	Laccase enzyme	25°C, 24hr	1	Resin – plywood	• SP + lignin + water, HCl, pH 4.5, 2hr • 21°C	150°C, 1.03MPa, 10min	5.8	-16	H9	[175]

	Hardwood kraft	Laccase enzyme + reduction	25°C, 3hr	50	Resin – plywood	• SP (Chitosan or PEI) + lignin + sodium acetate, ABTS, laccase, 25°C, 3hr	120°C, 2MPa, 15min	DLSP: 0.41 DLSP-R: 1.81	-84 -31	H10	[166]
	Alkali	1-dodecanethiol	130°C, 1.5hr	1, 2, 3, 4 + Cu additive	Resin – plywood	• Mix SP + lignin + water, 25°C, 15min	180g/m^2 120°C, 1MPa, 6min	DLSP-1: 1.77 DLSP-2: 1.91 DLSP-3: 1.88 DLSP-4: 1.84 DLSP-2-Cu: 1.90	5 13 11 9 12	H11	[164]
Amination	Enzymatic hydrolysis	$NaBH_4$	25°C, 20min	14, 23, 32, 42	Resin – plywood	• Mix SP + lignin + water + ESO	200g/m^2 130°C, 1MPa, 6min	ALSP-23: 0.94[a] ALSP-32: 1.07[a] ALSP-42: 0.99[a]	77 102 87	H12	[163]
	Depolymerized hydrolysis	$NaBH_4$	25°C, 20min	1	Resin – plywood	• Mix SP + water + NaOH, 60°C, 2hr • Add lignin, 30min	120°C, 1MPa, 5min	ALSP: 9.02 ADLSP: 7.02	31 2	H13	[9]
Epoxy	Enzymatic hydrolysis	EGDE	30°C, 4hr	41	Resin – plywood	• Mix SP + water+ lignin, 25°C, 20min	200g/m^2 120°C, 1MPa, 7min	1.02[a]	364	H14	[10]
	Enzymatic hydrolysis	EGDE	30°C, 4hr	41 + preservatives	Resin – plywood	• Mix SP + water+ lignin, 25°C, 20min	200g/m^2 120°C, 1MPa, 7min	EPLSP: 1.02[a] EPLSP-P: 0.86[a]	364 291	H15	[176]
Carboxy-methylation + hexagonal boron nitride functionalized	Kraft	Sodium chloroacetate	40°C, 4hr	5, 10, 15	Resin – plywood	• Mix lignin + water, ultrasonic, 2hr, 200W • Add SP + CAL, 5min • Add TGA, 10min	200g/m^2 120°C, 1MPa, 6min	SPI-BN: 1.76 CLSP-5-BN: 1.75 CLSP-10-BN: 2.07 CLSP-15-BN: 1.45	40 39 64 15	H16	[165]

a: wet strength

2.4.3 Lignin-Furfural Adhesive (LFA)

Furfural based resins are polymers derived primarily from furfural. Furfural is a naturally occurring compound produced through sugar dehydration and present in various agricultural byproducts. Hemicellulose, a key component of biomass, can be transformed into different furan-based chemicals, including furfural and furfuryl alcohol [177]. Due to its high reactivity, furfural exhibits similar reactions to other aldehydes and aromatic compounds [3], [178]. In 2022, the global market of furfural was estimated to be 365 thousand metric tons in 2022, with an estimated grown to 505 thousand metric ton by 2023 [179]. Furfural resins are widely used in both the materials and food industries. They serve as lubricating oils, binders in abrasive wheels, and wood adhesives [180], [181]. Additionally, they are integral in the production of PF resins, binders for refractory materials, rubber adhesion, moisture-cure adhesives, coatings, and laminates [182-185].

Furfural resins are known for their high resistance to acids and alkalis, making them suitable for applications requiring chemical durability [186]. They also exhibit good thermal stability, with continuous use at temperatures up to 120°C, and some grades can withstand up to 150°C [187]. With its unsaturated double bond, oxygen ether bond, diene, and aldehyde functional groups, furfural possesses high chemical activity along with excellent heat and water resistance [188]. Additionally, these resins are characterized by low flammability and minimal smoke emission, enhancing safety in various industrial applications [187]. They also offer good bonding strength, making them effective in adhesive and composite applications [189].

Furfural-based resins have several shortcomings that impact their usability. These resins can become brittle after curing, compromising their performance in flexible applications. Health hazards are also a concern, as furfural can irritate the skin and mucous membranes, potentially causing dermatitis or eczema [190]. Additionally, furfural is classified as a Category 3 carcinogen [191]. Environmental issues also arise from the production and use of furfural resins, particularly regarding waste management and emissions [192]. Furthermore, processing challenges exist, as furfural resins can degrade under prolonged acidic conditions, reducing yield and efficiency during production [193].

In theory, lignin could serve as a substitute for phenol, while furfural could replace formaldehyde. The mechanism for lignin-furfural resins can be seen in Figure 2-10. Under acidic conditions, lignin undergoes activation as electron density increases at the C2 and C6 positions due to inductive and resonance effects, making these sites highly reactive to electrophilic substitution [7]. In the next step, furfural, acting as an electrophile, reacts with these activated positions, leading to condensation and crosslinking [7]. This results in the formation of a lignin-furfural resin, though competing depolymerization and repolymerization reactions may also take place [7]. It is important to note that the lignin-furfural mechanism is not yet fully understood and requires further research. In literature, lignin furfural adhesives (LFA) have demonstrated a bonding strength from 0.24 MPa to 153 MPa (H7, H8).

Various types of lignin have been investigated in the development of a LFAs, such as, enzymatic hydrolysis, hydrolysis, softwood kraft, bagasse, sugar maple and plasticized lignin, which are all summarized in Table 2-10. The incorporation of furfural into PF resins has been examined by various researchers (I3, I4, I5, I8). Typically, it is seen that the bonding strength decreases with the incorporation of furfural. For example, a lignin-PF resins was synthesized using kraft lignin with various amounts of furfural (I4). As more furfural (0-30 wt%) was added to the system, the bonding strength decreased while free formaldehyde content increased [188]. The optimum amount of furfural in the lignin-furfural PF resin was found to be 15 wt% [188]. Oxidized lignin was used to develop a lignin-PF resin (I8). An increase in bonding strength of 7% was achieved with 15 wt% lignin [50].

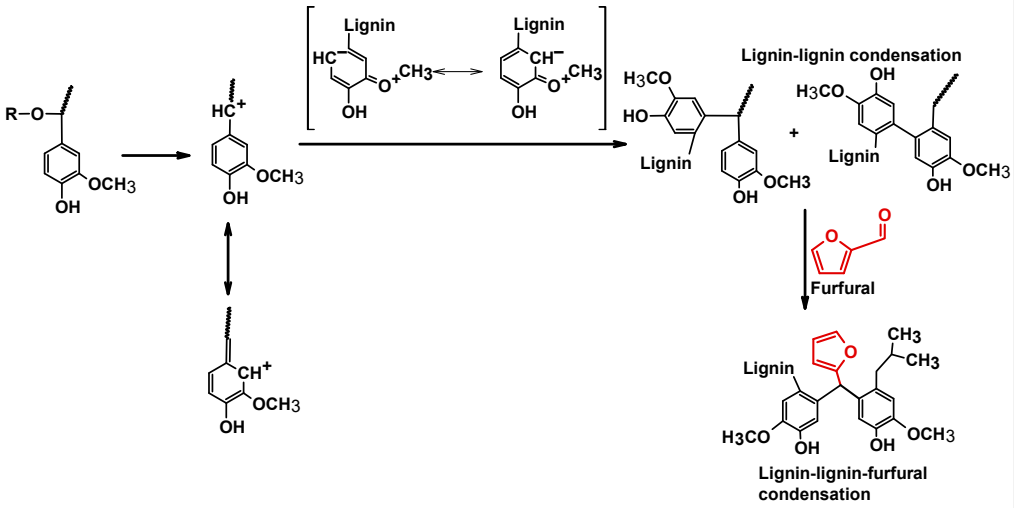

Figure 2-10: Mechanism for lignin-furfural resin [7].

Commented [PF7]: Move the lignin strcutre from the top to bottm in the second step to make use of space in the figure better

A lignin-furfural adhesive (LFA) was developed using phenolated depolymerized hydrolysis lignin (I6). With 50 wt% lignin, the bonding strength decreased by 18% and the resin required higher curing temperatures and longer times [178]. The thermal stability also increased being stable until 315°C (in air or N_2) when compared to phenol furfural adhesives [178]. In another work, lignin modified using a low transition temperature mixture (LTTM) was used to synthesize a lignin-phenol-furfural resin (I7). When the substitution of lignin was 50 wt%, the bonding strength decreased by 17% [189]. At this substitution level, the bonding strength was much greater than the Chinese national standard (0.7 MPa), however, the free aldehyde emission of 0.39% was slightly higher than the 0.30% of the Chinese national standard [189].

Modified lignin-furfural resins exhibit inferior mechanical properties compared to conventional phenol-formaldehyde resins, limiting their use in demanding applications [7]. The curing process increases brittleness, reducing flexibility and durability. Additionally, the high molecular weight and low reactivity of lignin would lead to longer curing times and higher temperatures during synthesis [7]. While lignin and furfuryl alcohol are sustainable, second-generation products from agricultural or paper industries, these raw materials are not ideal for resin fabrication compared to specialized polymers derived from synthetic routes, which are specifically engineered to meet specific performance criteria [194].

Table 2-10: Studies on lignin-furfural adhesives.

Modification	Lignin Type	Reagent	Conditions	Lignin Substitution, %	Application	Resin synthesis,	Hot press Conditions	Bonding Strength, MPa	Bonding strength percent difference, %	Free formaldehyde content [a], %	Symbol	References
Raw	Plasticized	----	----	20, 30	Resin	FF/MA: 50 • Add mix lignin + FF + MA, 110°C, 30min	160°C, 1.2MPa, 2hr	----	----	----	I1	[194]
	Softwood kraft	----	----	30	Resin	Lignin + FF + water + acid, 50°C, 60min	----	----	----	----	I2	[177]
	Sugar cane bagasse	Sodium periodate	25°C, 25min	100	Resin- mold	• Phenol + F + NaOH, 70°C, 1hr • Add resorcinol and lignin, 50°C, 30min	• 75°C, 2.5ton, 1hr • 85°C, 5ton, 30min • 95°C, 7.5ton, 30min • 105°C, 7.5ton, 30min • 115°C, 10ton, 30min	153	-31	----	I3	[195]
	Kraft	----	----	50 + 5, 10, 15, 20, 30 furfural substitution	Resin-plywood	F/P: 1.6 • 80°C, 180min+NaOH • 90°C, 50min, 70%F • 40min, 30%F + FF	250g/m^2 140°C, 17MPa, 4min	LFF-10: 1.19 LFF-15: 1.30 LFF-20: 1.11 LFF-30: 1.01	-6 2 -13 -20	0.21 0.24 0.47 0.71	I4	[188]
	Sugar maple acid hydrolyzed	----	----	5, 8, 16 furfural substitution	Resin-adhesive reinforced glass fibers	0, 5, 8, 16% FF • 90°C, 60min	250g/m^2 150/180°C, 3MPa, 4min	LFF-5: 9.96[b] LFF-8: 9.35[b] LFF-16: 7.33[b]	-11 -16 -34	----	I5	[7]
Depolymerization	Hydrolysis (phenolated)	Patent pending	150-250°C, 30-120min, <250psig	50 + additive	Resin	Mix lignin + FF + glucose + water + catalyst	----	89	-18	----	I6	[178]
Low transition temperature mixtures	Enzymatic hydrolysis	Oxalic acid, choline chloride	100°C, 6hr	20, 40, 50, 60, 80	Resin-plywood	FF/P: 0.8 • Mix P + NaOH, 45°C • Add furfural + urea, 135°C, 2hr	----	LTLFF-20: 2.05 LTLFF-40: 1.92 LTLFF-50: 1.84 LTLFF-60: 1.64 LTLFF-80: 0.98	-7 -13 -17 -26 -56	0.30[a] 0.33[a] 0.39[a] 0.45[a] 0.53[a]	I7	[189]
Oxidation	Bagasse	ClO_2, acetic acid	55°C	15	Resin- mold	F/P: 1.37 KOH/P: 0.06 • Mix P + F +KOH 70°C, 60min • Mix lignin + FF	250-300g/m^2 130°C, 1MPa, 7min	OLFF: 0.24	7	----	I8	[50]

a: free aldehyde content, b: N/(m*g)

2.5 Best sustainable lignin incorporated lignin and future directions

The best formulations, demonstrating the highest improvement in performance was achieved for LPFA with alkali lignin nanoparticles, which achieved a 64% increase in bonding strength (1.59 MPa) at 30 wt% lignin with a urea enhancer (A18). LUFA with glyoxalated Bagasse soda black liquor lignin saw a remarkable 295% increase (1.7 MPa) at 15 wt% lignin using an epoxy enhancer, eliminating formaldehyde (B5). LMFA with hydroxymethylated alkali lignin improved by 47% (1.34 MPa) at 6 wt% lignin with a urea enhancer (C2). LEPA with depolymerized reed magnesium bisulfite lignin showed a significant 228% increase (10.42 MPa) at 17 wt% lignin with T-31 as an enhancer (D12). LPUA foam with demethylated softwood lignin saw an outstanding 942% increase in compression strength (0.34 MPa) with 34 wt% lignin and PEG 200 as an enhancer (E8). LPEIA with poplar wood lignocellulose achieved the highest relative improvement, with a 2,957% increase (2.14 MPa) using 95 wt% lignocellulose and glutaraldehyde as an enhancer (F1). LTA with glyoxalated organosolv lignin showed a moderate 16% increase (0.81 MPa) at 10 wt% lignin (G1). LSPA with epoxidized enzymatic hydrolysis lignin experienced a strong 364% increase (1.02 MPa) at 41 wt% lignin (H15). LFA with oxidized bagasse lignin had a limited 7% increase (0.24 MPa) at 15 wt% lignin using a PF resin prepolymer enhancer (I8). While these formulations exhibit the most substantial improvements in performance, a key downside is that all rely on expensive enhancers to achieve these results.

Despite progress in lignin incorporated resins, they still face challenges. Future advancements in lignin-based adhesives should prioritize reducing formaldehyde emissions, enhancing water resistance, and increasing lignin content to improve sustainability of resins. Phenol-, urea-, and melamine-formaldehyde adhesives must minimize formaldehyde while maintaining cost-effectiveness and performance, while epoxy and polyurethane variants should replace petroleum-based components with sustainable alternatives for polyols and curing agents. Tannin and soy protein adhesives require improved curing efficiency and durability, whereas furfural and polyethyleneimine adhesives need optimized processing and scalability for broader applications. Enhancing bond strength, thermal stability, and overall adhesive performance is crucial for lignin-based systems to compete with conventional adhesives. Additionally, integrating circular economy principles by utilizing lignin from waste streams, developing formaldehyde-free formulations, and expanding applications into automotive, construction, and packaging industries will drive commercialization and environmental benefits. Lignin-based adhesives show strong potential across various formulations. Lignin-phenol-formaldehyde adhesives lead in research due to their ability to replace phenol while maintaining strong bonding properties. Lignin-epoxy and lignin-polyurethane adhesives offer excellent mechanical strength and versatility, with ongoing research optimizing curing and reactivity (Table 2-5 & 2-6). Lignin-polyethyleneimine adhesives demonstrate high bonding strength for wood applications. Additionally, soy proteins, PEI and furfural can be used as enhancers to improve adhesion in synthetic adhesives, such as LPF, LPU, and LEP. Lignin-tannin adhesives stand out for being fully bio-based with strong adhesive properties. Continued advancements focus on improving performance, sustainability, and scalability to enhance commercial viability. Lignin-phenol-formaldehyde (LPF) adhesives are among the most commercially available, with companies like Latvijas Finieris incorporating bio-based lignin from Stora Enso to reduce reliance on fossil-based phenols in plywood production, while maintaining performance and lowering carbon footprints [196]. Similarly, lignin-polyurethane (LPU) adhesives are advancing toward broader commercialization with efforts focused on improving sustainability and performance [197].

Despite their promise, lignin-based adhesives still face challenges in reactivity, chemical heterogeneity, and performance, often struggling to match the strength, durability, and water resistance of synthetic

alternatives. Issues like odor, color, and formaldehyde emissions further limit adoption, while high extraction and modification costs make scalability difficult. Market acceptance remains a hurdle as industries hesitate to transition from traditional adhesives. Additionally, a lack of standardized curing and resin synthesis procedures in the literature makes it difficult to compare formulations, even within the same adhesive type, further complicating research and development efforts.

2.6 Conclusion

Lignin shows promising potential for use as feedstock in industrial adhesive systems. Not only does the application of this biomass precursor reduce production costs, reduce environmental pollution and reduce our dependency on petroleum, but it also reduces lignin waste. Unfortunately, the use of lignin is not yet practical due to its low reactivity and complex heterogenous structure. Various modifications can enhance the reactivity of lignin. Among the most common methods are demethylation, depolymerization, phenolation, hydroxymethylation, and glyoxalation. The best-performing adhesive was reported to use enhancers. Alkali lignin nanoparticles in a PF resin adhesive with a urea enhancer (30 wt% lignin) increased tensile strength by 64% (1.59 MPa) while maintaining a free formaldehyde content of only 0.12%, well below the Chinese standard of 0.3% (A18). Similarly, hydroxymethylated lignin in a UF resin adhesive with a melamine enhancer (5 wt% lignin) acted as a polyacid catalyst, enhancing bonding strength by 67% (1.72 MPa) while lowering free formaldehyde emissions compared to commercial resin catalysts (B9). Though less researched, hydroxymethylated alkali lignin in an MF resin adhesive with a urea enhancer (6 wt% lignin) led to a 47% increase in bonding strength (1.34 MPa) with minimal formaldehyde emissions (0.06%) (C2). In epoxy resin systems, depolymerized lignin (reed magnesium bisulfite) with an E-57 resin enhancer (15 wt% lignin) improved bonding strength by 228% (10.42 MPa) compared to commercial epoxy resins (D12). In PU resin foam applications, demethylated softwood lignin with PEG 200 enhancer (34 wt% lignin) resulted in a remarkable 942% increase in compression strength (0.34 MPa) (E8). In tannin resin adhesives, glyoxalated lignin (oil palm empty fruit bunch) with a PEI enhancer (40 wt% lignin, 20 wt% PEI) achieved a 103% increase in bonding strength (63.16 MPa) over formulations without PEI (F7). Epoxidized enzymatic hydrolysis lignin in a soy protein resin adhesive (41 wt% lignin) boosted wet bonding strength by 364% (1.02 MPa), though the addition of a preservative reduced this increase to 291% (0.86 MPa) (G14). Oxidized bagasse lignin in a furfural-PF resin mold (15 wt% lignin) provided a modest 7% improvement in bonding strength (0.24 MPa) (H8). Finally, a poplar wood lignocellulose PEI resin adhesive with a glutaraldehyde enhancer (95 wt% lignin) exhibited the most dramatic increase, with bonding strength improving by 2,957% (2.14 MPa) (I1). These findings highlight the diverse applications of lignin-based resin materials, demonstrating their potential as sustainable, high-performance alternatives in adhesive and composite resin formulations. However, challenges in reactivity, consistency, and performance, often falling short of synthetic alternatives in strength, durability, and water resistance. Additionally, factors such as odor, color, and formaldehyde emissions hinder widespread adoption, while high processing costs limit scalability. Market reluctance to shift from conventional adhesives further slows progress. Continued research and innovation in lignin modification, cost-effective processing, and performance optimization will be essential for bridging the gap between lignin-based and synthetic resin adhesives, paving the way for wider industrial adoption.

Table 2-11: List of abbreviations.

Abbreviations	Full name
PF	Phenol-formaldehyde
LPF	Lignin-phenol-formaldehyde
LPFA	Lignin-phenol formaldehyde adhesive
UF	Urea-formaldehyde
UFA	Urea-formaldehyde adhesive
LUF	Lignin-urea-formaldehyde
LUFA	Lignin-urea formaldehyde adhesive
GDE	glycerol diglycidyl ether
MA-HL	Maleated lignin-based polyacid catalyst
MF	Melamine-formaldehyde
MUF	Melamine-urea-formaldehyde
LMF	Lignin-melamine-formaldehyde
LMFA	Lignin-melamine formaldehyde adhesive
LEA	Lignin-epoxy adhesive
BPA	Bisphenol-A
ECH	Epichlorohydrin
DGEBA	Diglycidyl ether of bisphenol A
TBAB	Tetrabutylammonium bromide
PU	Polyurethane
LPU	Lignin-polyurethane
LPUA	Lignin-polyurethane adhesive
TDI	Toluene dissocyanate
DEG	diethylene glycol
PEI	Polyethyleneimine
LPEIA	Lignin-polyethyleneimine adhesive
MAP	Marine adhesive protein
PVC	for polyvinyl chloride
OPP	oriented polypropylene
PET	polyethylene terephthalate
LTA	Lignin-tannin adhesive
SP	Soy protein
LSPA	Lignin-soy protein adhesive
KL	Kraft lignin
CNF	cellulose nanofiber
PDA-BN	dopamine-functionalized hexagonal boron nitride
LFA	Lignin-furfural adhesive
F/P	Formaldehyde/phenol, mol/mol
F/U	Formaldehyde/Urea, mol/mol
FF/MA	Furfural/ malic acid, mol/mol
FF/P	Furfural/phenol, mol/mol
NaOH/P	Sodium hydroxide/phenol
WBB-LPF	Whie birch bark lignin-phenol-formaldehyde
WSB-LPF	Whie spruce bark lignin-phenol-formaldehyde
LPF	Lignin-phenol-formaldehyde
PLPF	Phenolated lignin-phenol-formaldehyde
NLPF	Lignin nanoparticle-phenol-formaldehyde
MLPF	Lignin macroparticle-phenol-formaldehyde
B-LUF	Alkali bagasse lignin-urea-formaldehyde
M-LUF	Alkali molasse lignin-urea-formaldehyde
LUF	Lignin-urea-formaldehyde

GLUF	Glyoxalated lignin-urea-formaldehyde
ILUF	Ionic liquid modified lignin-urea-formaldehyde
HLUF	Hydroxymethyalted lignin-urea-formaldehyde
DLUF	Demethylated/depolymerized lignin-urea-formaldehyde
PLUF	Phenolated lignin-urea-formaldehyde
NLUF	Lignin nanoparticles-urea-formaldehyde
TLMF	Tosylated lignin-melamine-formaldehyde
HLMF	Hydroxymethyalted lignin-melamine-formaldehyde
LEP	Lignin-epoxy
WDLEP	water soluble lignin-epoxy
ADLEP	Ammonia water/ethanol soluble lignin-epoxy
EDLEP	ethylenediamine/ethanol soluble lignin-epoxy
DLEP	Demethylated/depolymerized lignin-epoxy
PLEP	Phenolated lignin-epoxy
ALEP	Aminated lignin-epoxy
NLEP	Lignin nanoparticles-epoxy
DLPU	Demethylated/depolymerized lignin-polyurethane
OLPU	Oxypropylated lignin-polyurethane
NLPU	Lignin nanoparticles-polyurethane
LPEI	Lignin-Polyethylenimine
DLPEI	Demethylated/depolymerized lignin-Polyethylenimine
OLPEI	Oxidized lignin-Polyethylenimine
NLPEI	Lignin nanoparticles-Polyethylenimine
GLT	Glyoxalated/glycidolated lignin-tannin
OLT	Oxypropylated lignin-tannin
LSP	Lignin-soy protein
DLSP	Demethylated/depolymerized lignin-soy protein
DLSP-R	Reduced-demethylated lignin-soy protein
ALSP	Phenolated lignin-soy protein
EPLSP	Lignin nanoparticles-soy protein
CLSP	Carboxymethylated + hexagonal boron nitride functionalized lignin-soy protein
LFF	Lignin-furfural
DLFF	Demethylated/depolymerized lignin-furfural
LTLFF	Low transition temperature mixture modified lignin-furfural
OLFF	Oxidized lignin-furfural
LTTM	Low temperature transition mixture

2.7 References

[1] R. D. Adams, Adhesive Bonding, 2nd ed. Woodhead, 2021.

[2] S. J. Marshall, S. C. Bayne, R. Baier, A. P. Tomsia, and G. W. Marshall, "A review of adhesion science," Dental Materials, vol. 26, no. 2, 2010, doi: 10.1016/j.dental.2009.11.157.

[3] C. Huang, Z. Peng, J. Li, X. Li, X. Jiang, and Y. Dong, "Unlocking the role of lignin for preparing the lignin-based wood adhesive: A review," Nov. 01, 2022, Elsevier B.V. doi: 10.1016/j.indcrop.2022.115388.

[4] C. S. P. Borges, A. Akhavan-Safar, P. Tsokanas, R. J. C. Carbas, E. A. S. Marques, and L. F. M. da Silva, "From fundamental concepts to recent developments in the adhesive bonding technology: a general view," Discover Mechanical Engineering, vol. 2, no. 1, May 2023, doi: 10.1007/s44245-023-00014-7.

[5] X. Gong, Y. Meng, J. Lu, Y. Tao, Y. Cheng, and H. Wang, "A Review on Lignin-Based Phenolic Resin Adhesive," Feb. 01, 2022, John Wiley and Sons Inc. doi: 10.1002/macp.202100434.

[6] Z. Yuan, C. Charles Xu, N. Mahmood, and J. Schmidt, "Valorization of Hydrolysis Lignin for Polyols/Polyurethane Foam VALORIZATION OF HYDROLYSIS LIGNIN FOR POLYOLS AND RIGID POLYURETHANE FOAM," 2013. [Online]. Available: https://www.researchgate.net/publication/264655151

[7] P. Dongre, M. Driscoll, T. Amidon, and B. Bujanovic, "Lignin-furfural based adhesives," Energies (Basel), vol. 8, no. 8, pp. 7897–7914, Aug. 2015, doi: 10.3390/en8087897.

[8] L. Chupin, B. Charrier, A. Pizzi, A. Perdomo, and F. Charrier-El Bouhtoury, "Study of thermal durability properties of tannin-lignosulfonate adhesives," J Therm Anal Calorim, vol. 119, no. 3, pp. 1577–1585, 2015, doi: 10.1007/s10973-014-4331-0.

[9] J. Xin, P. Zhang, M. P. Wolcott, J. Zhang, W. C. Hiscox, and X. Zhang, "A Novel and Formaldehyde-Free Preparation Method for Lignin Amine and Its Enhancement for Soy Protein Adhesive," J Polym Environ, vol. 25, no. 3, pp. 599–605, Sep. 2017, doi: 10.1007/s10924-016-0844-x.

[10] S. Chen, D. Fan, and C. Gui, "Investigation of humidity-heat aging resistance of a soy protein adhesive fabricated by soybean meal and lignin-based polymer," Polym Test, vol. 120, Mar. 2023, doi: 10.1016/j.polymertesting.2023.107971.

[11] M. S. Karunarathna and R. C. Smith, "Valorization of lignin as a sustainable component of structural materials and composites: Advances from 2011 to 2019," Jan. 01, 2020, MDPI. doi: 10.3390/su12020734.

[12] D. Zhao, Z. Li, Y. Zhang, and P. Fu, "The role of lignin in adhesives for lignin-based formaldehyde-based resins: a review," 2025, Springer Science and Business Media Deutschland GmbH. doi: 10.1007/s13399-024-06397-1.

[13] P. Fatehi and J. Chen, "Extraction of Technical Lignins from Pulping Spent Liquors, Challenges and Opportunities," in Production of Biofuels and Chemicals from Lignin, Biofuels and Biorefineries, 6th ed., vol. 6, 2016, pp. 35–54. doi: 10.1007/978-981-10-1965-4_2.

[14] B. Ahvazi, É. Cloutier, O. Wojciechowicz, and T. D. Ngo, “Lignin Profiling: A Guide for Selecting Appropriate Lignins as Precursors in Biomaterials Development,” Oct. 03, 2016, American Chemical Society. doi: 10.1021/acssuschemeng.6b00873.

[15] W. Gao and P. Fatehi, “Lignin for polymer and nanoparticle production: Current status and challenges,” Canadian Journal of Chemical Engineering, vol. 97, no. 11, pp. 2827–2842, Nov. 2019, doi: 10.1002/cjce.23620.

[16] J. Li, W. Wang, S. Zhang, Q. Gao, W. Zhang, and J. Li, “Preparation and characterization of lignin demethylated at atmospheric pressure and its application in fast curing biobased phenolic resins,” RSC Adv, vol. 6, no. 71, pp. 67435–67443, 2016, doi: 10.1039/c6ra11966b.

[17] Z. Peng, X. Jiang, C. Si, A. Joao Cárdenas-Oscanoa, and C. Huang, “Advances of Modified Lignin as Substitute to Develop Lignin-Based Phenol-Formaldehyde Resin Adhesives,” Aug. 07, 2023, John Wiley and Sons Inc. doi: 10.1002/cssc.202300174.

[18] Q. Liu, Y. Xu, F. Kong, H. Ren, and H. Zhai, “Synthesis of phenolic resins by substituting phenol with modified spruce kraft lignin,” Wood Sci Technol, vol. 56, no. 5, pp. 1527–1549, Sep. 2022, doi: 10.1007/s00226-022-01408-8.

[19] E. Feghali et al., “Thermosetting Polymers from Lignin Model Compounds and Depolymerized Lignins,” Aug. 01, 2018, Springer International Publishing. doi: 10.1007/s41061-018-0211-6.

[20] S. Zhang et al., “High-performance adhesives modified by demethylated lignin for use in extreme environments,” New Journal of Chemistry, vol. 47, no. 14, pp. 6721–6729, Mar. 2023, doi: 10.1039/d2nj06225a.

[21] H. Younesi-Kordkheili, A. Pizzi, and G. Niyatzade, “Reduction of Formaldehyde Emission from Particleboard by Phenolated Kraft Lignin,” Journal of Adhesion, vol. 92, no. 6, pp. 485–497, Jun. 2016, doi: 10.1080/00218464.2015.1046596.

[22] X. Chen et al., “Oxidized demethylated lignin as a bio-based adhesive for wood bonding,” Journal of Adhesion, vol. 97, no. 9, pp. 873–890, 2021, doi: 10.1080/00218464.2019.1710830.

[23] Y. Yuan, M. Guo, and F. Liu, “Preparation and Evaluation of Green Composites Using Modified Ammonium Lignosulfonate and Polyethylenimine as a Binder,” Bioresources, vol. 9, no. 1, pp. 836–848, 2014.

[24] P. Navarrete et al., “Low formaldehyde emitting biobased wood adhesives manufactured from mixtures of tannin and glyoxylated lignin,” J Adhes Sci Technol, vol. 26, no. 10–11, pp. 1667–1684, Jun. 2012, doi: 10.1163/156856111X618489.

[25] S. Gao, Y. Liu, C. Wang, F. Chu, F. Xu, and D. Zhang, “Synthesis of lignin-based polyacid catalyst and its utilization to improve water resistance of urea-formaldehyde resins,” Polymers (Basel), vol. 12, no. 1, Jan. 2020, doi: 10.3390/polym12010175.

[26] K. Sawamura, Y. Tobimatsu, H. Kamitakahara, and T. Takano, “Lignin Functionalization through Chemical Demethylation: Preparation and Tannin-Like Properties of Demethylated Guaiacyl-Type Synthetic Lignins,” ACS Sustain Chem Eng, vol. 5, no. 6, pp. 5424–5431, Jun. 2017, doi: 10.1021/acssuschemeng.7b00748.

[27] S. Kang, X. Li, J. Fan, and J. Chang, “Hydrothermal conversion of lignin: A review,” 2013. doi: 10.1016/j.rser.2013.07.013.

[28] X. F. Zhou, “Conversion of kraft lignin under hydrothermal conditions,” Bioresour Technol, vol. 170, pp. 583–586, Oct. 2014, doi: 10.1016/j.biortech.2014.08.076.

[29] J. Ou, S. Li, W. Li, C. Liu, J. Ren, and F. Yue, “Revealing the Structural Influence on Lignin Phenolation and Its Nanoparticle Fabrication with Tunable Sizes,” ACS Sustain Chem Eng, vol. 10, no. 45, pp. 14845–14854, Nov. 2022, doi: 10.1021/acssuschemeng.2c04701.

[30] F. Zhang, X. Jiang, J. Lin, G. Zhao, H. M. Chang, and H. Jameel, “Reactivity improvement by phenolation of wheat straw lignin isolated from a biorefinery process,” New Journal of Chemistry, vol. 43, no. 5, pp. 2238–2246, 2019, doi: 10.1039/c8nj05016c.

[31] L. R. Nahra, M. C. Rezende, M. P. Oliveira, and L. M. Guerrini, “Glyoxalation of Kraft lignin and optimization of electrospinning process parameters for producing polyacrylonitrile/KL nanomats for potential applications as carbon material,” Journal of Polymer Research, vol. 27, no. 11, Nov. 2020, doi: 10.1007/s10965-020-02304-0.

[32] E. Frollini, C. G. Silva, and E. C. Ramires, “Phenolic resins as a matrix material in advanced fiber-reinforced polymer (FRP) composites,” Advanced Fibre-Reinforced Polymer (FRP) Composites for Structural Applications, pp. 7–43, Jan. 2013, doi: 10.1533/9780857098641.1.7.

[33] M. E. Taverna, F. Felissia, M. C. Area, D. A. Estenoz, and V. V. Nicolau, “Hydroxymethylation of technical lignins from South American sources with potential use in phenolic resins,” J Appl Polym Sci, vol. 136, no. 26, Jul. 2019, doi: 10.1002/app.47712.

[34] S. Yang, J. L. Wen, T. Q. Yuan, and R. C. Sun, “Characterization and phenolation of biorefinery technical lignins for lignin-phenol-formaldehyde resin adhesive synthesis,” RSC Adv, vol. 4, no. 101, pp. 57996–58004, 2014, doi: 10.1039/c4ra09595b.

[35] C. Xu and F. Ferdosian, “Lignin-Based Phenol–Formaldehyde (LPF) Resins/Adhesives,” in Conversion of lignin into Bio-Based Chemicals and Materials, Springer, Berlin, Heidelberg, 2017, pp. 91–109. doi: 10.1007/978-3-662-54959-9_6.

[36] B. Zhu, X. Jiang, S. Li, and M. Zhu, “An Overview of Recycling Phenolic Resin,” May 01, 2024, Multidisciplinary Digital Publishing Institute (MDPI). doi: 10.3390/polym16091255.

[37] Y. Chen et al., “Demethylation of lignin with mild conditions and preparation of green adhesives to reduce formaldehyde emissions and health risks,” Int J Biol Macromol, vol. 242, Jul. 2023, doi: 10.1016/j.ijbiomac.2023.124462.

[38] Wu Shubin and Zhan Huaiyu, “Characteristics of Demethylation wheat straw soda lignin and its utilization in ligin based phenolic formaldehyde resins,” Cellulose Chemistry Technology , vol. 35, no. 3–4, pp. 253–262, 2001.

[39] N. Lewis and T. Lantzy, “Chapter 2 Lignin in Adhesives Introduction and Historical Perspective,” in Adhesives From Renewable Resources , 1989, pp. 13–26. [Online]. Available: https://pubs.acs.org/sharingguidelines

[40] S. Yang, T. Q. Yuan, M. F. Li, and R. C. Sun, “Hydrothermal degradation of lignin: Products analysis for phenol formaldehyde adhesive synthesis,” Int J Biol Macromol, vol. 72, pp. 54–62, 2015, doi: 10.1016/j.ijbiomac.2014.07.048.

[41] H. Wang, T. L. Eberhardt, C. Wang, S. Gao, and H. Pan, “Demethylation of alkali lignin with halogen acids and its application to phenolic resins,” Polymers (Basel), vol. 11, no. 11, Nov. 2019, doi: 10.3390/polym11111771.

[42] “7.22: Hydrolysis of Salts- Equations - Chemistry LibreTexts.” Accessed: Feb. 06, 2025. [Online]. Available: https://chem.libretexts.org/Courses/Brevard_College/CHE_104%3A_Principles_of_Chemistry_II/07%3A_Acid_and_Base_Equilibria/7.22%3A_Hydrolysis_of_Salts-_Equations

[43] Y. Song, Z. Wang, N. Yan, R. Zhang, and J. Li, “Demethylation of wheat straw alkali lignin for application in phenol formaldehyde adhesives,” Polymers (Basel), vol. 8, no. 6, May 2016, doi: 10.3390/polym8060209.

[44] “Phenol Formaldehyde (PF) - Properties.” Accessed: Feb. 11, 2025. [Online]. Available: https://matmake.com/materials-data/phenol-formaldehyde-properties.html

[45] “Urea Formaldehyde (UF) - Properties.” Accessed: Feb. 11, 2025. [Online]. Available: https://matmake.com/materials-data/urea-formaldehyde-properties.html

[46] “Melamine Formaldehyde (MF) - Properties.” Accessed: Mar. 12, 2025. [Online]. Available: https://matmake.com/materials-data/melamine-formaldehyde-properties.html

[47] “Overview of materials for Epoxy Cure Resin.” Accessed: Feb. 13, 2025. [Online]. Available: https://www.matweb.com/search/datasheet_print.aspx?matguid=956da5edc80f4c62a72c15ca2b923494

[48] “Polyurethane (PUR) - Properties.” Accessed: Feb. 17, 2025. [Online]. Available: https://matmake.com/materials-data/polyurethane-properties.html

[49] S. Feng, Z. Yuan, M. Leitch, and C. C. Xu, “Adhesives formulated from bark bio-crude and phenol formaldehyde resole,” Ind Crops Prod, vol. 76, pp. 258–268, Dec. 2015, doi: 10.1016/j.indcrop.2015.06.056.

[50] W. G. Trindade, W. Hoareau, J. D. Megiatto, I. A. T. Razera, A. Castellan, and E. Frollini, “Thermoset Phenolic Matrices Reinforced with Unmodified and Surface-Grafted Furfuryl Alcohol Sugar Cane Bagasse and Curaua Fibers: Properties of Fibers and Composites,” Biomacromolecules, vol. 6, pp. 2485–2496, 2005, doi: 10.1021/bm058006.

[51] P. Solt, B. Rößiger, J. Konnerth, and H. W. G. van Herwijnen, “Lignin phenol formaldehyde resoles using base-catalysed depolymerized kraft lignin,” Polymers (Basel), vol. 10, no. 10, 2018, doi: 10.3390/polym10101162.

[52] S. Cheng, Z. Yuan, M. Leitch, M. Anderson, and C. C. Xu, “Highly efficient de-polymerization of organosolv lignin using a catalytic hydrothermal process and production of phenolic resins/adhesives with the depolymerized lignin as a substitute for phenol at a high substitution ratio,” Ind Crops Prod, vol. 44, pp. 315–322, Jan. 2013, doi: 10.1016/j.indcrop.2012.10.033.

[53] B. Di et al., “Phenol-enriched hydroxy depolymerized lignin by microwave alkali catalysis to prepare high-adhesive biomass composites,” Polym Eng Sci, vol. 61, no. 5, pp. 1463–1475, May 2021, doi: 10.1002/pen.25664.

[54] J. Li, J. Zhang, S. Zhang, Q. Gao, J. Li, and W. Zhang, “Fast curing bio-based phenolic resins via lignin demethylated under mild reaction condition,” Polymers (Basel), vol. 9, no. 9, Sep. 2017, doi: 10.3390/polym9090428.

[55] Q. Liu, Y. Xu, F. Kong, H. Ren, and H. Zhai, “Synthesis of phenolic resins by substituting phenol with modified spruce kraft lignin,” Wood Sci Technol, vol. 56, no. 5, pp. 1527–1549, Sep. 2022, doi: 10.1007/s00226-022-01408-8.

[56] B. Luo, Z. Jia, H. Jiang, S. Wang, and D. Min, “Improving the reactivity of sugarcane bagasse kraft lignin by a combination of fractionation and phenolation for phenol-formaldehyde adhesive applications,” Polymers (Basel), vol. 12, no. 8, Aug. 2020, doi: 10.3390/POLYM12081825.

[57] H. Paananen, L. Alvila, and T. T. Pakkanen, “Hydroxymethylation of softwood kraft lignin and phenol with paraformaldehyde,” Sustain Chem Pharm, vol. 20, May 2021, doi: 10.1016/j.scp.2021.100376.

[58] S. Feng, T. Shui, H. Wang, X. Ai, T. Kuboki, and C. C. Xu, “Properties of phenolic adhesives formulated with activated organosolv lignin derived from cornstalk,” Ind Crops Prod, vol. 161, Mar. 2021, doi: 10.1016/j.indcrop.2020.113225.

[59] Y. Chen, X. Gong, G. Yang, Q. Li, and N. Zhou, “Preparation and characterization of a nanolignin phenol formaldehyde resin by replacing phenol partially with lignin nanoparticles,” RSC Adv, vol. 9, no. 50, pp. 29255–29262, 2019, doi: 10.1039/c9ra04827h.

[60] W. Yang et al., “Preparation and properties of adhesives based on phenolic resin containing lignin micro and nanoparticles: A comparative study,” Mater Des, vol. 161, pp. 55–63, Jan. 2019, doi: 10.1016/j.matdes.2018.11.032.

[61] I. A. Gilca, R. E. Ghitescu, A. C. Puitel, and V. I. Popa, “Preparation of lignin nanoparticles by chemical modification,” Iranian Polymer Journal (English Edition), vol. 23, no. 5, pp. 355–363, 2014, doi: 10.1007/s13726-014-0232-0.

[62] A. Dorieh, F. Pahlavan, K. Hájková, Š. Hýsek, M. Farajollah Pour, and E. H. Fini, “Advancing Sustainable Building Materials: Reducing Formaldehyde Emissions in Medium Density Fiber Boards with Lignin Nanoparticles,” Adv Sustain Syst, Sep. 2024, doi: 10.1002/adsu.202400102.

[63] S. Gao et al., “Unexpected role of amphiphilic lignosulfonate to improve the storage stability of urea formaldehyde resin and its application as adhesives,” Int J Biol Macromol, vol. 161, pp. 755–762, Oct. 2020, doi: 10.1016/j.ijbiomac.2020.06.135.

[64] H. Younesi-Kordkheili, S. Kazemi-Najafi, R. B. Eshkiki, and A. Pizzi, “Improving urea formaldehyde resin properties by glyoxalated soda bagasse lignin,” European Journal of Wood and Wood Products, vol. 73, no. 1, pp. 77–85, Jan. 2015, doi: 10.1007/s00107-014-0850-4.

[65] C. V. L. Natarelli et al., “Sulfonated Kraft lignin addition in urea–formaldehyde resin: Thermokinetic analysis,” J Therm Anal Calorim, vol. 137, no. 5, pp. 1537–1547, Sep. 2019, doi: 10.1007/s10973-019-08075-1.

[66] P. Bekhta et al., “Properties of eco-friendly particleboards bonded with lignosulfonate-urea-formaldehyde adhesives and PMDI as a crosslinker,” Materials, vol. 14, no. 17, Sep. 2021, doi: 10.3390/ma14174875.

[67] H. Younesi-Kordkheili, A. Pizzi, A. Honarbakhsh-Raouf, and F. Nemati, “The effect of soda bagasse lignin modified by ionic liquids on properties of the urea–formaldehyde resin as a wood adhesive,” Journal of Adhesion, vol. 93, no. 11, pp. 914–925, Sep. 2017, doi: 10.1080/00218464.2016.1188284.

[68] A. Boussetta, A. A. Benhamou, F. J. Barba, M. EL Idrissi, N. Grimi, and A. Moubarik, “Experimental and theoretical investigations of lignin-urea-formaldehyde wood adhesive: Density functional theory analysis,” Int J Adhes Adhes, vol. 104, Jan. 2021, doi: 10.1016/j.ijadhadh.2020.102737.

[69] H. Younesi-Kordkheili and A. Pizzi, “A comparison between lignin modified by ionic liquids and glyoxalated lignin as modifiers of urea-formaldehyde resin,” Journal of Adhesion, vol. 93, no. 14, pp. 1120–1130, Sep. 2017, doi: 10.1080/00218464.2016.1209741.

[70] H. Younesi-Kordkheili, S. Kazemi-Najafi, R. B. Eshkiki, and A. Pizzi, “Improving urea formaldehyde resin properties by glyoxalated soda bagasse lignin,” European Journal of Wood and Wood Products, vol. 73, no. 1, pp. 77–85, Jan. 2015, doi: 10.1007/s00107-014-0850-4.

[71] W. Qi et al., “Preparation of carbon microspheres from lignin–urea–formaldehyde resin for application in high-performance supercapacitor,” Wood Sci Technol, vol. 56, no. 2, pp. 367–387, Mar. 2022, doi: 10.1007/s00226-022-01357-2.

[72] W. Qi et al., “Preparation of carbon microspheres from lignin–urea–formaldehyde resin for application in high-performance supercapacitor,” Wood Sci Technol, vol. 56, no. 2, pp. 367–387, Mar. 2022, doi: 10.1007/s00226-022-01357-2.

[73] A. Boussetta, A. A. Benhamou, F. J. Barba, M. EL Idrissi, N. Grimi, and A. Moubarik, “Experimental and theoretical investigations of lignin-urea-formaldehyde wood adhesive: Density functional theory analysis,” Int J Adhes Adhes, vol. 104, Jan. 2021, doi: 10.1016/j.ijadhadh.2020.102737.

[74] H. Younesi-Kordkheili and A. Pizzi, “Improving the properties of urea-lignin-glyoxal resin as a wood adhesive by small addition of epoxy,” Int J Adhes Adhes, vol. 102, Oct. 2020, doi: 10.1016/j.ijadhadh.2020.102681.

[75] P. Bekhta et al., “Properties of eco-friendly particleboards bonded with lignosulfonate-urea-formaldehyde adhesives and PMDI as a crosslinker,” Materials, vol. 14, no. 17, Sep. 2021, doi: 10.3390/ma14174875.

[76] H. Younesi-Kordkheili and A. Pizzi, “Improving the properties of urea-lignin-glyoxal resin as a wood adhesive by small addition of epoxy,” Int J Adhes Adhes, vol. 102, Oct. 2020, doi: 10.1016/j.ijadhadh.2020.102681.

[77] X. Chen et al., “Particleboard bio-adhesive by glyoxalated lignin and oxidized dialdehyde starch crosslinked by urea,” Wood Sci Technol, vol. 56, no. 1, pp. 63–85, Jan. 2022, doi: 10.1007/s00226-021-01344-z.

[78] H. Younesi-Kordkheili, A. Pizzi, and A. Mohammadghasemipour, “Improving the properties of ionic liquid-treated lignin-urea-formaldehyde resins by a small addition of isocyanate for wood

adhesive," Journal of Adhesion, vol. 94, no. 5, pp. 406–419, Apr. 2018, doi: 10.1080/00218464.2017.1282350.

[79] J. Li, J. Zhang, S. Zhang, Q. Gao, J. Li, and W. Zhang, "Alkali lignin depolymerization under eco-friendly and cost-effective NaOH/urea aqueous solution for fast curing bio-based phenolic resin," Ind Crops Prod, vol. 120, pp. 25–33, Sep. 2018, doi: 10.1016/j.indcrop.2018.04.027.

[80] H. Younesi-Kordkheili, "Reduction of formaldehyde emission from urea-formaldehyde resin by maleated nanolignin," Int J Adhes Adhes, vol. 132, Jun. 2024, doi: 10.1016/j.ijadhadh.2024.103677.

[81] D. Li et al., "Melamine–Urea–Formaldehyde Resin Adhesive Modified with Recycling Lignin: Preparation, Structures and Properties," Forests, vol. 14, no. 8, Aug. 2023, doi: 10.3390/f14081625.

[82] "Melamine Resins | Hexion," Hexion. Accessed: Feb. 12, 2025. [Online]. Available: https://www.hexion.com/our-products/products-by-chemistry/amino-resins/melamine-resins

[83] "What Melamine Resin Is Used For," Capitalresin. Accessed: Feb. 12, 2025. [Online]. Available: https://capitalresin.com/what-melamine-resin-is-used-for/

[84] "Top Uses and Benefits of Melamine Resin | Atlas Fibre," AtlasFibre. Accessed: Feb. 12, 2025. [Online]. Available: https://www.atlasfibre.com/top-uses-and-benefits-of-melamine-resin/

[85] A. Field, "Melamine Plastic," Michigan state University. Accessed: Feb. 12, 2025. [Online]. Available: https://web.archive.org/web/20140327144152/http://www.msue.msu.edu/objects/content_revision/download.cfm/revision_id.493538/workspace_id.-4/01500096.html/

[86] S. Akhurst, "The Rise and Fall of Melamine Tableware," plastiquarian. Accessed: Feb. 12, 2025. [Online]. Available: https://web.archive.org/web/20080625052055/http://www.plastiquarian.com/styr3n3/pqs/pq32.htm

[87] "Melamine-formaldehyde resin | Synthetic Polymer, Thermosetting, Molding | Britannica." Accessed: Feb. 12, 2025. [Online]. Available: https://www.britannica.com/technology/melamine-formaldehyde-resin

[88] Y. Wang et al., "A review of application, modification, and prospect of melamine foam," Jan. 01, 2023, Walter de Gruyter GmbH. doi: 10.1515/ntrev-2023-0137.

[89] M. G. Kim, Adhesives and Finishes for Wood: For Practitioners and Students. Wiley, 2023. doi: 10.1002/9783527842780.

[90] A. Diop, K. Adjallé, B. Boëns, D. Montplaisir, and S. Barnabé, "Synthesis and characterization of lignin-melamine-formaldehyde resin," Journal of Thermoplastic Composite Materials, vol. 30, no. 9, pp. 1255–1266, Sep. 2017, doi: 10.1177/0892705716632856.

[91] X. Lu and X. Gu, "A review on lignin-based epoxy resins_Lignin effects on their synthesis and properties," Biological Macromolecules, vol. 229, pp. 778–790, 2023.

[92] "Epoxy Resin Market Size, Growth & Forecast, 2030." Accessed: Feb. 13, 2025. [Online]. Available: https://www.chemanalyst.com/industry-report/epoxy-resin-market-597

[93] H. Z. Chen, Z. Y. Li, X. Y. Liu, Y. M. Tian, L. Yang, and Z. C. Wang, "Depolymerization of renewable resources-lignin by sodium hydroxide as a catalyst and its applications to epoxy resin," J Appl Polym Sci, vol. 132, no. 26, Jul. 2015, doi: 10.1002/app.42176.

[94] F. Wang, J. Kuai, H. Pan, N. Wang, and X. Zhu, "Study on the demethylation of enzymatic hydrolysis lignin and the properties of lignin–epoxy resin blends," Wood Sci Technol, vol. 52, no. 5, pp. 1343–1357, Sep. 2018, doi: 10.1007/s00226-018-1024-z.

[95] Y. Zhu, B. Di, H. Chen, X. Wang, and Y. Tian, "In situ synthesis of novel biomass lignin/silica based epoxy resin adhesive from renewable resources at different pHs," J Adhes Sci Technol, vol. 33, no. 16, pp. 1806–1820, Aug. 2019, doi: 10.1080/01694243.2019.1617511.

[96] X. Lu and X. Gu, "A review on lignin-based epoxy resins_Lignin effects on their synthesis and properties," Biological Macromolecules, vol. 229, pp. 778–790, 2023.

[97] X. Zhen et al., "Demethylation, phenolation, and depolymerization of lignin for the synthesis of lignin-based epoxy resin via a one-pot strategy," Ind Crops Prod, vol. 173, Dec. 2021, doi: 10.1016/j.indcrop.2021.114135.

[98] H. Zhang, T. Chen, Y. Li, Y. Han, Y. Sun, and G. Sun, "Novel lignin-containing high-performance adhesive for extreme environment," Int J Biol Macromol, vol. 164, pp. 1832–1839, Dec. 2020, doi: 10.1016/j.ijbiomac.2020.07.307.

[99] X. Yang et al., "Preparation of single O-methoxyphenol from lignin and related liquor products as reinforcement for epoxy resin," Renew Energy, vol. 162, pp. 1285–1291, Dec. 2020, doi: 10.1016/j.renene.2020.07.143.

[100] G. Lui, J. Can, S. Huo, Z. Kong, and F. Chu, "Preparation and properties of novel bio-based epoxy resin thermosets from lignin oliogmers and Cardanol," Biological Macromolecules, vol. 193, pp. 1400–1408, 2021.

[101] B. Chen et al., "Synthesis of a novel lignin-based epoxy resin curing agent and study of cure kinetics, thermal, and mechanical properties," J Appl Polym Sci, vol. 138, no. 23, Jun. 2021, doi: 10.1002/app.50523.

[102] S. Nikafshar, O. Zabihi, Y. Moradi, M. Ahmadi, S. Amiri, and M. Naebe, "Catalyzed synthesis and characterization of a novel lignin-based curing agent for the curing of high-performance epoxy resin," Polymers (Basel), vol. 9, no. 7, Jul. 2017, doi: 10.3390/polym9070266.

[103] J. Liu et al., "One-Step Synthesis of Waterborne Epoxidized Lignin Nanoparticles with High Epoxy Value and Stability for High-Strength Adhesives," ACS Sustain Chem Eng, Oct. 2024, doi: 10.1021/acssuschemeng.4c02695.

[104] K. A. Henn et al., "Interfacial catalysis and lignin nanoparticles for strong fire- and water-resistant composite adhesives," Green Chemistry, vol. 24, no. 17, pp. 6487–6500, Aug. 2022, doi: 10.1039/d2gc01637k.

[105] C. Yu, Y. Chen, R. Li, J. Jiang, and X. Wang, "A Narrative Review: Modification of Bio-Based Wood Adhesive for Performance Improvement," Coatings, vol. 14, no. 9, p. 1153, Sep. 2024, doi: 10.3390/coatings14091153.

[106] “Polyurethane Resin | Formula, Properties & Application.” Accessed: Feb. 17, 2025. [Online]. Available: https://material-properties.org/polyurethane-resin/

[107] S. Nikafshar, J. Wang, K. Dunne, P. Sangthonganotai, and M. Nejad, “Choosing the Right Lignin to Fully Replace Bisphenol A in Epoxy Resin Formulation,” ChemSusChem, vol. 14, no. 4, pp. 1184–1195, Feb. 2021, doi: 10.1002/cssc.202002729.

[108] C. Gioia et al., “Lignin-Based Epoxy Resins: Unravelling the Relationship between Structure and Material Properties,” Biomacromolecules, vol. 21, no. 5, pp. 1920–1928, May 2020, doi: 10.1021/acs.biomac.0c00057.

[109] G. Lui, J. Can, S. Huo, Z. Kong, and F. Chu, “Preparation and properties of novel bio-based epoxy resin thermosets from lignin oliogmers and Cardanol,” Biological Macromolecules, vol. 193, pp. 1400–1408, 2021.

[110] F. Ferdosian, Z. Yuan, M. Anderson, and C. Xu, “Synthesis of lignin-based epoxy resins: Optimization of reaction parameters using response surface methodology,” RSC Adv, vol. 4, no. 60, pp. 31745–31753, 2014, doi: 10.1039/c4ra03978e.

[111] X. Zhao, Z. Zhang, J. Pang, and L. Su, “Study on the preparation of epoxy resin materials from nano-lignin polyols,” Ind Crops Prod, vol. 185, Oct. 2022, doi: 10.1016/j.indcrop.2022.115158.

[112] “Polyurethane global market volume 2030 | Statista.” Accessed: Feb. 17, 2025. [Online]. Available: https://www.statista.com/statistics/720341/global-polyurethane-market-size-forecast/

[113] B. L. Xue, P. L. Huang, Y. C. Sun, X. P. Li, and R. C. Sun, “Hydrolytic depolymerization of corncob lignin in the view of a bio-based rigid polyurethane foam synthesis,” RSC Adv, vol. 7, no. 10, pp. 6123–6130, 2017, doi: 10.1039/c6ra26318f.

[114] N. Mahmood, Z. Yuan, C. Charles Xu, and J. Schmidt, “VALORIZATION OF HYDROLYSIS LIGNIN FOR POLYOLS AND RIGID POLYURETHANE FOAM,” 2013. [Online]. Available: https://www.researchgate.net/publication/264655151

[115] N. Mahmood, Z. Yuan, J. Schmidt, and C. Xu, “Preparation of bio-based rigid polyurethane foam using hydrolytically depolymerized Kraft lignin via direct replacement or oxypropylation,” Eur Polym J, vol. 68, pp. 1–9, Jul. 2015, doi: 10.1016/j.eurpolymj.2015.04.030.

[116] H. Chung and N. R. Washburn, “Improved lignin polyurethane properties with lewis acid treatment,” ACS Appl Mater Interfaces, vol. 4, no. 6, pp. 2840–2846, Jun. 2012, doi: 10.1021/am300425x.

[117] X. Ma, J. Chen, J. Zhu, and N. Yan, “Lignin-Based Polyurethane: Recent Advances and Future Perspectives,” Feb. 01, 2021, Wiley-VCH Verlag. doi: 10.1002/marc.202000492.

[118] Y. Li and A. J. Ragauskas, “Kraft lignin-based rigid polyurethane foam,” Journal of Wood Chemistry and Technology, vol. 32, no. 3, pp. 210–224, Jul. 2012, doi: 10.1080/02773813.2011.652795.

[119] “All information about Polyurethane resin,” Europlas. Accessed: Feb. 17, 2025. [Online]. Available: https://europlas.com.vn/en-US/blog-1/all-information-about-Polyurethane-resin

[120] A. Van Schoor, “Polyurethane Resin Guide – Everything you need to Know.” Accessed: Feb. 17, 2025. [Online]. Available: https://resin-expert.com/en/guide/polyurethane-resin

[121] M. S. Karunarathna and R. C. Smith, “Valorization of lignin as a sustainable component of structural materials and composites: Advances from 2011 to 2019,” Jan. 01, 2020, MDPI. doi: 10.3390/su12020734.

[122] C. Huang, Z. Peng, J. Li, X. Li, X. Jiang, and Y. Dong, “Unlocking the role of lignin for preparing the lignin-based wood adhesive: A review,” Nov. 01, 2022, Elsevier B.V. doi: 10.1016/j.indcrop.2022.115388.

[123] E. Feghali et al., “Thermosetting Polymers from Lignin Model Compounds and Depolymerized Lignins,” Aug. 01, 2018, Springer International Publishing. doi: 10.1007/s41061-018-0211-6.

[124] Y. C. Chen, S. Fu, and H. Zhang, “Signally improvement of polyurethane adhesive with hydroxy-enriched lignin from bagasse,” Colloids Surf A Physicochem Eng Asp, vol. 585, Jan. 2020, doi: 10.1016/j.colsurfa.2019.124164.

[125] C. A. Xu et al., “Effect of modified bamboo lignin replacing part of C5 petroleum resin on properties of polyurethane/polysiloxane pressure-sensitive adhesive and its application on the wood substrate,” J Colloid Interface Sci, vol. 602, pp. 394–405, Nov. 2021, doi: 10.1016/j.jcis.2021.06.033.

[126] E. Rusen et al., “Synthesis and Mechanical Performances of Polyurethane Bio-Based Adhesives Resulted from the Depolymerization of Lignocellulose Biomass,” ACS Omega, vol. 8, no. 41, pp. 38178–38190, Oct. 2023, doi: 10.1021/acsomega.3c04393.

[127] D. J. Dos Santos, L. B. Tavares, J. R. Gouveia, and G. F. Batalha, “Lignin-based polyurethane and epoxy adhesives: A short review,” 2021, International OCSCO World Press. doi: 10.5604/01.3001.0015.0242.

[128] J. Hu, M. Huang, X. Zhou, R. Luo, L. Li, and X. Li, “Research Status of Lignin-Based Polyurethane and Its Application in Flexible Electronics,” Aug. 01, 2024, Multidisciplinary Digital Publishing Institute (MDPI). doi: 10.3390/polym16162340.

[129] K. Wysocka, K. Szymona, A. G. McDonald, and M. Maminski, “Characterization of thermal and mechanical properties of lignosulfonate- and hydrolyzed lignosulfonate-based polyurethane foams,” Bioresources, vol. 11, no. 3, pp. 7355–7364, 2016, doi: 10.15376/biores.11.3.7355-7364.

[130] K. M. Torr, D. J. van de Pas, E. Cazeils, and I. D. Suckling, “Mild hydrogenolysis of in-situ and isolated Pinus radiata lignins,” Bioresour Technol, vol. 102, no. 16, pp. 7608–7611, 2011, doi: 10.1016/j.biortech.2011.05.040.

[131] E. Rusen et al., “Synthesis and Mechanical Performances of Polyurethane Bio-Based Adhesives Resulted from the Depolymerization of Lignocellulose Biomass,” ACS Omega, vol. 8, no. 41, pp. 38178–38190, Oct. 2023, doi: 10.1021/acsomega.3c04393.

[132] C. A. Xu et al., “Effect of modified bamboo lignin replacing part of C5 petroleum resin on properties of polyurethane/polysiloxane pressure-sensitive adhesive and its application on the wood substrate,” J Colloid Interface Sci, vol. 602, pp. 394–405, Nov. 2021, doi: 10.1016/j.jcis.2021.06.033.

[133] J. Podschun, B. Saake, and R. Lehnen, “Catalytic demethylation of organosolv lignin in aqueous medium using indium triflate under microwave irradiation,” React Funct Polym, vol. 119, pp. 82–86, Oct. 2017, doi: 10.1016/j.reactfunctpolym.2017.08.007.

[134] L. Wu et al., “High strength and multifunctional polyurethane film incorporated with lignin nanoparticles,” Ind Crops Prod, vol. 177, Mar. 2022, doi: 10.1016/j.indcrop.2022.114526.

[135] T. He, F. Chen, W. Zhu, and N. Yan, “Functionalized lignin nanoparticles for producing mechanically strong and tough flame-retardant polyurethane elastomers,” Int J Biol Macromol, vol. 209, pp. 1339–1351, Jun. 2022, doi: 10.1016/j.ijbiomac.2022.04.089.

[136] D. Fan, Y. Huang, Y. Niu, Y. Lv, and G. Li, “Sustainable waterborne polyurethane/lignin nanoparticles composites: Durability meets degradability,” Polymer (Guildf), vol. 305, Jun. 2024, doi: 10.1016/j.polymer.2024.127179.

[137] Y. Liu and K. Li, “Preparation and characterization of demethylated lignin-polyethylenimine adhesives,” Journal of Adhesion, vol. 82, no. 6, pp. 593–605, Jun. 2006, doi: 10.1080/00218460600766632.

[138] Y. Li and D. Ju, “The Application, Neurotoxicity, and Related Mechanism of Cationic Polymers,” Neurotoxicity of Nanomaterials and Nanomedicine, pp. 285–329, Jan. 2017, doi: 10.1016/B978-0-12-804598-5.00012-X.

[139] Y. Yan et al., “Preparation and characterization of high-strength and water resistant lignocelluloses based composites bonded by branched polyethylenimine (PEI),” Int J Biol Macromol, vol. 141, pp. 369–377, Dec. 2019, doi: 10.1016/j.ijbiomac.2019.09.004.

[140] “Polyethyleneimine: EPOMIN™ | Products | NIPPON SHOKUBAI,” Nippon Shokubai. Accessed: Feb. 23, 2025. [Online]. Available: https://www.shokubai.co.jp/en/products/detail/epomin1/?utm_source=chatgpt.com

[141] X. Geng and K. Li, “Investigation of wood adhesives from kraft lignin and polyethylenimine,” J Adhes Sci Technol, vol. 20, no. 8, pp. 847–858, 2006, doi: 10.1163/156856106777638699.

[142] W. Peng, C. Dong, J. An, G. Zhang, P. Wang, and Y. Xie, “A Novel Formaldehyde-Free Wood Adhesive Synthesized by Straw Soda Lignin and Polyethyleneimin,” Bioresources, vol. 18, no. 2, pp. 3123–3143, 2023.

[143] A. H. Faris, A. A. Rahim, M. N. M. Ibrahim, A. M. Alkurdi, and I. Shah, “Combination of lignin polyol-tannin adhesives and polyethylenimine for the preparation of green water-resistant adhesives,” J Appl Polym Sci, vol. 133, no. 20, May 2016, doi: 10.1002/app.43437.

[144] K. Li and X. Geng, “Formaldehyde-free wood adhesives from decayed wood,” Macromol Rapid Commun, vol. 26, no. 7, pp. 529–532, Apr. 2005, doi: 10.1002/marc.200400594.

[145] G. Shulga et al., “Lignin containing Adhesion Enhancers for wood-plastic,” Bioresources, pp. 2804–2823, 2021.

[146] S. Sain, L. Matsakas, U. Rova, P. Christakopoulos, T. Öman, and M. Skrifvars, “Spruce bark-extracted lignin and tannin-based bioresin-adhesives: Effect of curing temperatures on the thermal properties of the resins,” Molecules, vol. 26, no. 12, Jun. 2021, doi: 10.3390/molecules26123523.

[147] ReporLinker, “Global Tannin Market to Reach 2 Million Tons by 2027,” GlobeNewswire by notified. Accessed: Feb. 23, 2025. [Online]. Available: https://www.globenewswire.com/news-release/2021/05/04/2222758/0/en/Global-Tannin-Market-to-Reach-2-Million-Tons-by-2027.html

[148] S. Liang, “Characterization of different tannins for possible industrial resin production,” Abo akademi University, 2022. doi: 10.06.2022.

[149] X. Zhou and G. Du, “Applications of Tannin Resin Adhesives in the Wood Industry,” in Tannins - Structural Properties, Biological Properties and Current Knowledge, Intehopen, 2019. doi: DOI:10.5772/intechopen.86424.

[150] J. Torres et al., “Removal of mercury(II) and methylmercury from solution by tannin adsorbents,” J Radioanal Nucl Chem, vol. 240, no. 1, pp. 361–365, 1999, doi: 10.1007/BF02349180/METRICS.

[151] T. Sakaguchi and A. Nakajima, “Recovery of Uranium from Seawater by Immobilized Tannin,” Sep Sci Technol, vol. 22, no. 6, pp. 1609–1623, Jun. 1987, doi: 10.1080/01496398708058421.

[152] S. Vijay et al., “Tannin as a renewable raw material for adhesive applications: a review,” Material advances , vol. 3, p. 3365, 2022, doi: 10.1039/d1ma00841b.

[153] M. A. Aristri et al., “Bio-Based Polyurethane Resins Derived from Tannin: Source, Synthesis, Characterisation, and Application,” Forests 2021, Vol. 12, Page 1516, vol. 12, no. 11, p. 1516, Nov. 2021, doi: 10.3390/F12111516.

[154] J. Saražin, D. Schmiedl, A. Pizzi, and M. Šernek, “Bio-based Adhesive Mixtures of Pine Tannin and Different Types of Lignins,” BioResources , vol. 15, no. 1, pp. 9401–9412, 2020.

[155] I. Dababi, O. Gimello, E. Elaloui, F. Quignard, and N. Brosse, “Organosolv lignin-based wood adhesive. Influence of the lignin extraction conditions on the adhesive performance,” Polymers (Basel), vol. 8, no. 9, Sep. 2016, doi: 10.3390/polym8090340.

[156] F. Bertaud, S. Tapin-Lingua, A. Pizzi, P. Navarrete, and M. Petit-Conil, “DEVELOPMENT OF GREEN ADHESIVES FOR FIBREBOARD MANUFACTURING, USING TANNINS AND LIGNIN FROM PULP MILL RESIDUES,” 2012.

[157] H. Lei, A. Pizzi, and G. Du, “Environmentally friendly mixed tannin/lignin wood resins,” J Appl Polym Sci, vol. 107, no. 1, pp. 203–209, Jan. 2008, doi: 10.1002/app.27011.

[158] R. El Hage, N. Brosse, P. Navarrete, and A. Pizzi, “Extraction, characterization and utilization of organosolv Miscanthus lignin for the conception of environmentally friendly mixed tannin/lignin wood resins,” J Adhes Sci Technol, vol. 25, no. 13, pp. 1549–1560, 2011, doi: 10.1163/016942410X524110.

[159] C. Jiang, J. Hu, C. Zhang, G. Hota, J. Wang, and N. G. Akhmedov, “Lignin oligomers from mild base-catalyzed depolymerization for potential application in aqueous soy adhesive as phenolic blends,” React Chem Eng, vol. 8, no. 10, pp. 2455–2465, Jun. 2023, doi: 10.1039/d3re00224a.

[160] K. Makwana, “Soybeans for Global Nutrition: A Numbers Story - Sustainable Nutrition Initiative®,” sustainable Nutrition Initiative . Accessed: Feb. 23, 2025. [Online]. Available: https://sustainablenutritioninitiative.com/soybeans-for-global-nutrition-a-numbers-story/

[161] “Adhesives | Soy New Uses,” US Soy. Accessed: Feb. 19, 2025. [Online]. Available: https://soynewuses.org/common-uses/adhesive/

[162] C. R. Frihart, C. G. Hunt, and M. J. Birkeland, “Chapter 16: Soy Proteins as Wood Adhesives,” Recent advances in adhesion science and technology, 2014.

[163] S. Chen, Y. Chen, Z. Wang, H. Chen, and D. Fan, “Renewable bio-based adhesive fabricated from a novel biopolymer and soy protein,” RSC Adv, vol. 11, no. 19, pp. 11724–11731, Mar. 2021, doi: 10.1039/d1ra00766a.

[164] Z. Liu et al., “Performance of soybean protein adhesive cross-linked by lignin and cuprum,” J Clean Prod, vol. 366, Sep. 2022, doi: 10.1016/j.jclepro.2022.132906.

[165] F. Cao, C. Sun, Y. Xu, J. Li, Z. Fang, and Z. Qiao, “Design of high performance multifunctional protein adhesive by incorporating of polydopamine-functionalized boron nitride and carboxymethylated lignin,” Ind Crops Prod, vol. 212, Jun. 2024, doi: 10.1016/j.indcrop.2024.118355.

[166] V. Ibrahim, G. Mamo, P. J. Gustafsson, and R. Hatti-Kaul, “Production and properties of adhesives formulated from laccase modified Kraft lignin,” Ind Crops Prod, vol. 45, pp. 343–348, Feb. 2013, doi: 10.1016/j.indcrop.2012.12.051.

[167] J. Luo et al., “An eco-friendly wood adhesive from soy protein and lignin: Performance properties,” RSC Adv, vol. 5, no. 122, pp. 100849–100855, Nov. 2015, doi: 10.1039/c5ra19232c.

[168] C. Yu, Y. Chen, R. Li, J. Jiang, and X. Wang, “A Narrative Review: Modification of Bio-Based Wood Adhesive for Performance Improvement,” Coatings 2024, Vol. 14, Page 1153, vol. 14, no. 9, p. 1153, Sep. 2024, doi: 10.3390/COATINGS14091153.

[169] S. Pradyawong et al., “Improved soy protein adhesives by lignin and polyamide-epichlorohydrin: Adhesion performance and properties,” J Appl Polym Sci, vol. 139, no. 44, Nov. 2022, doi: 10.1002/app.53086.

[170] S. Pradyawong, G. Qi, N. Li, X. S. Sun, and D. Wang, “Adhesion properties of soy protein adhesives enhanced by biomass lignin,” Int J Adhes Adhes, vol. 75, pp. 66–73, Jun. 2017, doi: 10.1016/j.ijadhadh.2017.02.017.

[171] X. Zhang, Y. Zhu, Y. Yu, and J. Song, “Improve performance of soy flour-based adhesive with a lignin-based resin,” Polymers (Basel), vol. 9, no. 7, Jul. 2017, doi: 10.3390/polym9070261.

[172] M. Podlena, M. Böhm, D. Saloni, G. Velarde, and C. Salas, “Tuning the adhesive properties of soy protein wood adhesives with different coadjutant polymers, nanocellulose and lignin,” Polymers (Basel), vol. 13, no. 12, Jun. 2021, doi: 10.3390/polym13121972.

[173] Z. Xiao et al., “Utilization of sorghum lignin to improve adhesion strength of soy protein adhesives on wood veneer,” Ind Crops Prod, vol. 50, pp. 501–509, Oct. 2013, doi: 10.1016/j.indcrop.2013.07.057.

[174] X. Zhu, D. Wang, N. Li, and X. S. Sun, “Bio-Based Wood Adhesive from Camelina Protein (a Biodiesel Residue) and Depolymerized Lignin with Improved Water Resistance,” ACS Omega, vol. 2, no. 11, pp. 7996–8004, Nov. 2017, doi: 10.1021/acsomega.7b01093.

[175] S. Pradyawong, G. Qi, X. S. Sun, and D. Wang, “Laccase/TEMPO-modified lignin improved soy-protein-based adhesives: Adhesion performance and properties,” Int J Adhes Adhes, vol. 91, pp. 116–122, Jun. 2019, doi: 10.1016/j.ijadhadh.2019.03.005.

[176] S. Chen, H. Chen, S. Yang, and D. Fan, “Developing an antifungal and high-strength soy protein-based adhesive modified by lignin-based polymer,” Ind Crops Prod, vol. 170, Oct. 2021, doi: 10.1016/j.indcrop.2021.113795.

[177] X. Zhu, B. Bruijnaers, T. V. Lourençon, and M. Balakshin, “Structural Analysis of Lignin-Based Furan Resin,” Materials, vol. 15, no. 1, Jan. 2022, doi: 10.3390/ma15010350.

[178] Y. Zhang, Z. Yuan, N. Mahmood, S. Huang, and C. C. Xu, “Sustainable bio-phenol-hydroxymethylfurfural resins using phenolated de-polymerized hydrolysis lignin and their application in bio-composites,” Ind Crops Prod, vol. 79, pp. 84–90, Jan. 2016, doi: 10.1016/j.indcrop.2015.10.048.

[179] “Furfural global market volume 2030 | Statista.” Accessed: Feb. 23, 2025. [Online]. Available: https://www.statista.com/statistics/1310459/furfural-market-volume-worldwide/

[180] J. Zhang, H. Chen, A. Pizzi, Y. Li, Q. Gao, and J. Li, “Characterization and Application of Urea-Formaldehyde-Furfural Co-condensed Resins as Wood Adhesives,” Bioresources.com.

[181] “Foundry - IFC.” Accessed: Feb. 23, 2025. [Online]. Available: https://www.furan.com/markets/foundry/?utm_source=chatgpt.com

[182] L. H. Brown, C. Lake, D. D. Watson, and A. Barrington, “Fiber glass laminates containing furfuryl resin binder,” May 31, 1968

[183] T. Türel, B. Eling, A. M. Cristadoro, T. Mathieu, M. Linnenbrink, and Ž. Tomović, “Novel Furfural-Derived Polyaldimines as Latent Hardeners for Polyurethane Adhesives,” ACS Appl Mater Interfaces, vol. 16, no. 5, pp. 6414–6423, Feb. 2024, doi: 10.1021/ACSAMI.3C17416/ASSET/IMAGES/LARGE/AM3C17416_0007.JPEG.

[184] P. Vaithanomsat, P. Janchai, V. Punsuvon, and W. Smitthipong, “EFFECT OF FURFURAL ON THE PROPERTIES OF NATURAL LATEX: POSSIBILITY FOR ADHESIVE APPLICATION,” Rubber Chemistry and Technology, vol. 90, no. 4, pp. 642–650, Dec. 2017, doi: 10.5254/RCT.82.83731.

[185] M. Depta, S. Napiórkowski, K. Zielińska, K. Gębura, D. Niewolik, and K. Jaszcz, “Environmentally Friendly o–Cresol–Furfural–Formaldehyde Resin as an Alternative to Traditional Phenol–Formaldehyde Resins for Paint Industry,” Materials, vol. 17, no. 13, p. 3072, Jul. 2024, doi: 10.3390/MA17133072.

[186] “Furfural resin - CAMEO.” Accessed: Feb. 23, 2025. [Online]. Available: https://cameo.mfa.org/wiki/Furfural_resin?utm_source=chatgpt.com

[187] M. Biron, “Thermosets and Composites: Material Selection, Applications, Manufacturing ... - Michel Biron - Google Books,” Elseivier. Accessed: Feb. 23, 2025. [Online]. Available: https://books.google.ca/books?id=IZwlAAAAQBAJ&printsec=frontcover&source=gbs_ge_summary_r&cad=0#v=onepage&q&f=false

[188] Y. Zhang et al., “Synthesis of high-water-resistance lignin-phenol resin adhesive with furfural as a crosslinking agent,” Polymers (Basel), vol. 12, no. 12, pp. 1–14, Dec. 2020, doi: 10.3390/polym12122805.

[189] J. Liu, J. Wang, Y. Fu, and J. Chang, “Synthesis and characterization of phenol-furfural resins using lignin modified by a low transition temperature mixture,” RSC Adv, vol. 6, no. 97, pp. 94588–94594, 2016, doi: 10.1039/c6ra17877d.

[190] I. W. G. on the E. of C. R. to Humans, “Dry Cleaning, Some Chlorinated Solvents and Other Industrial Chemicals,” in IARC Monographs on the Evaluation of Carcinogenic Risks to Humans, vol. 63, International Agency for Research on Cancer, 1995, ch. Furfural, pp. 33–475. Accessed: Feb. 23, 2025. [Online]. Available: https://www.ncbi.nlm.nih.gov/books/NBK464353/

[191] “OPINION OF THE SCIENTIFIC COMMITTEE ON COSMETIC PRODUCTS AND NON-FOOD PRODUCTS INTENDED FOR CONSUMERS CONCERNING FURFURAL.”

[192] D. Tien Vu, “What is furan resin sand casting Definition, Advantage & Application,” Vietnam Cast Iron. Accessed: Feb. 23, 2025. [Online]. Available: https://vietnamcastiron.com/furan-resin-sand-casting/?utm_source=chatgpt.com

[193] L. Almhofer, R. H. Bischof, M. Madera, and C. Paulik, “Kinetic and mechanistic aspects of furfural degradation in biorefineries,” Can J Chem Eng, vol. 101, no. 4, pp. 2033–2049, Apr. 2023, doi: 10.1002/CJCE.24593.

[194] N. Guigo, A. Mija, L. Vincent, and N. Sbirrazzuoli, “Eco-friendly composite resins based on renewable biomass resources: Polyfurfuryl alcohol/lignin thermosets,” Eur Polym J, vol. 46, no. 5, pp. 1016–1023, May 2010, doi: 10.1016/j.eurpolymj.2010.02.010.

[195] W. G. Trindade, W. Hoareau, I. A. T. Razera, R. Ruggiero, E. Frollini, and A. Castellan, “Phenolic thermoset matrix reinforced with sugar cane bagasse fibers: Attempt to develop a new fiber surface chemical modification involving formation of quinones followed by reaction with furfuryl alcohol,” Macromol Mater Eng, vol. 289, no. 8, pp. 728–736, Aug. 2004, doi: 10.1002/mame.200300320.

[196] “Lignin-based glue used in plywood production | Stora Enso,” StoraEnso. Accessed: Feb. 24, 2025. [Online]. Available: https://www.storaenso.com/en/newsroom/news/2022/3/lignin-based-glue-used-in-plywood-production?utm_source=chatgpt.com

[197] “Lignin-Based Adhesives for Engineered Wood Products and Cross Laminated Timber (CLT) : Centre for Research & Innovation in the Bio-economy.” Accessed: Feb. 24, 2025. [Online]. Available: https://cribe.ca/projects/roseburg-forest-products/?utm_source=chatgpt.com

Chapter 3: Demethylation of sulfobutylated lignin and its application as PF resin

Abstract

Phenol-formaldehyde (PF) resins are widely used in adhesives due to their excellent bonding strength, thermal stability, and weather resistance. However, the use of petroleum-based phenol and the release of formaldehyde during curing raise environmental and health concerns. Lignin, a renewable and aromatic-rich biopolymer, has been explored as a partial phenol substitute in PF resins. However, its complex structure and low reactivity limit its effectiveness, reducing bonding strength and increasing free formaldehyde emissions. To address these challenges, this study investigated the effect of sulfobutylation (SB) pretreatment to improve the water solubility of lignin and facilitate its subsequent demethylation in aqueous systems to generate lignin derivative that is compatible and reactive in PF resins. With sulfobutylation, methoxy and hydroxyl content decreased by 20% and 27%, respectively, while sulfonate content, charge density, and solubility increased by 14%, 25% and 508%, respectively. The rise in sulfonate content being the primary driver of enhanced charge density and solubility. Following demethylation of sulfobutylated lignin, both sulfonate content and methoxy content decreased by 6% and 27%, respectively, hydroxyl content showed a slight increase of 4%. Additionally, molecular weight and β-O-4 interunit linkages increased, all indicating condensation. Compared with demethylated lignin, SB pretreated and demethylated enhanced the resin's dry and wet bonding strength by 25% and 108% (DSBPF60), respectively, and improved its fire retardancy. However, it reduced thermal stability and increased water absorption, likely due to lignin condensation primarily occurring at the β-O-4 interunit linkage and the incorporation of DSH and SB aliphatic chains. These findings suggest that sulfobutylated and demethylated lignin can be used as a new process for producing lignin derivatives for sustainable PF resin manufacturing, but strategies should be taken into account for improving the thermal stability, water absorption, and formaldehyde emissions (3.18% in DSBPF60) of the resin.

Commented [KK8]: Please add Key Quantitative Findings here

3.1 Introduction

Adhesives serve as essential supporting materials across multiple industries. Among different types of adhesives, resole phenol-formaldehyde (PF) is the most widely used for exterior applications [1]. Phenol-formaldehyde (PF) adhesives are thermosetting polymers formed through the reaction of phenol and formaldehyde in the presence of a basic catalyst [2]. PF adhesives are extensively used in engineered wood products, including particle board, plywood, oriented strand board, waferboard, hardboard, and laminated veneer lumber [2-3]. Additionally, PF resins are applied in moldings, electrical insulators, brake linings, and brake pads. The distinctive network-crosslinked structure of this polymer provides outstanding heat resistance and bond strength, along with good aging and weather resistance, as well as satisfactory chemical stability [2]. A major drawback of PF resins is the release of formaldehyde during production and curing, posing significant health and environmental risks [4]. Additionally, their synthesis relies on petroleum-based raw materials (phenol and formaldehyde), raising sustainability concerns [4]. Due to rising petroleum demand, increasing costs, potential supply shortages, and associated environmental and health risks, researchers have explored more sustainable alternatives.

Lignin is the second most abundant renewable resource after cellulose and the primary source of aromatic compounds on Earth [5]. It is a high-molecular-weight, amorphous, and highly branched macromolecule, primarily produced as a by-product of the pulp and paper industry, where it is burned for energy recovery [6]. Though chemically complex, it features various functional groups, including aliphatic and phenolic hydroxyls, carboxyl, methoxyl, and terminal aldehyde groups, along with aryl, alkyl, ester, and ether linkages [6-7]. Due to its similar structure to phenol, it has been studied for phenol substitution in the PF resin. However, incorporating lignin into PF adhesives has been challenging due to its heterogeneous molecular weight, complex structure, and low reactivity, which lead to lower performance compared to conventional PF adhesives [2]. This low reactivity is primarily due to the methoxy groups occupying the meta position in lignin, hindering its ability to crosslink during the PF adhesive reaction [1]. Consequently, lignin addition generally reduces bonding strength while increasing free formaldehyde and phenol emissions [8], hindering the use of lignin in PF resins.

Chemical modification via demethylation, depolymerization, phenolation, and hydroxymethylation has been conducted to improve the reactivity of lignin in PF resin synthesis [1, 9-12]. Among these methods, demethylation has been the most widely studied for PF resins. Demethylation involves converting the unreactive methoxy groups of lignin into reactive hydroxyls. Typically, the demethylation reaction is performed using reagents such as 1-dodecanethiol, iodocyclohexane (ICH), sodium sulfite, or halogens acids in the presence of a base catalyst [1, 13-17]. It is generally conducted at elevated temperatures (130 °C), which increases production costs and energy consumption, using DMF as the solvent, a petroleum-derived compound [1, 13-17].

The use of demethylated lignin in PF resin adhesives has been investigated by various researcher [1, 13-17]. The effects of temperature and time on demethylation reaction were investigated by Song et al. who demethylated wheat straw alkali lignin using iodocyclohexane (ICH) to develop a lignin-PF adhesive. It was observed that 145°C and 3 hr were optimum reaction conditions. Crosslinking side reactions with hydroxyl groups were seen with a further increasing time and temperature [1]. With a 40 wt% lignin content, bonding strength decreased by 10% compared to PF resin [1]. The effect of various lignin substitutions on resin properties has also been investigated [15-16, 18-19]. Generally, bonding strength decreased as more lignin was added to the system. For example, Wang et al. demethylated alkali lignin with different halogen acids (HBr and HI) to produce a lignin-PF adhesive. At 10 wt% lignin, the bonding strength decreased by 10% and 20% with HI and HBr, respectively. With 50 wt% lignin substitution, bonding strength decreased by 40% and 60% with HI and HBr, respectively [15]. Lui et al. produced a lignin-PF adhesive using kraft lignin demethylated with sodium sulfite and sodium hydroxide. At 30 wt% lignin, bonding strength increased by 70% but only by 52% at 50 wt% lignin and decreased by 6% at 70 wt% lignin [16]. It is important to consider that all of the studies on lignin demethylation use either DMF, a petroleum-derived solvent harmful to the environment, or highly concentrated NaOH (33%), which poses significant environmental and health risks if not handled properly.

In this work, kraft lignin was first sulfobutylated to enhance its solubility, allowing demethylation to be conducted in an aqueous medium rather than in organic solvents like DMF. The objectives of this study are to: (1) perform demethylation in an aqueous medium via sulfobutylation, (2) investigate the effect of sulfobutylation on demethylation efficiency, (3) produce a lignin-phenol-formaldehyde (LPF) adhesive from the modified lignin, and (4) to examine the impact of sulfonate groups on the flame retardancy of the final product. The novelty of this approach lies in: (1) conducting demethylation in water instead of traditional organic solvents like DMF, and (2) performing a double modification of lignin—sulfobutylation followed by demethylation—for improving its performance in PF resin systems. By introducing sulfonate functional groups, sulfobutylation not only facilitates aqueous demethylation but may also enhance the flame-retardant properties of the resulting resin. In this work, 1-Dodecanethiol (DSH) was selected as the demethylation reagent due to its safer profile compared to iodocyclohexane and halogen acids. The modifications were characterized using FTIR, NMR (^{1}H, ^{31}P, HQSC), and static light scattering (SLS) to evaluate reaction efficiency. The resulting demethylated sulfobutylated lignin was then incorporated into an LPF resin to assess its adhesive performance and flame-retardant properties.

3.2 Experimental method

3.2.1 Materials

Softwood kraft lignin (KL) was obtained from a mill in Hinton, Alberta. Sodium hydroxide (NaOH), hydrochloric acid (HCl), sulfuric acid (H_2SO_4), 1,4-butane sultone (BS), N, N-Dimethylformamide (DMF), hexane, 1-dodecanethiol (DSH), phenol, formaldehyde (37 wt%), pyridine, chromium (III) acetylacetonate, cyclohexanol, deuterated chloroform, deuterated dimethyl sulfoxide (DMSO-d_6), 3–2-chloro-4,4,5,5-tetramethyl-1,3,2-dioxaphospholane (CDP), 3-(trimethylsilyl) propionic-2,2,3,3-d4 acid sodium salt (TMSP), potassium nitrate (KNO_3), hydroxylamine hydrochloride, and poly (diallyldimethylammonium chloride) (PDADMAC) were all purchased from Sigma-Aldrich Company. Sodium methoxide (NaMeO) was obtained from thermos scientific. For plywood testing, yellow birch veneer was purchased from Roarockit, and the wheat flour was purchased from Walmart.

3.2.2 Lignin modification

3.2.2.1 Sulfobutylation of kraft lignin

The sulfobutylation of lignin was conducted according to the literature [20]. First, 5 g of KL were mixed with 200 mL of H_2O. The pH was then adjusted to 12 using 1 M NaOH and left overnight. The reaction was conducted in a three-neck flask. BS was added at 0.0125:1 mole ratio (BS:KL), and the mixture was allowed to react at 70 °C for 3 hrs and 150 rpm. Following the reaction, the pH of the mixture was neutralized to 7 using 1M H_2SO_4. The modified lignin was then purified with membrane dialysis in deionized water for 48 hrs, in which the water was changed twice a day. After purification, the sulfobutylated lignin (SB) was dried in a convection oven at 105 °C. The control sample of sulfobutylation reaction (SB-C) underwent the same procedure without the addition of the BS reagent in the reaction medium.

3.2.2.2 Demethylation of sulfobutylated lignin

The demethylation of sulfobutylated lignin was adapted from literature [13]. First, 5 mL of DSH and 21 mL of H_2O were added into a 250 mL three-neck flask under a nitrogen atmosphere. The flask was then placed in an ice bath and cooled to 5-10°C. Once the temperature was below 10°C, 3.25 g of NaMeO was added to the flask. The flask was then taken out of the ice bath and allowed to warm up to 20-25°C. Once the mixture was stabilized to room temperature, 5 g of lignin was mixed with 12.5 mL of H_2O, and the mixture was transferred to a three-neck flask. The flask was placed in an oil bath at 130°C and allowed to react for 3 hrs under a nitrogen atmosphere. The reaction was then quenched with 6.25 mL of H_2O before being placed in an ice bath. Then, HCl (1 N) was added dropwise to the solution until a pH of 1. The precipitated lignin was then separated using a centrifuge at 4500 rpm for 10 min. The precipitated lignin was then neutralized using NaOH (1 M) and placed in membrane dialysis for 48 hrs, changing the water twice a day. After membrane dialysis, the demethylated sulfobutylated lignin (DSB) was dried in a convection oven at 70 °C. The dried lignin was further purified by mixing with 12.5 mL of hexane for 1 hr and filtered. The filtered lignin was then mixed with hexane one more time, and then it was placed in an oven at 70 °C and left to dry overnight. The product was a light-brown powder (DSB). The control of the demethylated reaction was denoted as DSB-C, and it was produced using the SB control sample (SB-C) followed by the demethylation reaction but in the absence of DSH. On the other hand, demethylated kraft lignin (DKL) was produced following the same procedure using KL instead of SB in the presence of DMF as the solvent instead of H_2O, as KL was water insoluble. Similarly, the control of the demethylated kraft lignin (DKL) sample was denoted as DKL-C.

3.2.3 Lignin characterization

3.2.3.1 Molecular structure of lignin derivatives

The FTIR analysis were carried out to observe the chemical structure of all lignin samples in powder form using a Bruker Tensor 37 instrument (Germany, Germany, ATR accessory). The chemical characterization of the samples was conducted using ^{1}H-NMR and H-C (HSQC) NMR. For each sample, 70 mg of lignin and 7 mg of internal standard, TMSP, were mixed with 1 mL of DMSO-d_6. The samples were then left over night to mix. The spectra were developed using a Bruker AVANCHE NEO 500 MHz instrument at 25 °C. The parameters used for the ^{1}H-NMR analysis were 64 scans, a relaxation delay of 2s, an acquisition time of 3.28s, and a 30° pulse angle. The parameters used for HSQC analysis were 8 scans, a 2s relaxation delay, with a spectral width of 250 ppm in the F1 (^{13}C) and 20 ppm in F2 (^{1}H). The NMR spectra were processed using TopSpin 4.3.0 and 4.4.0 software.

The hydroxyl groups of lignin were quantified using the ^{31}P NMR method described in the literature [21]. A solvent mixture that consisted of a 1:1.6 v/v solution of chloroform-d and pyridine, respectively. For each

test, 70-75 mg of the sample was dissolved in 1 mL of the solvent. 140 µL of 5 mg/mL chromium (III) acetylacetonate was added as a relaxing agent. The mixture was allowed to mix overnight. It was then mixed with 200 µL of CDP and allowed to react for 30 min. lastly, 70 µL of 20 mg/mL cyclohexanol was added as the internal standard and allowed to mix for 30 min before testing the sample. The spectra were measured using the same NMR instrument stated above at 25 °C.

3.2.3.2 Solubility, charge density, organic element and molecular weight analyses

The water solubility and charge density of the samples were determined as previously discussed [22]. A 20 g solution of 1 wt.% lignin was prepared and placed into a water bath shaker, where it is left overnight at 30 °C. The solution was then placed in a centrifuge at 1000 rpm for 5 minutes in order to ensure there were no suspended solids in the solution. A portion of the solution (15 mL) was used for the water solubility analysis, while the rest was titrated against PDADMAC (0.00525 M) (for anionic samples) to determine the charge density using a PCD-04+Titrator (Mütek, Germany). For water solubility, 5 mL of the solution was placed in a dry desiccated foil tray and left in the oven at 100 °C until dry, which facilitated the determination of concentration measurement.

The organic elemental analysis (carbon, hydrogen, nitrogen, and sulfur) was conducted by combusting 2 mg of each sample at 1200 °C. The elemental analyzer from Vario EL cube, (Elementar Analyse System Ronkonkoma, NY) was used to conduct the analysis [23].

The molecular weight of the samples was determined using a static light scatter (SLS) analyzer (BI-200SM Brookhaven Instrument Corp., Holtsville, NY, USA.). The samples of varying concentrations (0.2, .06, 1.2, 1.6, 2.0 mg/mL) were prepared in 20 mL of 2 M NaOH stirring at 300 rpm and 25 °C and left overnight. The samples were then filtered using 0.45 µm nylon syringe filters and transferred to 20 mL glass vials. In the SLS measurement, time-averaged intensity measurements were made at variable angles from 15° to 155° and a wavelength of 637 nm at room temperature. The measured data was then processed using Zimm plot software (Holtsville, NY, USA) in order to obtain the absolute molecular weights. Using the same samples from SLS, the samples' refractive index increment (dn/dc) was determined by a differential refractometer (Brookhaven Instruments BI-DNDC, Holtsville, USA) at 25 °C.

3.2.4 PF resin synthesis

The PF resin synthesis was adapted from the literature [24]. Lignin phenol formaldehyde resole resins with various substitution degrees of lignin (20 and 60 wt%) were synthesized in a 250 mL three-neck flask with a pressure equalizing addition funnel. In a typical run, 20 g of lignin/phenol, 4 g H_2O, 4 g of 50 wt% NaOH (10 wt% of phenolic feed) and 10 mL of ethanol were mixed into a three-neck flask, which was then placed into a water bath at 80 °C for 2 hrs. Then, 22.4 g of formaldehyde (37 wt%) was added to the three-neck flask dropwise using the pressure equalizing funnel. Formaldehyde was added with a mole ratio of 1.3:1 formaldehyde to phenol. After allowing the reaction to proceed for an additional 2 hours following the addition of formaldehyde, the reaction was quenched by placing the three-neck flask in a water bath until the flask temperature dropped to room temperature. The resins made from DSB with 20 wt.% and 60 wt.% lignin substitution was denoted as DSBPF20 and DSBPF60, respectively. Control resin samples with KL, SB and DKL were also made at 20 wt.% lignin substitution and denoted as LPF20, SBLPF20, DKLPF20.

3.2.5 PF resin characterization

3.2.5.1 Chemical structure

The structural insights of the PF and lignin-based PF resins was investigated using ^{1}H-NMR, ^{13}C-NMR, and HSQC NMR. For each analysis, 80 mg of resin was mixed with 750 µL of DMSO-d_6. The samples

were then left over night to mix. The ^{1}H-NMR and HSQC NMR analyses were conducted as described in section 3.2.3.1. For ^{13}C-NMR analysis, the parameters were 800 scans with an 8s relaxation delay [14].

3.2.5.2 Free formaldehyde and non-volatile content

The free formaldehyde content of the resins was determined according to the literature [24]. In this set of experiments, 2 g of resin was diluted in 25 mL of water. The pH was then adjusted to 4 using 0.1 M HCl. Then, 30 mL of hydroxylamine hydrochloride (0.5 M, pH= 4.0) was added to the resin, and the mixture was allowed to stir for 10 minutes. The free formaldehyde content was then determined by back titration to pH 4.0 using 0.1 M NaOH. The non-volatile content was determined according to ASTM D4426-01, in which 1 g of resin was placed in a dry aluminum tray and then placed in the oven at 125 °C for 105±3 min, and its non-volatile content was determined following a mass balance for the sample before and after the drying [9]. After the non-volatile test, the cured resin was then grinded into a powered and used for water absorption and TGA

3.2.5.3 Molecular weight analysis

The molecular weight of the resins were analyzed similarly to the methods stated in section 3.2.3.2. The samples of varying concentrations (0.2, .06, 1.2, 1.6, 2.0 mg/mL) were prepared using 20 mL of 10 mM KNO_3 and then left stirring at 25 °C with 300 rpm overnight. The samples were then filtered using 0.45 µm cellulose syringe filters and transferred to 20 mL glass vials.

3.2.5.4 Thermal analysis

The thermal stability of the resins was observed by means of thermogravimetric analysis (TGA) using a TGA 1000i (Instrument Specialists, Inc. Twin lakes, WI). For each sample, 10 mg of the non-volatile resin powder was heated in a platinum pan at a rate of 10 °C/min, with a nitrogen flow of 30 mL/min from 25 °C to 700 °C [24].

3.2.5.5 Water absorption

The water absorption of the resins was evaluated using tensiometry. For each sample, 150 mg of non-volatile resin powder was placed in a Theta Light tensiometer (Bolin Scientific, Finland) at room temperature for 3 hours. The weight measurements obtained were used to calculate the water absorption, following established methods from the literature [25].

3.2.5.6 Rheology

The rheological properties of PF and lignin-based-PF resins were studied by amplitude sweep, dynamic frequency sweep, and temperature sweep. The rheological studies were conducted using a Discovery Hybrid Rheometer (DHR) (TA Instruments, New Castle, DE). A 40 mm flat plate with a fixed gap of 500 µm and a purge gas cover were used to minimize any evaporation during the analysis. According to the literature [26], the amplitude sweep was conducted in the range of 0.01-10% at 25°C with 1 rad/s. It was performed first to determine the strain % for the remaining experiments. The operating parameters for frequency sweep were 0.0015 to 1.5 Hz at 25°C. The time sweep was performed for 2 hr with 1 rad/s at 25 °C. The temperature sweep was performed at 25-80°C with a heating rate of 3 °C/min and 1 rad/s.

3.2.6 Plywood analysis

3.2.6.1 Plywood preparation

All PF and lignin PF resins were tested as adhesives for the manufacturing of three-layer plywood. The method for plywood preparation was adapted from the literature [24]. Yellow birch veneer (11” x 11” x 1/16”) were conditioned at 20 °C and 60% relative humidity in a conditioning chamber to obtain a 10-12% moisture content. The resin was mixed with wheat flour (15 wt%), then the mixture was applied to both

sides of the center layer of the plywood with a spread rate of 250 g/m^3 per glue line. The face and center piece of veneer were bonded in perpendicular directions to each other (outer layer grain was vertical; center layer grain was horizontal). The plywood was then put in a hot press at 140 °C for 4 min at 2000 psi. Two panels of each sample were produced for statistical purposes.

3.2.6.2 Tensile strength test

In accordance with ASTM D906-98, the 11" x 11" x 1/16" plywood sheets were cut into 20 specimens (3¼" x 1" x 1/16"). The specimens were tested by shear stress tension loading until failure using a Bench-top universal testing machine (Model H10K-T UTM, Tinus Olsen Material Testing Machine Co. Horsham, PA) at a loading rate of 10 mm/min. Half of the specimen were tested in the open direction while the other half in the closed (ASTM D906-98). The wet tensile strength and water resistance of the plywood were analyzed by boiling 20 specimen in water for 3 hrs before testing. The percentage of wood failure was assed visually in accordance with ASTM D5266-13 (2020).

3.2.6.3 SEM/EDX/EDS

Scanning electron microscopy (SEM) was used to analyze the surface morphology of the resin samples after dry and wet tensile tests. The samples were analyzed using FE-SEM; Hitachi Su-70 with a voltage of 5 kV. The surface element mapping and elemental analysis of the samples were also carried out by energy dispersive spectroscopy (EDS) and energy-dispersive X-ray spectroscopy (EDX) at a voltage of 200 kV, where the samples were coated with gold and carbon glue [27].

3.2.7 Flame Retardancy

The flame test was conducted according to the literature [28]. Plywood samples were cut into 1" x 1" specimen. The specimen was then ignited directly using a torch. Once the flame was established, the torch was removed, and the specimen was recorded on video to observe the burning process. If the fire was quenched upon ignition, the torch was reapplied until the specimen reignited. Once fully ignited, the specimen was allowed to burn until the flame either consumed it completely or extinguished itself. The smoke density analysis was performed in conjunction with the literature [28]. Plywood samples were cut into 1" x 1" specimen. The samples were then placed in a smoke density apparatus (Model ACI-2843, Advance Instruments CO., Limited. Suzhou, Jiangsu, China). The samples were ignited by a direct contact with flame and exposed to 0.14 MPa of propane gas for 240s after ignition. The sample's smoke density rating (SDR) and light absorption was assessed and reported. The SDR is a measure of the concentration of smoke, while light absorption is the amount of light absorbed by smoke particles during combustion.

3.3 Results

3.3.1 lignin derivative characterization

3.3.1.1 Chemical structure of lignin derivatives

The FTIR spectra of lignin derivatives is seen in Figure 3-1. It can be observed that the stretching vibrations of (S–O) bonds at 660 cm^{-1} and (O=S=O) bonds at 1040 and 1120 cm^{-1} increased with sulfobutylation when compared KL [29-30]. The aromatic hydroxy, aliphatic hydroxy and methoxy can also be seen at 1218, 1039, and 1457 cm^{-1}, respectively, which were reduced via sulfobutylation. This is attributed to the sulfonate functional group grafted onto the lignin. For the control sample of sulfobutylation (SB-C), a decrease in the stretching vibrations for the S–O and S=O, methoxy, aliphatic hydroxyl, and aromatic hydroxyl bonds was observed. The presence of S=O and S–O vibrations, despite the absence of a sulfobutylation reaction, indicates that sulfur containing groups were attached to kraft lignin during pulping and lignin extraction

processes. However, these vibrations, and thus the concentrations of such groups decreased for the control sample (SB-C vs KL) because the control sample went through membrane dialysis.

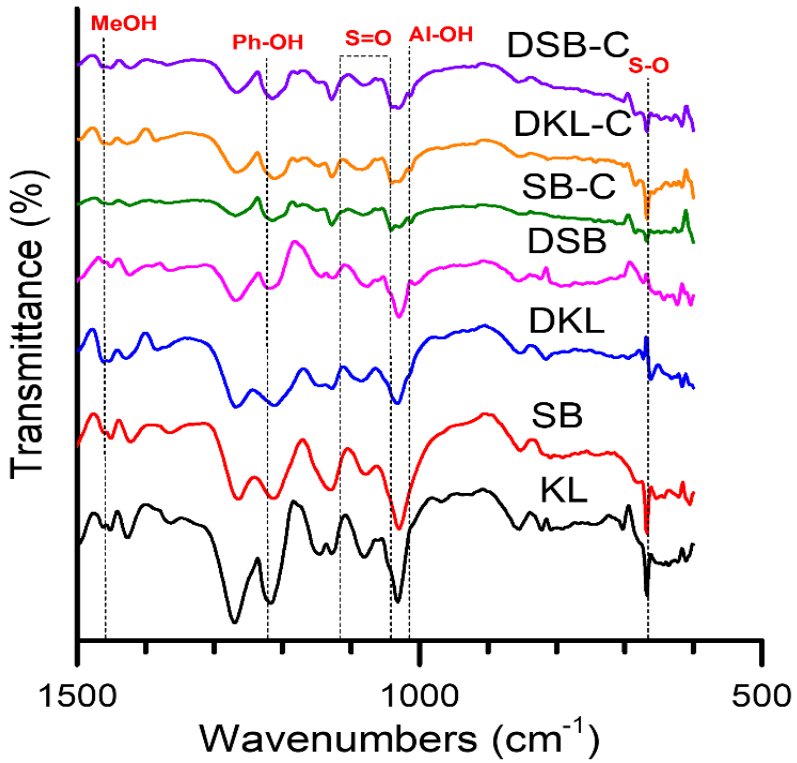

Figure 3-1: FTIR of lignin derivatives.

After the demethylation of the SB sample, it is evident that the stretching vibrations of (S–O) and (O=S=O) bonds decreased for DSB compared to SB, which suggests that DSB lost almost all of the grafted sulfonate functional group were cleaved during the demethylation. The remaining S-O and O=S=O bonds are attributed to kraft lignin. The signals for the C–H deformation in methoxyl groups, the stretching in phenolic hydroxyl groups and the primary aliphatic hydroxyl signal at 1457, 1222, and 1032 cm^{-}, respectively, decreased, which echoes the results presented by ^{1}H NMR and ^{31}P NMR assessments [13]. A similar decrease in methoxy, aromatic hydroxyl, and aliphatic hydroxy can be observed in DKL. It should be noted that all the controls (SB-C, DSB-C and DKL-C), exhibited a decrease in aromatic hydroxyl, aliphatic hydroxyl, methoxy.

The ^{1}H NMR spectra of kraft, modified lignin derivatives can be seen in Figure 3-2a. The solvent DMSO-d_6 and internal standard, TMPS, can be seen in all samples at 2.5 and 0 ppm, respectively [23]. In all the spectra, the signals corresponding to aromatic protons, methoxy groups and sulfur attached to lignin (4) are observed at 6.95, 3.82, 3.4 ppm, respectively, highlighting the structural characteristics of lignin [15], [31].

Commented [KK9]: Why would you have AL in Lignin samples?

Commented [JP10R9]: Al-OH is present in all lignin

Commented [JP11]: I left previous changes highlighted but did not comment as I assume you read already

Commented [JP12]: new

In the spectra of SB, protons 1, 1' and 1" appear in the aliphatic regions at 3.2, 2.8, and 2.1 ppm, respectively. These peaks are associated with the carbons of the aliphatic chain of the sulfobutyl functional group and are not present in KL [20].

The intensity of the methoxy signal in SB decreased compared to KL (Table 3-1). The methoxy content decreased from 2.43 to 1.93 mmol/g for SB, which is ascribed to the breakage of the aromatic ring and methoxy groups seen during sulfoalkylation reaction [20]. The control lignin of sulfobutylation reaction, SB-C, did not have peaks at 1, 1', and 1", which is scribed to the absence of BS reagent during the reaction.

For the demethylated and sulfobutylated lignin (DSB), peaks of 1, 1', and 1" did not exist and a new peak of 2' appeared at 1.3 ppm. It is also seen that the methoxy content further decreased from 1.93 to 1.40 mmol/g via demethylation. The disappearance of peaks of 1, 1', and 1" suggest that the sulfonate functional group, which had been grafted onto KL via sulfobutylation was cleaved, which is also supported by organic element, FTIR, HSQC NMR analyses (will be discussed below). The appearance of peak 2' is a result of the aliphatic chain of DSH (demethylation reagent) incorporated into the lignin monomeric structure, which is also corroborated with HSQC NMR analysis [32]. The lack of peak 2' in the DSB-C (i.e., demethylated control samples of sulfobutylation reaction) is due to the lack of DSH in the demethylation reaction. In KL, peak 2 can be seen in the same place as peak 2'. However, peak 2 is associated with aliphatic protons of the β-1 linkages of lignin in KL [23]. In the DKL spectra, the same peaks as DSB can be seen except for those of 3 and 3' at 7.96, 2.86-2.73 ppm, respectively. These new peaks are the signals for DMF, which is attributed to the fact that DMF was used as the solvent for demethylation reaction of KL compared to water for DSB [33]. Similar to DSB, peak 2' in DKL spectrum appears at 1.3 ppm, which is also associated with DSH suggesting the incorporation of the reagent's aliphatic chain. The spectra for both DKL-C and DSB-C are very similar to that of KL, which is due to the exclusion of DSH from the demethylation reaction for the control sample fabrication.

Table 3-1: NMR quantification of lignin derivatives

Linkage	KL	SB	DSB	DKL	SB-C	DSB-C	DKL-C	Spectra range, ppm
Methoxy, mmol/g	2.43	1.93	1.4	1.56	2.33	1.96	1.48	4 – 3.25 [13]
Ph-OH, mmol/g	3.31	2.28	2.42	2.97	2.31	2.90	2.97	Syringyl: 143.5 – 139.3, Guaiacyl: 139.32 – 137.2, p-hydroxyphenyl: 137.2 –136.1 [21]
Al-OH, mmol/g	1.73	1.42	1.43	1.2	1.51	1.69	1.00	148.4 – 144.4 [21]
β-O-4	127.88	80.4	153.06	130.2	106.46	143.4	80.48	δ_C/δ_H: 71.8/4.86 [34]
β-β	120.76	92.34	118.04	168.3	92.60	130.4	159.48	δ_C/δ_H: 84.8/4.66 [34]
β-5	29.88	18.08	42.88	72	34.34	48.6	30.42	δ_C/δ_H: 87.1/5.49 [34]

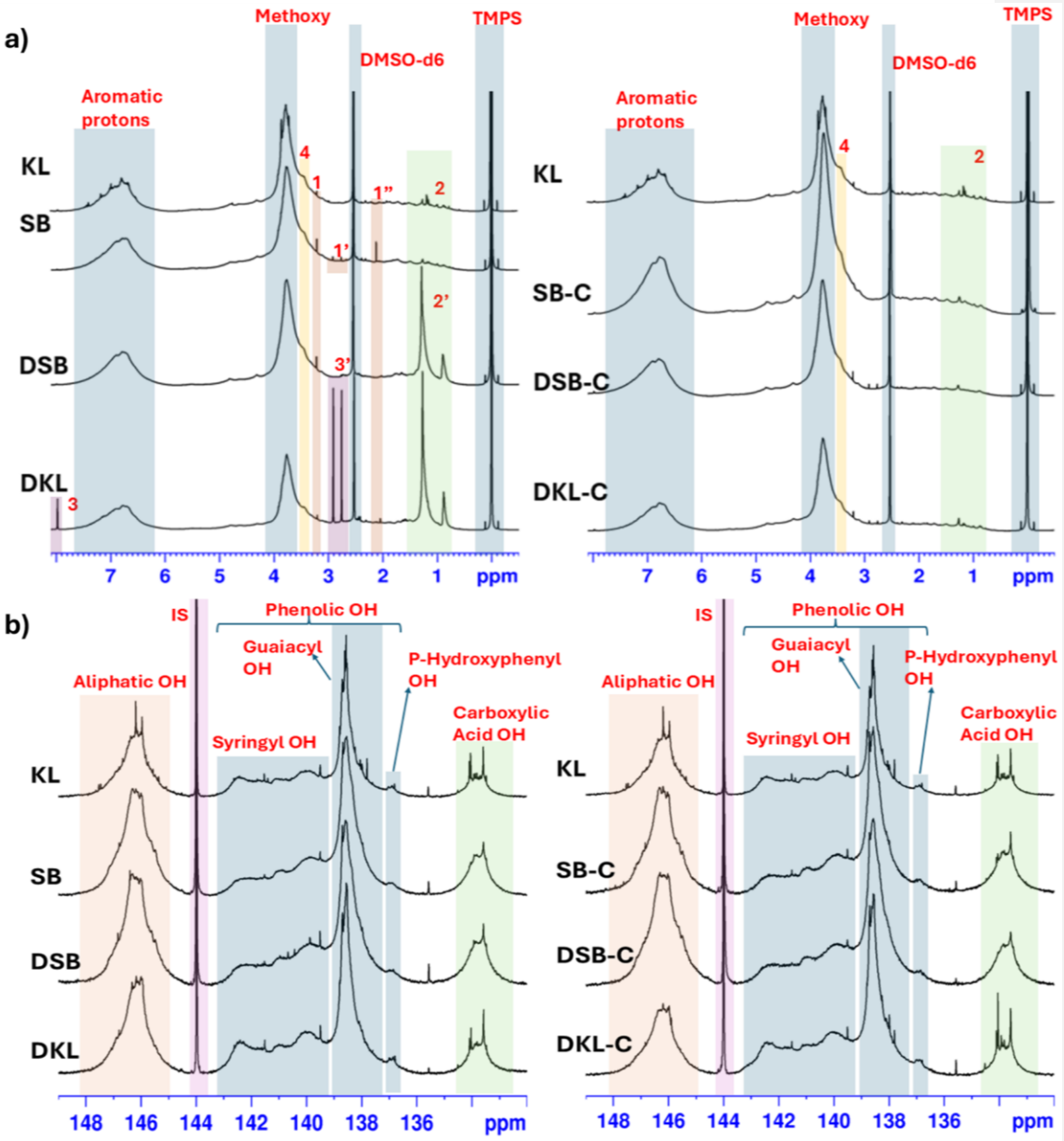

Figure 3-2: a) ^{1}H NMR spectra of lignin derivatives, b) ^{31}P NMR spectra of lignin derivatives.

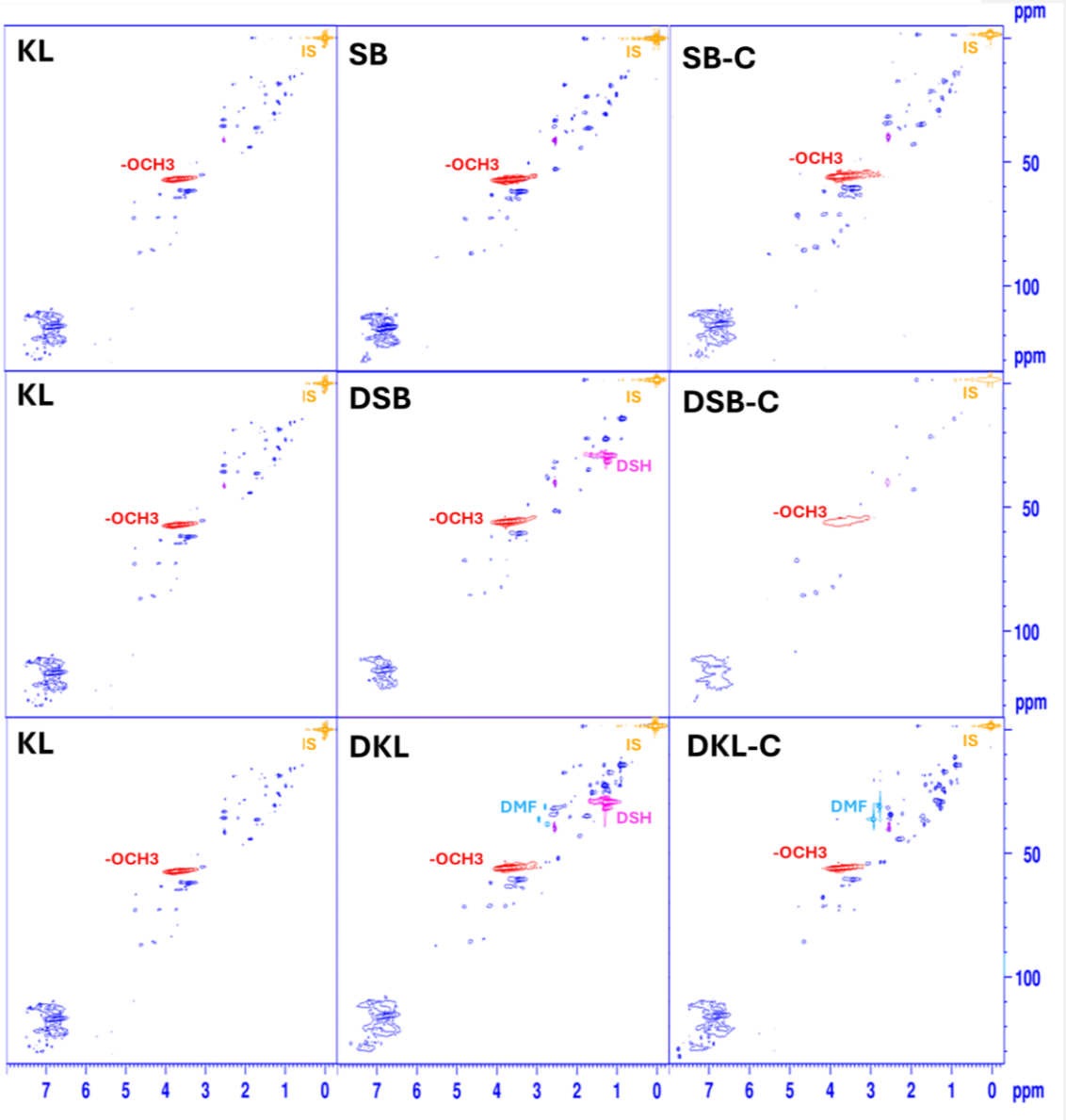

Figure 3-3: HSQC NMR spectra of lignin derivatives.

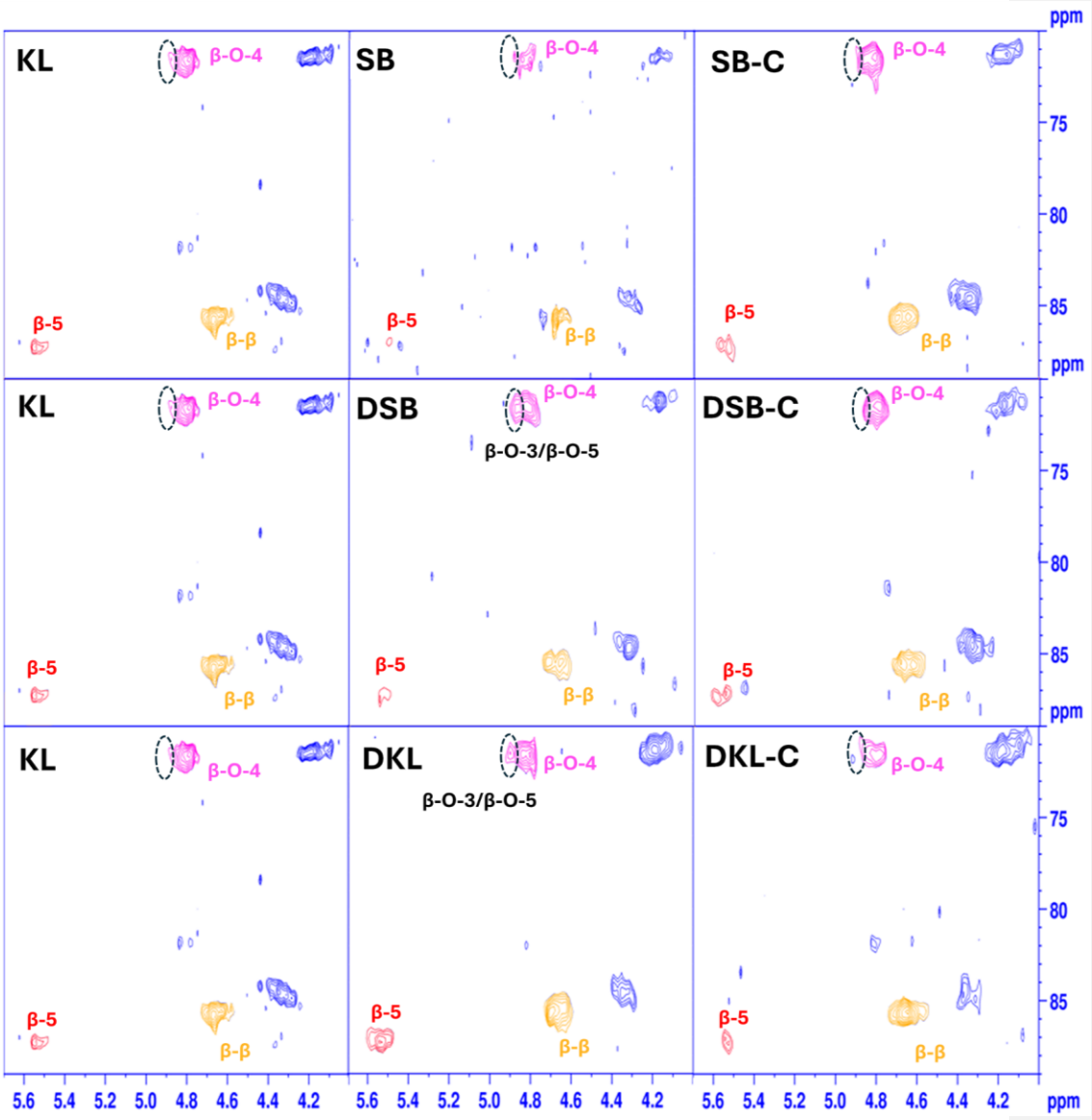

Figure 3-4: HSQC NMR of interunit linkages of lignin derivatives.

HSQC NMR spectra of lignin derivatives are observed in Figure 3-3 for full spectra and Figure 3-4 for spectra on interunit linkages. The signal for the internal standard (TMSP) and the solvent DMSO-d_6 can be seen in all the samples at δ_C/δ_H 0/-1.3 and δ_C/δ_H 41/2.5, respectively [23]. The signal for the aromatic units (δ_C/δ_H 122.9-110.6/7.5-6.7 ppm), C-O aliphatic (δ_C/δH 95-50/6-2.75), and C-C aliphatic (δ_C/δ_H 50-5/3-0.5 ppm) can be seen in all spectra [28]. The spectrum of SB is very similar to KL, with only a slight increase in the C-C aliphatic region from the aliphatic chain of the sulfobutyl functional group. This increase in the C-C aliphatic region was not seen in SB-C. In demethylated lignin derivatives (DSB and DKL), a new signal can be seen at δ_C/δ_H 29.3/1.3 ppm, which is associated with the aliphatic chain of the DSH being incorporated into the lignin monomeric structure [32], which confirms the ^{1}H-NMR results (Figure 3-2a). The DSH signal is not seen in either of the demethylated lignin controls (DSB-C and DKL-C). The signal for DMF can be seen in both DKL and DKL-C (control) at δ_C/δ_H 35.73-30.73/2.89-2.73 ppm [33]. This is because DMF was used as the solvent for DKL and DKL-C, whereas H_2O was used as the solvent for DSB and DSB-C. Furthermore, the interunit linkages (β-O-4, β-β, and β-5) of lignin were quantified in Table 3-1. It is seen that all the interunit linkages decreased with sulfobutylation. All three interunit linkages increased via demethylation of KL (for DKL), with β-β being the dominant linkage. Similarly, for DSB, all three interunit linkages increased, while the dominant one was the β-O-4 linkage.

For DSB, it is possible that β-O-4 linkages quantified in this report include β-O-3 and β-O-5 linkages. These β-O-3 and β-O-5 linkages would present themselves in the overlapping regions as β-O-4 due to the fact that β-O-4, and both of β-O-3 and β-O-5 have very similar molecular environments. However, for both of DSB and DKL, the β-O-4 signal changes in shape, gaining what looks like a second signal. This possible new signal is not present in KL or SB. Additionally, this signal is not seen in DSB-C and DKL-C. The presence of this new bond as the β-O-3 and β-O-5 can only be achieved if the oxygen in the 3 and 5 position was made available through the cleavage of the methyl group of the methoxy, which is cleaved using DSH via nucleophilic attack.

The ^{31}P NMR spectra of the lignin derivatives is observed in Figure 3-2b. All of the samples contained five characteristic hydroxyl peaks of aliphatic hydroxyl (148.4-144.4 ppm), syringyl hydroxyl (143.5-139.3 ppm), guaiacyl hydroxy (139.3-137.2 ppm), p-hydroxyphenyl (137.2-136.1 ppm), and carboxylic acid hydroxyl (134.8-132.8 ppm) [21]. The internal standard (cyclohexanol) can also be seen in all of the samples at 144 ppm. The quantification of the hydroxyl groups seen in Table 3-1. The phenolic and aliphatic hydroxyl contents decreased with sulfobutylation from 3.31 to 2.28 mmol/g, and 1.73 to 1.42 mmol/g, respectively. This is because the sulfobutyl functional group is generally grafted on the aliphatic and aromatic hydroxyl groups of lignin [20]. SB-C demonstrated a decrease in phenolic and aliphatic hydroxyls but to less extent than SB.

With the demethylation of sulfobutylated lignin (DSB), the methoxy group dropped 42 mol%, and the aromatic content increased slightly from 2.28 to 2.42 mmol/g (6 mol%) (Table 3-1). This is still lower than that of KL (3.31 mmol/g), despite the removal of 42 mol% of the methoxy groups. Similarly, a 36 % methoxy group and a 10 % aromatic and aliphatic hydroxyls group removals for DKL compared to KL were observed. DSB-C and DKL-C had a similar trend but to a lesser extent than DSB and DKL. The potential mechanism will be explained below.

3.3.1.2 Physicochemical properties

The solubility and charge density analysis for all the samples can be seen in Table 3-2. It is observed that the charge density of lignin increased for KL at 1.05 to SB at 1.31 meq/g and its solubility increased from 2.15 to 10.94 g/L, which is due to the grafting of the sulfonate functional group on the lignin structure. With the demethylation of sulfobutylated lignin, it is seen that the charge density dropped from 1.31 to 1.01

meq/g, while maintaining its solubility at 10.07 g/L, which can be attributed to the sulfonate functional group leaving the sulfobutylated lignin structure during demethylation as seen in FTIR, CHNSO and ^{1}H NMR. For DKL, it is seen that the solubility decreased from 2.15 g/L for KL to 0.54 g/L, while it was not possible to determine its charge density due to lack of solubility. The difference in solubility between DSB and DKL could be related to the condensation difference of lignin derivatives. Specifically, DSB predominantly condensed in β-O-4 (possibly β-O-3) linkage, which is water soluble, while DKL predominately condensed in β-β and β-5 interunit linkages, which is more hydrophobic affecting the solubility of demethylated lignin derivatives [35], [36]. After purification, DSB and DKL were obtained with a high yield of over 95%, while SB had a lower yield of 75%.

The organic elemental analysis for all the lignin samples can also be seen in Table 3-2. Apparently, the sulfur content decreased from 1.77% to 1.63% for SB compared to KL. As explained earlier, KL contained sulfur impurities that were purified after membrane dialysis. The lower sulfur content of SB-C than KL confirms this phenomenon since this sample was produced via purifying via membrane dialysis. However, it is observed that SB had more sulfur and oxygen than SB-C, which is the indicative of grafting sulfonate functional groups on lignin [20]. The carbon and hydrogen contents of SB increased slightly compared to SB-C, which could be due to the grafting of aliphatic chain of the sulfobutyl functional group to lignin. Such results are consistent with FTIR, ^{1}H NMR, and ^{31}P NMR results. The sulfur content can be seen to decrease from 1.63 to 1.48% in DSB relative to SB. This suggests that sulfonate functional group that were grafted during sulfobutylation left the structure of sulfobutylated lignin after demethylation, as seen with FTIR. The remaining sulfur is mainly contributed by KL. This could be a result of the high reaction temperature (130 °C) of the demethylation reaction and the acidic conditions present during precipitation of demethylated lignin (pH 1) after the reaction.

Table 3-2: Characterization properties of lignin derivatives.

Sample	C%	H%	N%	S%	O%	Charge Density, meq/g	Solubility, g/L	Molecular Weight, g/mol
KL	63.3	7	0	1.8	27.9	1.05	2.15	$(1.76\pm0.09)\times10^{5}$
SB	60.6	6.8	0	1.6	31	1.31	10.94	$(7.93\pm0.05)\times10^{5}$
DKL	63.5	8.3	1.4	2.7	24.1	N/A	0.54	$(3.65\pm0.17)\times10^{6}$
DSB	64.1	8.7	0	1.5	25.8	1.01	10.07	$(3.85\pm0.05)\times10^{6}$
SB-C	61.4	7	0	1.4	30.3	1.06	9.97	$(8.72\pm0.53)\times10^{5}$
DKL-C	62.3	7.4	1.8	1.5	27	N/A	0.42	$(2.81\pm0.12)\times10^{5}$
DSB-C	61.8	7	0	1.4	29.8	1.14	9.89	$(2.03\pm0.14)\times10^{5}$

The carbon and hydrogen contents of DSB was higher than those of SB and DSB-C. This increase could be a result of the DSH aliphatic chain incorporated into the lignin structure as seen in ^{1}H-NMR (Figure 3-2a) and HSQC results (Figure 3-3). The organic element analysis is a relative analysis. Therefore, the decrease in oxygen content would seem to increase hydrogen and carbon, which is consistent with the NMR results. It is also seen that the oxygen content of DKL was less than DSB. This is also supported by the HSQC NMR interunit linkage quantification (Figure 3-4). DKL was observed to consist of predominantly β-β, while DSB was dominated by β-O-4 linkage. This could be the reason for DSB containing a higher oxygen content. For the DKL and DKL-C samples, it was seen that the nitrogen increased, which might be a result of traces of the solvent DMF. The increase in the sulfur content could be due the CHNSO being a relative analysis. The oxygen content of DKL was lower as a result of increased β-β interunit linkages (Table 3-1), which would cause the relative carbon, hydrogen and sulfur content to increase.

The results of the molecular weight analysis can be seen in Table 3-2. The molecular weight of SB was higher than KL, which is attributed to the grafting of sulfobutyl function group to KL [20]. With demethylation of DSB and DKL, the molecular weight of lignin derivatives increased. This increase in molecular weight is consistent with NMR results (Figure 3-2) confirming that the molecular weight increase was aligned with interunit linkage increase and ultimately condensation of lignin for both DSB and DKL. This would explain why the removed methoxy groups weren't converted to hydroxy. After the demethylation reaction, before the O^- was protonated, the lignin began to condense. Interestingly, HSQC analysis (Table 3-1, Figure 3-4), confirmed that DSB condensed predominantly in β-O-4 (possibly β-O-3) linkage, while DKL condensed predominantly in β-5 linkage. The difference in molecular structure could be due to the different solvents used during the demethylation reaction since DSB used water while DKL used DMF [37]. Additionally, the cleaving of the sulfonate group during the acidic precipitation of demethylated lignin would leave an aliphatic chain that could introduce steric hinderance affecting the condensation. Molecular weight increased for SB-C, DSB-C and DKL-C. In conjunction with FTIR (Figure 3-1) and NMR (Table 3-1), this suggests that condensation occurred.

3.3.2 Reaction mechanisms

The sulfobutylation reaction mechanism can be seen in Figure 3-5. The mechanism has two stages. In the first stage, the hydroxyls of lignin are deprotonated using NaOH (pH 12). The deprotonated lignin nucleophiles then attack the BS's electrophilic sultone ring, opening the sultone ring. After nucleophilic addition, a stable sulfobutyl ether linkage is formed in the second step. The sulfobutylation of lignin conducted in this study was observed to follow these steps. A decrease in phenolic and aliphatic hydroxyls was observed (Table 3-1), along with an increase in (O=S=O) and (S–O) bonds (Figure 3-1), sulfur content (Table 3-2), and molecular weight (Table 3-2) via FTIR, ^{1}H-NMR, ^{31}P NMR, CHNSO and SLS. An increase in molecular weight, which was observed is in corroboration with literature and is due to converting low weight hydroxyls with larger molecular weight sulfobutyl groups [20]. The grafting of the sulfobutyl functional group was further corroborated by the increase in charge density and solubility that is typically seen in sulfoalkylated lignin (Table 3-2).

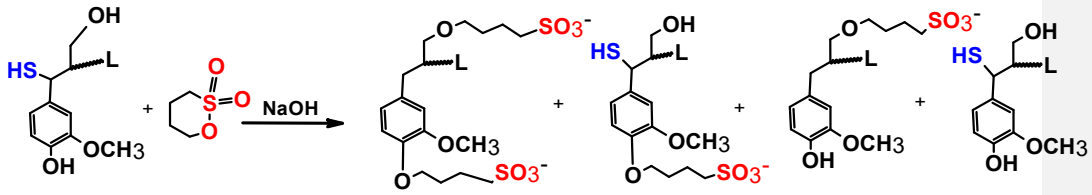

Figure 3-5: Lignin sulfobutylation reaction mechanism.

The mechanism for demethylation takes place in 3 stages. First, DSH was deprotonated using NaMeO as a catalyst. Then, the deprotonated thiol was mixed with lignin where it removes the methyl group from the methoxy through nucleophilic attack. In the third stage, the negatively charged oxygen is protonated, and lignin was precipitated using HCl. The demethylation of sulfobutylated lignin generally followed these same step. The first two steps of the reactions were the same. However, in the third step, it was observed using ^{1}H NMR, ^{31}P NMR (Figure 3-2a and 3-2b) that the methoxy content decreased by 26 mol%, while phenolic hydroxyl increased by 5 mol%. This low conversion suggests that although some negatively charged oxygens were not protonated properly, the already negatively charged oxygens interacted with some other molecules. This low conversion could be explained with HSQC and SLS results (Table 3-2).

Also, it was observed that the β-O-4 (possibly β-O-3) interunit linkages were increased by 20 mol% (Table 3-1) with increase in molecular weight from $1.76x10^5$ g/mol to $3.85x10^6$ g/mol (Table 3-2). This increase in β-O-4 (possibly β-O-3) bonds and molecular weight, along with the low conversion of methoxy to hydroxyls suggests that the lignin underwent condensation.

Another important change was the possible cleavage of the sulfonate group from the sulfobutyl functional group during the acidic precipitation of DSB, leaving its aliphatic chain [38]. The cleavage of the sulfonate group during the acidic precipitation of DSB was supported by FTIR (Figure 3-1) and organic element results (Table 3-2). As discussed in section 3.3.1.1 and 3.3.1.2, FTIR and organic element analyses observed a decrease in the (O=S=O) and (S–O) bonds and a decrease in the sulfur content, respectively. The cleaved sulfonate group would have left the lignin structure as H_2SO_3, then decomposed to H_2O and SO_2 [39]. It should also be noted that ^{1}H NMR and HSQC results suggest that the aliphatic chain of the DSH reagent could be incorporated into the lignin monomeric structure (Figure 3-2a & 3-3). Although this lines up with literature, its exact location is unknown [32].

The proposed mechanism for the demethylation of kraft lignin can be seen in Figure 3-7. Interestingly, it was observed that DKL followed a similar pathway as DSB. The methoxy, phenolic hydroxyl and aliphatic hydroxyl content was observed to decrease by 36 mol%, 10 mol%, and 31 mol% respectively (Table 3-1). This decrease, along with an increase in molecular weight (Table 3-2), and β-β and β-5 interunit linkage bonds (Table 3-1) suggests that DKL underwent condensation. However, unlike DSB, which predominantly condensed with β-O-4 (possibly β-O-3) bonds, DKL condensed primarily with β-β and β-5 bonds. This could be due the decrease in aliphatic hydroxyls seen in DKL but not in DSB (Tables 1).

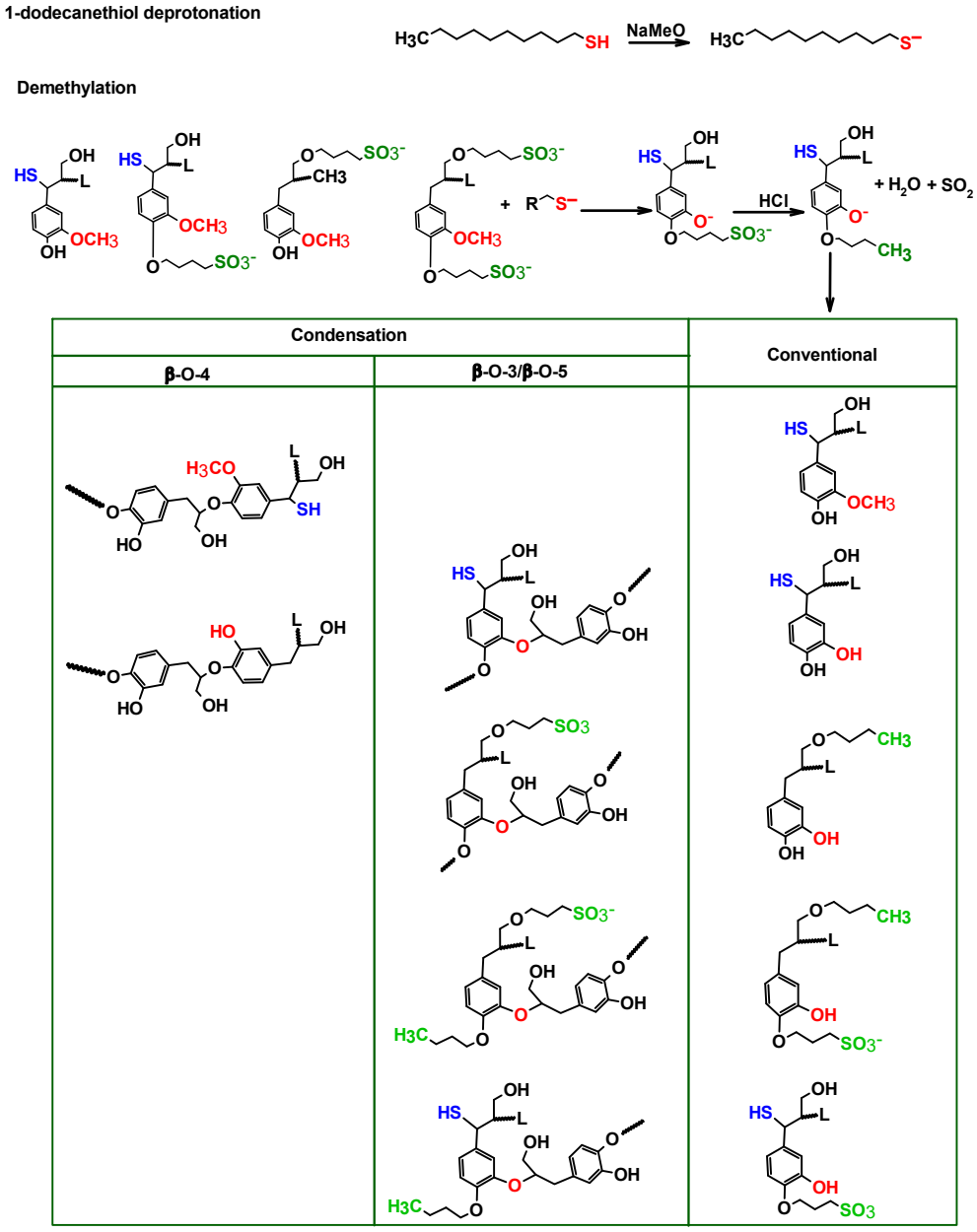

Figure 3-6: The proposed mechanism for the demethylation of sulfobutylated lignin.

Commented [PF13]: I do not see any S group in your final product, but you indeed have some S in the final product

Commented [JP14R13]: I think SO2 + water. But I cant find source. Chatgpt and bingcopilot

Commented [PF15R13]: ADD the S containing group to the sturcutre! We have discussed this many times back and forth!

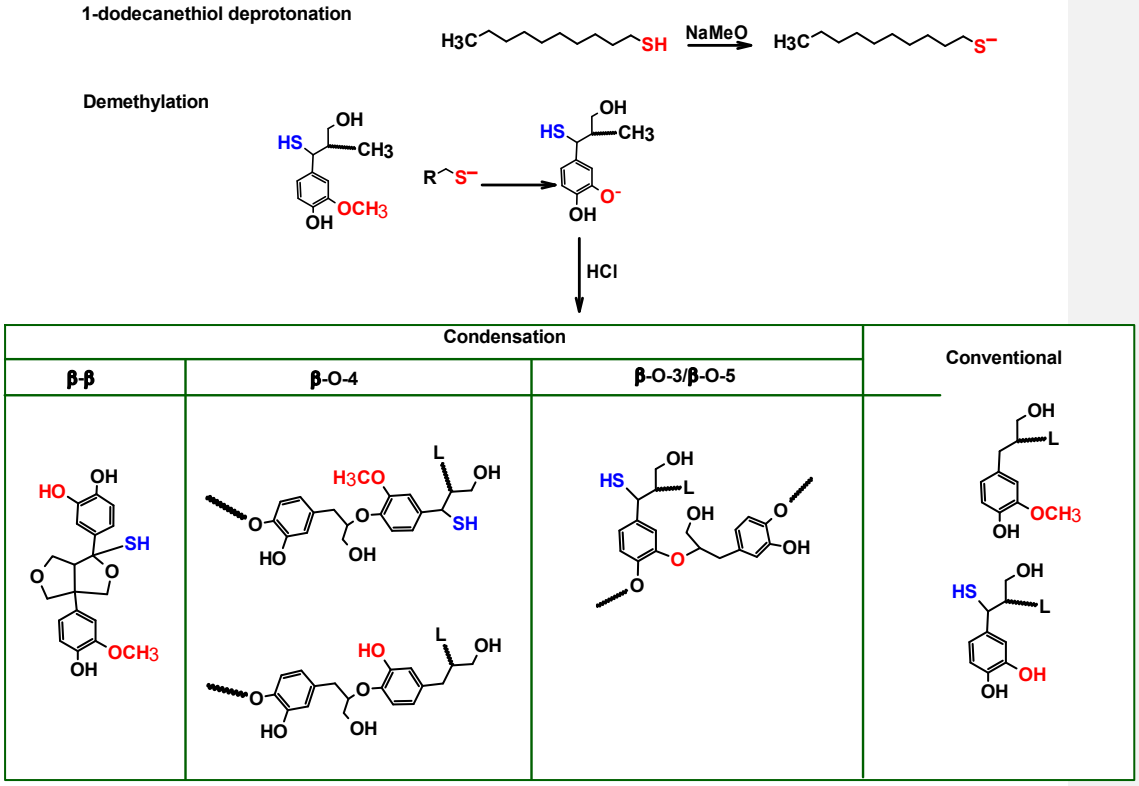

Figure 3-7: The proposed mechanism for the demethylation of kraft lignin.

Commented [JP16]: wrong

Commented [JP17R16]: Fixed

3.3.3 PF resin characterization

3.3.3.1 Chemical structure of resin derivatives

The ^{1}H-NMR, ^{13}C NMR, HSQC spectra for all of the resin samples can be seen in Figure 3-8a, 3-8b, and 3-9, respectively. All of the assigned peaks for ^{1}H-NMR, ^{13}C NMR, HSQC spectra are listed in Table 3-3. No major structural difference can be seen in any of the lignin derived-PF resins compared to PF resin. The NMR analysis identified DMSO-d_6 in ^{1}H-NMR, ^{13}C-NMR, and HSQC NMR, along with signals for methanol and ethanol across all three spectra. Reactive formaldehyde adducts were observed in ^{13}C-NMR and HSQC results. Key methylolation reaction products, including methylol (ortho/para) and methylene bridges (para-para/ortho-para), were detected in ^{13}C-NMR and HSQC spectra, with unsubstituted ortho and substituted ortho/para positions indicating different stages of methylolation. However, methylene bridges in ^{13}C-NMR spectra were difficult to distinguish due to overlap with DMSO-d_6, and no unsubstituted para positions were observed in ^{13}C-NMR. The phenoxy carbon was identified in ^{13}C-NMR spectra. Aromatic protons were clearly seen in ^{1}H-NMR spectra. In HSQC spectra, an ethanol signal overlapped with methoxy, making differentiation more challenging. The methoxy appeared in ^{1}H-NMR and HSQC spectra, where it overlapped with methanol, formaldehyde adducts, and methylol in ^{1}H-NMR spectra. Additionally, the

signal for protons adjacent to strong polar functional groups seen in ^{1}H-NMR spectra along with a C=O bond in ^{13}C-NMR spectra suggest the presence of formyl groups.

The NMR results confirmed that the main difference in all resin samples was the amount of reactive formaldehyde adducts present as the amount of lignin substituted was increased (Figure 3-9). They were not present in any of the control sample (PF, KLPF20, SBLPF20, DKLPF20). For DSBPF20, they were hardly visible, however, with increased substitution to 60 % for DSBPF60 sample, the signal strength became very prominently. This trend was also seen in ^{13}C NMR (Figure 3-8b) and HSQC NMR results (Figure 3-9). The decrease in aromatic protons and unsubstituted ortho position carbons in DSBPF60 seen in ^{1}H NMR (Figure 3-8a) and ^{13}C NMR (Figure 3-8b), respectively, could suggest a higher degree of crosslinking. Considering ^{1}H, ^{13}C, and HSQC NMR results, it is observed that the chemical structure of all lignin-based resins was very similar to that of the PF resin, with no major structural changes. In ^{1}H NMR spectra, the region with the methoxy, methylol, methanol and free formaldehyde adducts for DSBPF60 shifted slightly compared to the other resin samples. This shift could be due the amount of reactive formaldehyde adducts that was increased in DSBPF60 as seen in ^{13}C NMR (Figure 3-8b) and HSQC NMR (Figure 3-9) compared to the other resin samples. The signals were proposed using ^{13}C NMR and HSQC NMR analysis. It should be noted that the methoxy, methylol, and free formaldehyde regions in ^{1}H NMR spectra were difficult to identify due to overlapping signals.

Table 3-3: The assigned peaks for 1H-NMR, 13C NMR, HSQC spectra.

Linkage	**^{1}H-NMR, ppm**	**^{13}C-NMR, ppm**	**HSQC, ppm, δ_C/δ_H**
DMSO-d_6	2.5 [23]	34.7-39.8 [14]	40/2.5
ethanol	1.06, 3.44, 4.63 [33]	18.51, 56.07 [33]	2-36/1.08, 19/3.5, 42.8-73.0/3.48, 136.5/1.1
Methanol	3.4, 4.7 [33]	49 [14], [33]	49/3.2
Reactive formaldehyde adducts	–	80-100 [15]	80-100/3.8-5.5
Methylols, ortho	–	61.1-62.4 [14]	34-83/4.0-4.9
Methylols, para	–	63.3-64.5 [14]	
Unsubstituted, ortho	–	119.1-120.5 [14]	101-123.2/6-7.4
Unsubstituted, para	–	115.1-117.8 [14]	
Substituted, ortho	–	154.4-160.2 [14]	123.2-145/6.3-7.5
Substituted, para	–	160.7-162.8 [14]	
Phenoxy carbon	–	154-163 [14]	–
Methylene bridge, para-para	–	39.8-41.1 [14]	41/3.6
Methylene bridge, para-ortho	–	34.7-35.4 [14]	36/3.7
Methoxy	3.8 [13]	–	53-57/3.3-4 [40]
Aromatic protons	6.8 [15]	–	–
Protons adjacent to strong polar functional group	8.5 [13]		–
C=O	–	166 [41]	

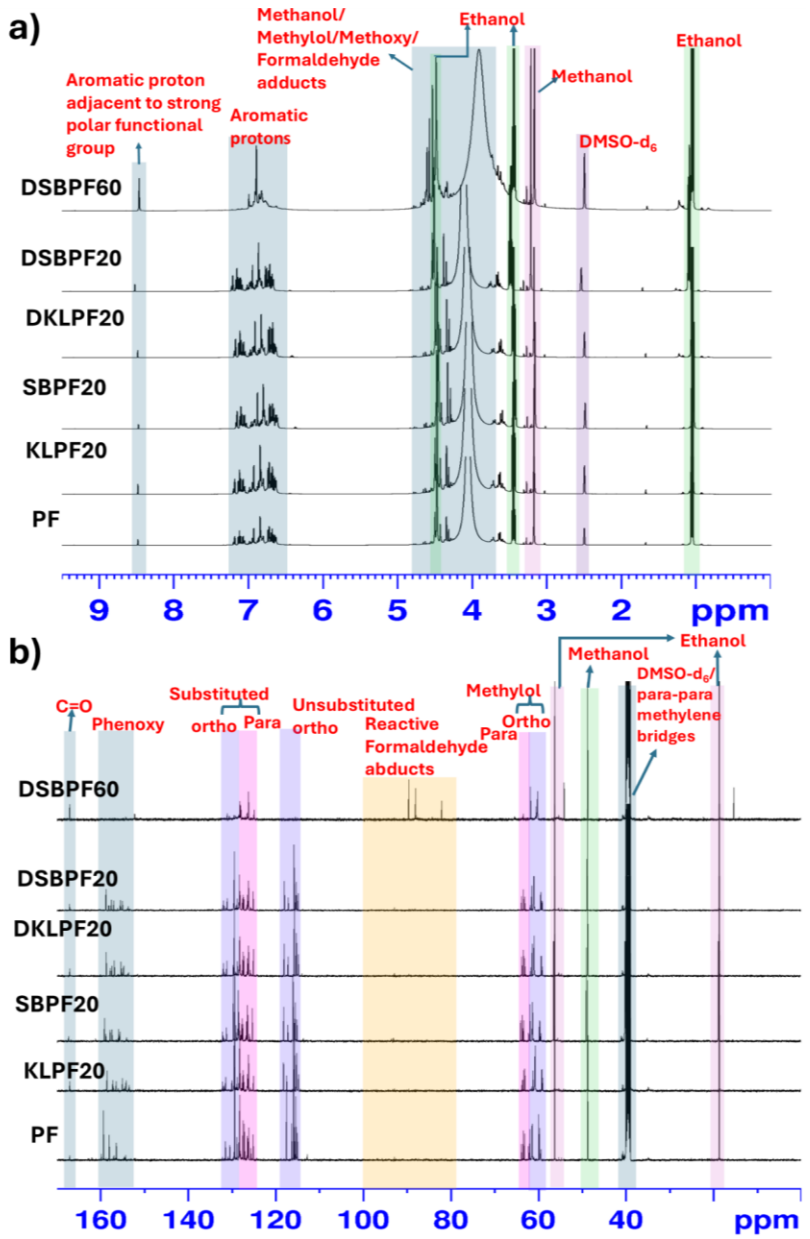

Figure 3-8: a) ^{1}H NMR spectra of lignin-PF and PF resin samples, b) ^{13}C NMR spectra of lignin-PF and PF resin samples.

Commented [PF18]: Poor figure quality

Commented [PF19R18]: Put them beside each other, like figure 2a

Commented [PF20R18]: Combine with figure 9 and make it like 2a

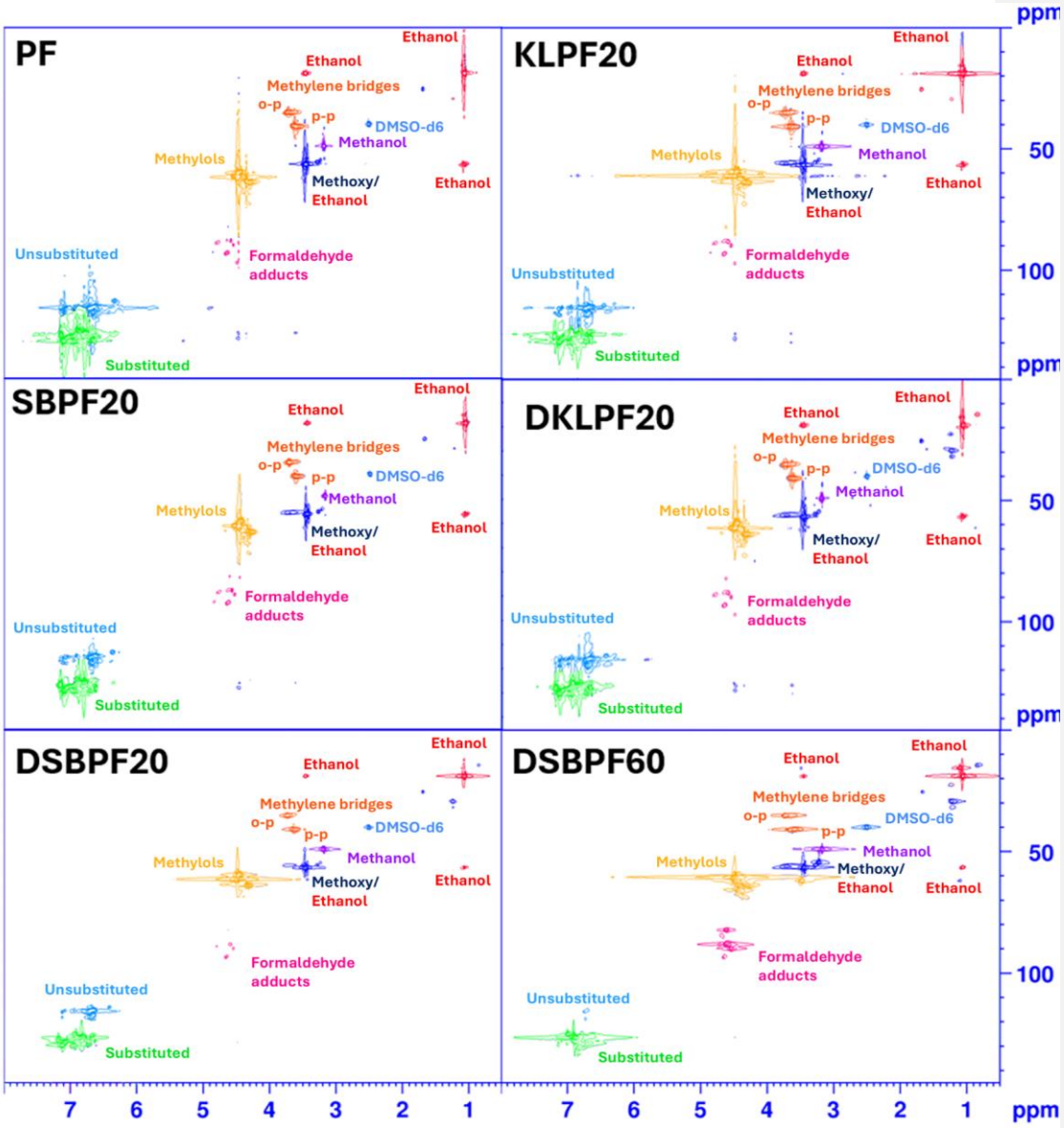

Figure 3-9: HSQC spectra of lignin-PF and PF resin samples.

3.3.3.2 Free formaldehyde, non volatile and molecular weight of resins

The molecular weight results of all PF resin derivatives are listed in Table 3-4. The Molecular weight of the resins increased with the substitution of lignin from $9.9\pm1.2\times10^4$ g/mol to $2.3\pm0.16\times10^5$ g/mol. This is because the molecular weight of lignin was larger than the molecular weight of phenol. The molecular weight of the lignin derived resins essentially followed the same trend as their corresponding lignin's molecular weight (Table 3-2). DSB has a much larger molecular weight than phenol and the other lignin samples, which would increase the molecular weigh of the resin as the 'building blocks' for crosslinking. The molecular weight of SBPF20 was larger than that of KLPF20. The molecular weight of DSBPF20 was much larger than that of DKLPF20. Although both DSB and DKL had large molecular weights, this difference was likely a result of the structural influence of condensed lignin. DSB predominantly condensed in β-O-4, which would retain its reactivity more than β-β, allowing for more crosslinking (Table 3-1) [42], [43], [44].

Table 3-4: Properties of lignin-PF and PF resin samples.

Sample	pH	Non-volatile Content, %	Free Formaldehyde Content, %	Molecular Weight, g/mol	Viscosity, cp @ 50 °C
PF	11.2	40.85± 0.89	0.18± 0.00	$(9.90\pm1.2)\times10^4$	103
KLPF20	10.3	42.70± 0.55	0.35± 0.02	$(2.30\pm0.16)\times10^5$	121
SBPF20	11.1	41.98± 0.29	0.34± 0.01	$(2.35\pm0.16)\times10^5$	39.1
DKLPF20	11.2	42.81± 0.83	0.36± 0.00	$(3.43\pm0.058)\times10^5$	127
DSBPF20	11.6	42.16± 0.17	0.35± 0.00	$(1.99\pm0.088)\times10^6$	20,051
DSBPF60	11.3	44.48± 0.26	3.18± 0.02	$(2.14\pm0.014)\times10^6$	1,773,797
GB/T 14074 [19]	**>7**	**>35**	**<0.3**	**-**	**>70**

Commented [JP21]: Fixed

The free formaldehyde emissions and non-volatile content of resins are listed in Table 3-4. As reported in the literature, the free formaldehyde content of PF resin would be increased with the additions of lignin [1]. These higher emissions are the result of the lesser reactivity of lignin compared to phenol due to the presence of methoxy in the lignin's aromatic structure [15]. For all samples with 20% lignin substitution, i.e., KLPF20, SBPF20, DKLPF, and DSBPF20, the free formaldehyde content was approximately 0.35%. This suggests that the different type of lignin used contain comparable reactivity with phenol. This level is slightly above the maximum allowable free formaldehyde content of 0.3% (GB/T-14074) [19], [45]. However, with further optimization of the PF reaction, it should be possible to reduce the free formaldehyde content to meet the standard. The hampered reactivity of DSB, compared to the controls (KL, SB, DKL) could be because although the methoxy content of lignin decreased with DSB, they were not effectively converted to hydroxy. Instead, the DSB condensed in predominantly in β-O-4 linkage of lignin (Figure 3-5), which would decrease its reactivity.

With concentrating lignin in the resin, the free formaldehyde content increased from 0.35% (DSBPF20) to 3.18% (DSBPF60) (Table 3-4) [1], [14], [16]. However, the 3.18% free formaldehyde emissions of DSBPF60 were much higher than those reported and was much higher than the standard maximum allowable free formaldehyde content of 0.3 (GB/T-14074) [19], [45]. The reason could be due to the condensation that occurred in DSB, which would hinder its reactivity (Tables 1 and 2). The pH of the PF resin and all of the lignin-PF resins was observed to be very similar, around pH 11, which follows the results of the literature [1], [16], [19]. Furthermore, with an increase in the lignin concentration to 60%, the non-

volatile content increased slightly from 42% to 44% (DSBPF60). This increase is due to the large molecular weight of lignin (Table 3-2), which decreased its volatility [46].The non-volatile content was very similar for all samples with 20% lignin substitution (KLPF20, SBPF20, DKLPF20, DSBPF20). All of the properties of the lignin derivative PF resins, except for the free formaldehyde, met the standard (GB/T-14074).

3.3.3.3 Thermal analysis

The thermal stability of PF resin derivatives are observed in Figure 3-10a & 3-10b. The TGA analysis was conducted using non-volatile resin samples. These samples were cured at 145°C for 105 minutes, ensuring that any water, moisture, ethanol, and methanol used as solvents or produced during PF resin synthesis were removed or evaporated. The degradation of phenolic resins is known to consist of three major thermal steps: post-curing, thermal reforming, and ring stripping [24]. Post-curing, which occurs from 70 to 325 °C, consists of the removal of terminal groups and further crosslinking or condensation reactions; the second event occurring from 310 to 440 °C, is attributed to the thermal reforming, where the bridged methylene linkages are cleaved; the third event, which occurs from 430 to 650 °C, is due to the breakage of the ring network [24]. The TGA analysis for all lignin-PF and PF resins contained similar decomposition pattern with all three major thermal events.

The decomposition temperatures and mass loss of each thermal event, along with the residual mass at 700 °C can be seen in Table 3-5. The KLPF20 and SBPF20 resins exhibited comparable thermal stability to the PF resin. The KLPF20 performed better in the first two thermal events, while SBPF20 showed higher thermal decomposition in the first thermal event than KLPF20 and PF. The decreased performance of SBPF20 in the first thermal event could be due to the presence of sulfobutyl functional groups in sulfobutylated lignin that were not cleaved during curing. Sulfoalkyl functional groups are known to not be very thermally stable[47]. Additionally, the decrease in thermal stability could be attributed to the aliphatic chain of the sulfobutyl functional group. If the sulfonate group was cleaved, it is possible that the aliphatic chain was left behind. This aliphatic chain could reduce crosslinking density and thermal stability as aliphatic chains are generally less thermally stable than aromatic structures [48]. The three resins synthesized with demethylated lignin (DKLPF20, DSBPF20, and DSBPF60) exhibited lower thermal stability compared to PF, KLPF20 and SBPF20. This decrease in thermal stability could be a result of the condensed structure of both DKL and DSB. DKL consists of more β-β bonds than KL, while DSB contains a higher number of β-O-4 (possibly β-O-3) linkages (Table 3-1, Figure 3-4). This would explain the decrease in thermal stability as KL is known to be more thermally stable than lignin with higher β-β and β-O-4 bonds [49].

Additionally, the bulky aliphatic chain of the sulfobutyl functional group and DSH may adversely affect thermal stability [50]. This decrease in thermal stability compared to raw PF resin is corroborated in the literature [15]. Typically, the thermal stability of PF resins decreases with the addition of lignin. With DKLPF20, the thermal stability of the resin increased compared the KLPF resin but decreased compared to PF resin. This trend is a result of the inherently less reactivity of lignin compared to phenol followed by the improved reactivity of lignin after demethylation [14], [15]. In this case, the thermal stability decreased with demethylation (DKL and DSB). This could be due to the condensation and increase molecular weight associated with DSB and DKL. The residual mass for all the resins was in the range of 60-70% [15], [17].

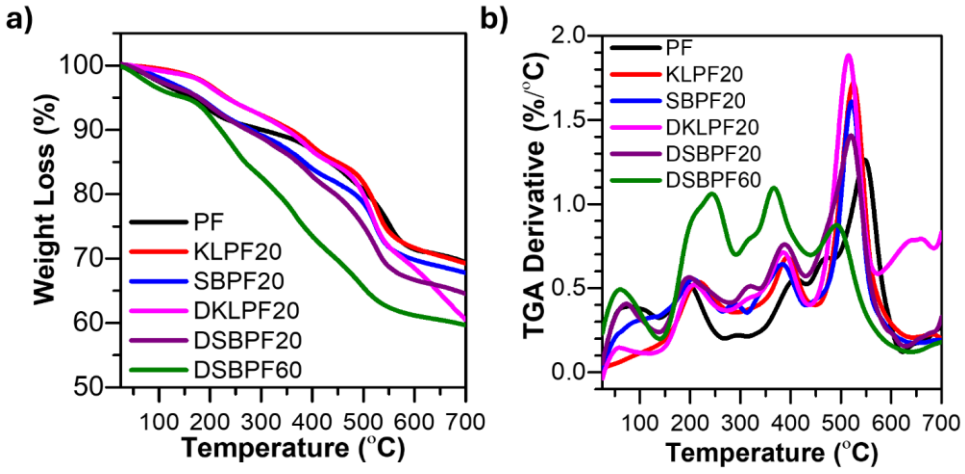

Figure 3-10: TGA profile and b) DTG profile for lignin-PF and PF resin samples.

Table 3-5: TGA and DTG results for lignin-PF and PF resin samples.

Sample	First Thermal Event $T_{onset}/T_{peak}/T_{endset}$, °C	Second Thermal Event $T_{onset}/T_{peak}/T_{endset}$, °C	Third Thermal Event $T_{onset}/T_{peak}/T_{endset}$, °C	Residual mass @ 700 °C, %
PF	70/197/300 (10%)	325/408/433 (4%)	433/448/627 (14%)	69
KLPF20	145/216/285 (6%)	334/395/447 (6%)	447/526/623 (14%)	69
SBPF20	46/206/310 (11%)	310/383/431 (6%)	431/525/640 (14%)	68
DKLPF20	61/207/330 (9%)	345/387/438 (6%)	438/515/625 (18%)	61
DSBPF20	70/198/325 (11%)	345/390/430 (6%)	430/521/625 (15%)	64
DSBPF60	63/242/291 (15%)	291/366/441 (13%)	441/492/645 (10%)	60

3.3.3.4 Water absorption

The water absorption of resins was shown in Figure 3-11. The water absorption can be seen to decrease with the addition of lignin in KLPF20. This is most likely associated with the hydrophobic properties of lignin. The water absorption further decreased for SBPF20, possibly due to the cleavage of sulfonate functional groups, which are unstable at elevated curing temperatures (Table 3-2, Figure 3-1) [47]. During the hot press curing process, which applies direct heat at 145°C, these groups may have broken down. If the aliphatic chain remained intact after cleavage, it could have increased the resin's hydrophobicity [51]. Additionally, water absorption could have decreased due to the condensation that occurred during curing, which led to increased crosslinking and reduced availability of hydrophilic sites in the resin matrix. DKLPF20 had similar water absorption to KLPF20 since β-β bonds in DKL reinforced its hydrophobicity [35]. DSBPF20 and DSBPF60 contain the highest water absorption. This increase in water absorption could be due to the increased β-O-4 (possibly β-O-3) bonds present in DSB, which are hydrophilic in nature [36].

Commented [PF22]: Unclear, why curing affect it, you still had some S groups after curing? Is it because of condensation? I think, that would be the reason? Or not?

Commented [JP23R22]: They all underwent very similar condensation so im assuming you would see similar trends with all resin, however its not true. The only different between them could be the aliphatic chain from sulfobutyl

Commented [PF24R22]: State condensation as a reason too.

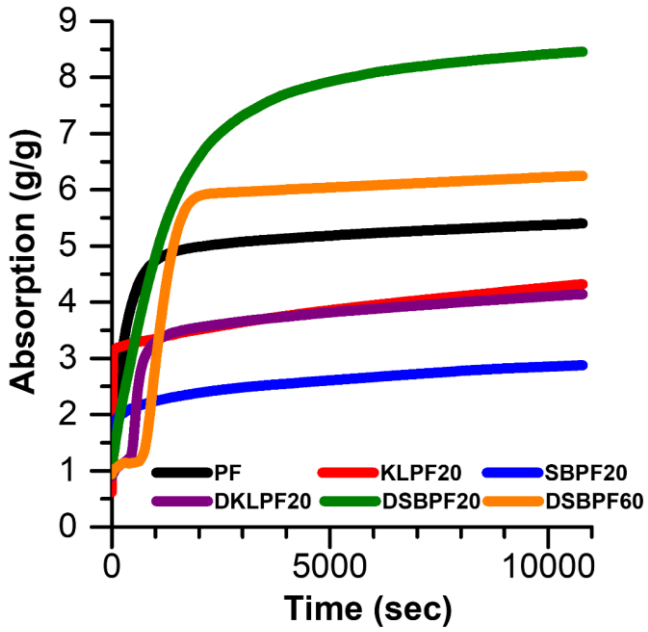

Figure 3-11: Water absorption of lignin-PF and PF resin samples

3.3.3.5 Rheological behavior

Frequency and temperature sweep tests were conducted for the rheological analysis of the samples, and the results are presented in Figure 3-12 and 3-13, respectively. Frequency sweep analysis reveals that all the PF and lignin-PF resins—specifically PF, DKLPF20, DSBPF20, and DSBPF60—exhibit shear thickening behavior in both storage and loss moduli, while their viscosity demonstrates shear thinning behavior. This behavior is common in PF resins and has been reported in the literature [26], [52]. In contrast, KLPF20 and SBPF20 show the opposite trend, with shear thinning behavior in their storage and loss moduli and shear thickening viscosity, which could be related to the shear thickening properties of lignin [53]. As the primary objective of sulfobutylation was to increase its water solubility without introducing many sulfobutyl functional groups onto the structure, the behavior of KLPF20 and SBPF20 were similar. DKLPF20 demonstrated trends comparable to KLPF20. However, data could not be recorded at low frequencies, potentially due to the low strain percentage selected during the amplitude sweep (supplementary material Figure S1), which may have exceeded the sensitivity limits of the rheometer. DSBPF20 and DSBPF60 showed the similar trends to PF. The G', G" and viscosity increased as the substitution of lignin increased. The main difference between the DSBPF resins (DSBPF20 and DSBPF60) and the rest of the PF and lignin-PF resins is that, for DSBPF20 and DSBPF60, G' > G", while the rest of the PF and lignin-PF resins have G" > G'. This suggest that the DSBPF resins (DSBPF20 and DSBPF60) exhibit more viscoelastic properties while PF and KLPF20, SBPF20, DKLPF20 exhibited more viscous properties [54]. This could be a result of a higher degree of crosslinking seen with an increased molecular weight (Table 3-2). This viscoelastic behaviour suggests that DSBPF20 and DSBPF60 could demonstrate better performance as an adhesive.

A temperature sweep experiment was conducted to observe the viscosity of the resin at different temperatures. The temperature sweep and viscosity at 50 °C can be seen in Figure 3-13 and Table 3-4, respectively. The temperature sweep results were very similar for all samples, except for DSBPF20, which exhibited slightly different behavior. As the temperature increased, DSBPF20 softened, i.e., a behavior not observed in DSBPF60. The softening behavior of DSBPF20 with increasing temperature could be due to the type of bonds present in DSB compared to PF, KLPF20, SBLP20, and DKLPF20. DSBPF20 was synthesized using DSB, which consists mainly of β-O-4 (possibly β-O-3) bonds, known to be more flexible than the β-β bonds predominant in DKL. The lower bond dissociation energy (BDE) of β-O-4 bonds (69.5–71.8 kcal/mol) compared to β-β bonds (112.5–118.5 kcal/mol) suggests lower thermal stability, possibly explaining why DSBPF20 softened with increasing temperature [44].

Additionally, the viscosity of PF, KLPF20, and DKLPF20 was similar at 103 cp, 121 cp, and 127 cp and 50 °C, respectively. The viscosity of KLPF20 and DKLPF20 was slightly higher due to the larger molecular weight and bulkier structure of lignin in KLPF20 and the higher molecular weight of DKL in DKLPF20. In contrast, SBPF20 had a significantly lower viscosity of 39.1 cp, attributing to the improved solubility of sulfobutylated lignin. For DSBPF20 and DSBPF60, viscosity increased dramatically to 20,051 cp, 242,040 cp, and 1,733,797 cp, respectively.

In contrast, DSBPF60 did not exhibit this behavior, likely due to their larger molecular weight (Table 3-4), which resulted in greater intermolecular entanglement and molecular packing. The significant increase in viscosity for DSBPF20 samples compared to DKLPF20 may be due to differences in reactivity and molecular weight. DKL primarily consists of β-β bonds, which are less reactive, while DSBPF20 contains more reactive β-O-4 (possibly β-O-3) bonds. This higher reactivity could lead to increased crosslinking, resulting in a more interconnected network, higher molecular weight, and increased viscosity [52].

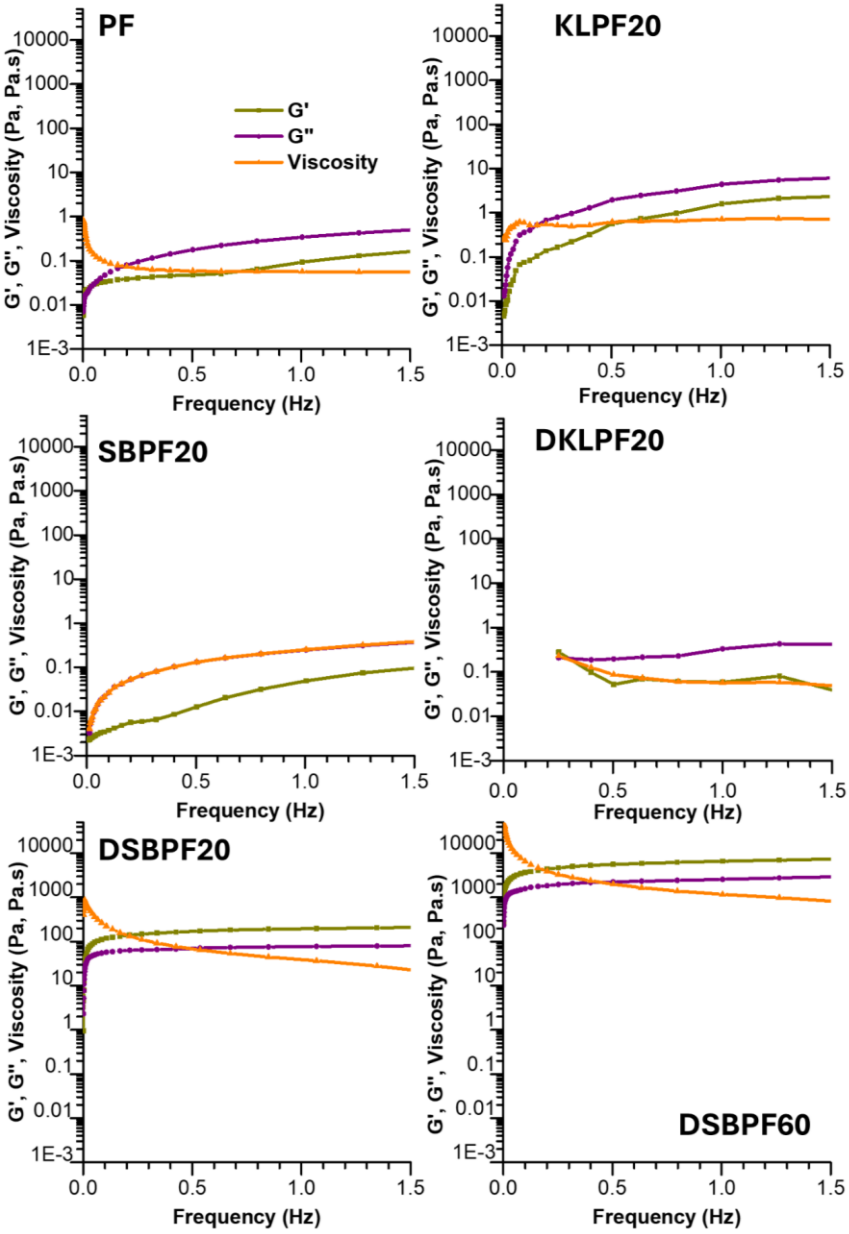

Figure 3-12: Frequency sweep of lignin-PF and PF resin samples.

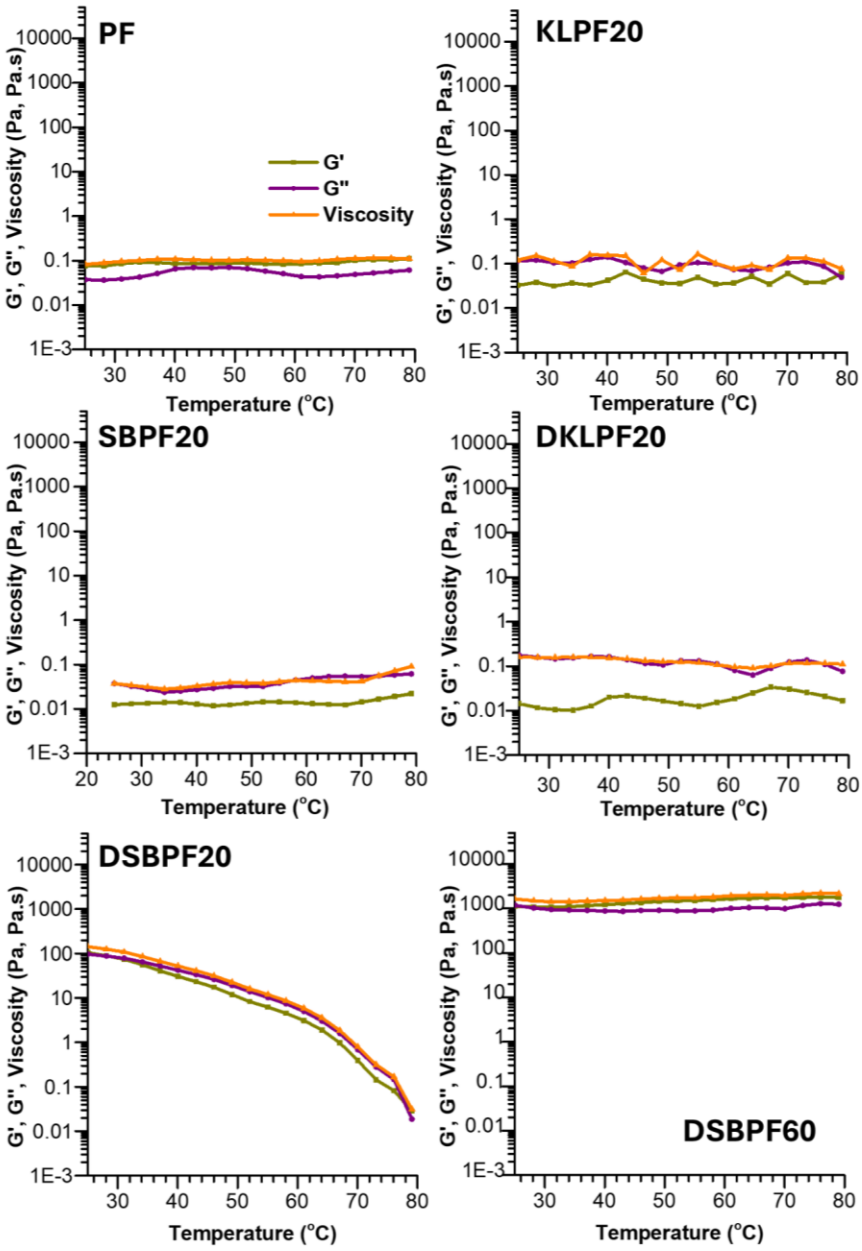

Figure 3-13: Temperature sweep of lignin-PF and PF resin samples.

3.3.4 Plywood analysis

3.3.4.1 Morphology

SEM images of the resin samples can be seen in Figure 3-14. No significant differences were observed between PF and lignin-derivative PF resins, with the main visible feature being wood fibers. This indicates that all PF and lignin PF resins (KLPF20, SBPF20, DKLPF20, DSBPF20) successfully penetrated the wood interior and adhered to the wood catheter and rays [55]. However, DSBPF60 shows fewer visible wood fibers, suggesting less penetration compared to PF resin, which is due to the larger viscosity of DSBPF60 compared to the other resin sample (Table 3-4). Despite this, no brittle fractures were observed, indicating that the adhesives withstood external forces, likely due to the viscoelastic properties of DSBPF resins (Figure 3-12). Quantified EDX results can be seen in Table 3-6. Cl, K and Ca are identified as impurities, while Na could be attributed to the NaOH used in resin synthesis. In wet samples, Na is absent because it dissolved into the water when plywood was boiled for the wet tensile test. Compared to PF, KLPF20 exhibited an increase in carbon and a decrease in oxygen content due to the larger molecular weight of lignin. SBPF20 showed a further decrease in oxygen content compared to KLPF20, reflecting the lower oxygen content in SB (Table 3-2). DKLPF20 had more carbon and less oxygen content due to a rise in β-β bonds (Table 3-1), while DSBPF20 exhibited an increase in oxygen content due to higher β-O-4 bonds (Table 3-1). Wet test samples follow a similar trend as dry samples.

Table 3-6: EDX quantification of lignin-PF and PF resin plywood samples after dry and wet tensile tests.

	PF		**KLPF20**		**SBPF20**		**DKLPF20**		**DSBPF20**		**DSBPF60**		**Wood**
Element, %	Dry	Wet	Dry	Wet	Dry	Wet	Dry	Wet	Dry	Wet	Dry	Wet	Dry
C	70.12	70.47	73.27	72.93	72.02	71.9	72.72	74.5	70.84	69.42	67.96	68.77	70.37
O	26.04	28.8	24.43	27.07	22.98	26.46	20.88	25.5	27.53	30.58	29.27	31.23	29.63
Na	3.84	-	1.4	-	2.26	0.75	2.78	-	1.63	-	1.60	-	-
Cl	-	0.73	0.9	-	1.52	-	2.47	-	-	-	1.17	-	-
K	-	-	-	-	1.22	0.66	1.15	-	-	-	-	-	-
Ca	-	-	-	-	-	0.23	-	-	-	-	-	-	-
total	100.00	100.00	100.0	100.00	100.00	100.00	100.00	100.00	100.00	100.00	100.00	100.00	100.00

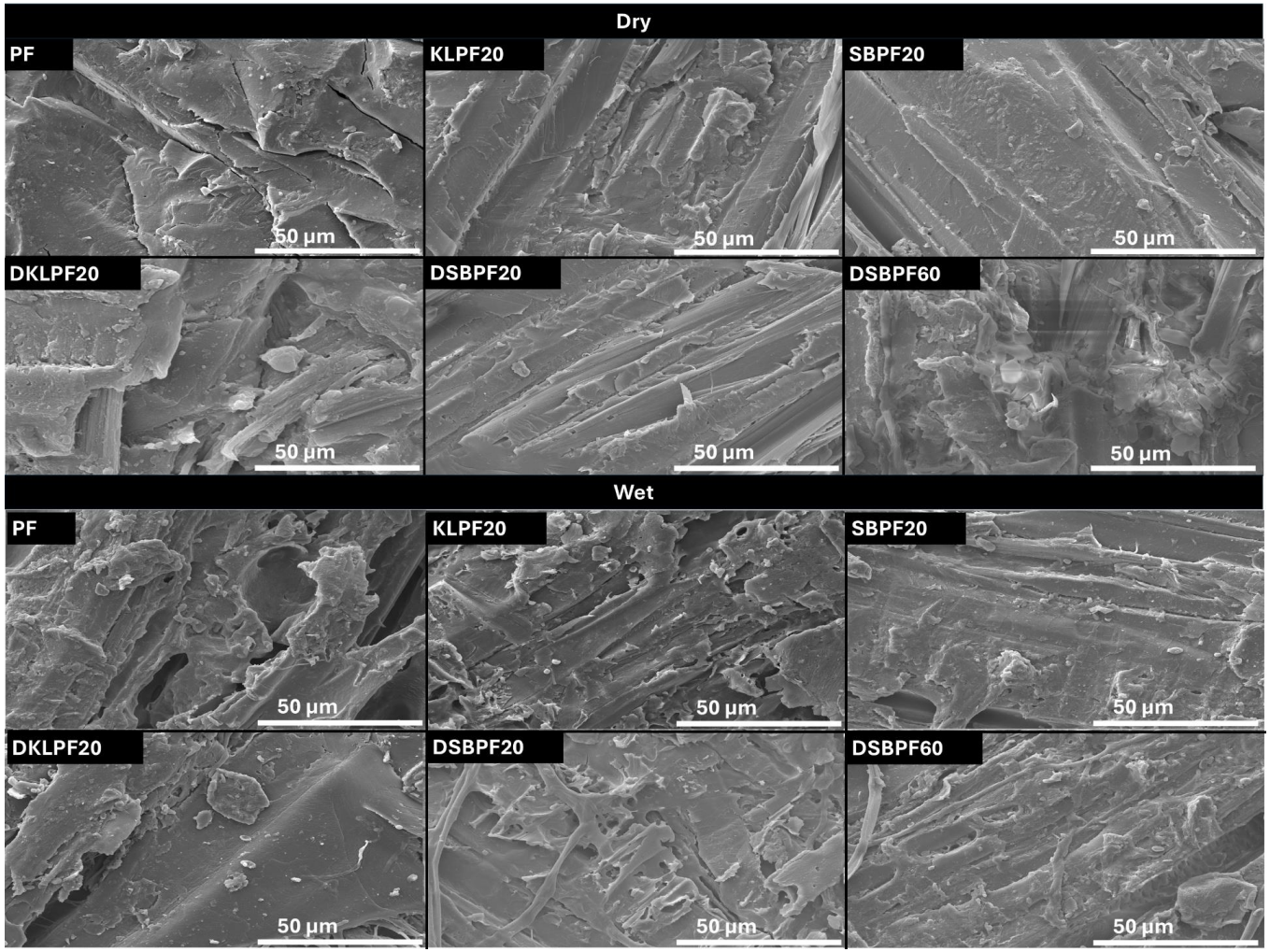

Figure 3-14: SEM images of lignin-PF and PF resin plywood samples after dry and wet tensile tests.

3.3.4.2 Mechanical characteristics

The dry and wet tensile strength for all the cured lignin-PF and PF resins can be seen in Figure 3-15. All the resins passed the JIS K-6852 standard test for dry and wet samples of 1.2 MPa and 1.0 MPa, respectively[24]. The tensile strength for PF resin was observed to be 7.63 MPa. With the addition of lignin, the tensile strength decreased to 7.40 MPa. This was expected as lignin is inherently less reactive than phenol, due to the two or less active sites of lignin, which are occupied by $^{-}OCH_3$ [14-15]. The tensile strength decreased to 7.16 MPa for SBPF20. This could potentially be due to the sulfonate functional group of SB in the resin. The sulfobutyl functional group has a bulky aliphatic chain (Figure 3-2a, Table 3-1) that could provide steric hinderance when crosslinking. The bonding strength of DKLPF20 further decreased to 6.88 MPa. Despite having a larger molecular weight, which should have improved tensile strength, this decrease can be related to relatively weak β-β bond (Table 3-1). This would increase rigidity and reduce reactive sites for crosslinking [56].

The tensile strength for DSBPF20 increased to 9.10 MPa. This increase was attributed to the large molecular weight of DSB and the inter-unit linkages. DSB predominately condensed in the β-O-4 (possibly β-O-3) linkage, which is more flexible and retains its reactivity allowing crosslinking with formaldehyde [42], [57]. Upon further lignin substitution, the tensile strength of DSBPF60 increased to 9.51 MPa. This increase in tensile strength is associated with the increased viscosity and molecular weight of DSBPF60 when compared to all the other samples (Table 3-4). The wet tensile strength closely resembles the trend of the dry tensile strength. The only difference is that the tensile strength of SBPF20 was higher than PF, KLPF20 and DKLPF20, which could be related to the decreased water absorption properties of SBPF20. It is possible that the sulfonate functional group was cleaved during the elevate curing temperatures, leaving the aliphatic chain of the sulfobutyl, reducing water solubility and improving wet performance. As seen in literature the sulfonate functional groups are not stable at elevated temperatures [47]. The wood failure for the samples can be seen in Table 3-7. The trend for the wood failure is very similar to that of the dry tensile strength. DSBPF20 and DSBPF60 where the only two samples which met the wood failure requirement (85%) [24]. The wet wood failure also followed similar tends and the tensile strength except for SBPF20. This is probably due to the decreased hydrophilicity of SBPF20, which could improve the resins performance under wet conditions.

Table 3-7: Wood failure for lignin-PF and PF resins.

Wood Failure, %						
Sample	**PF**	**KLPF20**	**SBPF20**	**DKLPF20**	**DSBPF20**	**DSBPF60**
Dry	82±9	76±11	77±18	73±25	83±7	88±6
Wet	20±11	18±8	17±12	29±18	68±15	75±14

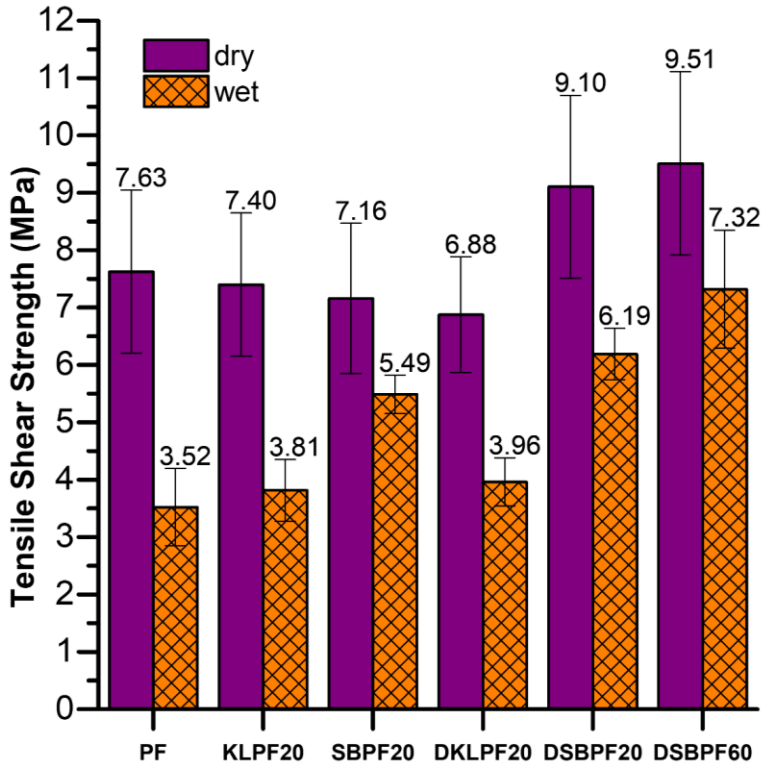

Figure 3-15:Tensile shear strength for lignin-PF and PF resins.

3.3.4.3 Flammability performance

The flame test analysis for the plywood samples can be seen in Figure 3-16. It is observed that upon ignition, the flame continuously burned the PF sample until flame extincted halfway through the plywood sample. The KLPF20 was similar to the PF in terms of ignition on the first attempt. The flame burned through the sample, consuming the entire KLPF20 sample. The SBPF20 sample showed signs of fire retardancy by self-quenching twice after ignition before the sample finally continuously burned, consuming half the sample. This self-quenching is a result of the sulfonate functional group containing fire retardant properties or the aliphatic chain of the sulfobutyl functional group [48], [58]. The DKLPF20 sample also demonstrated self-quenching, with two ignitions before the sample finally caught flame. Once ignited, the flame consumed the entire sample. This self-quenching could be due to its high molecular weight (Table 3-2), resulting from the condensation of DKL. The condensation of lignin may enhance its fire-retardant properties by increasing its molecular weight (Table 3-2), as supported by TGA analysis (Figure 3-10). DSBPF20 and DSBPF60 demonstrated fire retardancy, i.e., self-quenching twice before final ignition. Even after ignition, the flame consumed less than a quarter of the sample. The fire-retardant properties of the resins with DSB are due to its large molecular weight and high viscosity (Table 3-4), which reduce resin absorption into the veneer, leaving a thicker bond line for the fire to burn through. Additionally, the

incorporation of aliphatic chains from the sulfobutyl functional group and the DSH reagent may contribute to char formation during pyrolysis [50].

The discrepancy between the increase in flame retardancy while thermal stability of the resin decreased could be due to the difference in their curing. For the flame test plywood samples, the sample were cured for 4min at 145C and 2000 psi, while the non-volatile content was cured at 145C for

The max smoke density (MSD), average smoke density (ASD) and smoke density rate (SDR) for the smoke density analysis were all reported in Table 3-8. The MSD for the PF resin was 11.26%. With the substitution of lignin, the MSD decreased to 9.90%. This could be due to the flame-retardant characteristics of lignin, which would produce large amounts of char residue when heated at elevated temperatures [59]. The MSD of SBPF20 increased to 12.93%, likely due to the incorporation of sulfobutyl functional group. When sulfur is combusted, it produces SO_2 gas possibly increasing MSD [60]. The MSD increased for DKLPF20 compared to KLPF20. This increase is attributed to the larger molecular weigh of DKL compared to KL. It has been reported that higher molecular weight compounds would produce higher emissions [61]. DLFP20 observed a decrease in MSD to 9.18% compared to its demethylation counterpart. As mentioned earlier, DSB was primarily composed of β-O-4 bonds (358 kJ/mol), which were more thermally stable than the β-β bonds (304 kJ/mol) that were most abundant in DKL [62] The lower bond energy of β-β bonds reduced thermal stability, leading to increased combustion and smoke production. The MSD continued to increase with DSBPF60 due to the increased substitution of lignin. The light absorption reported in Figure 3-17 shows a similar pattern to that of the MSD for all samples.

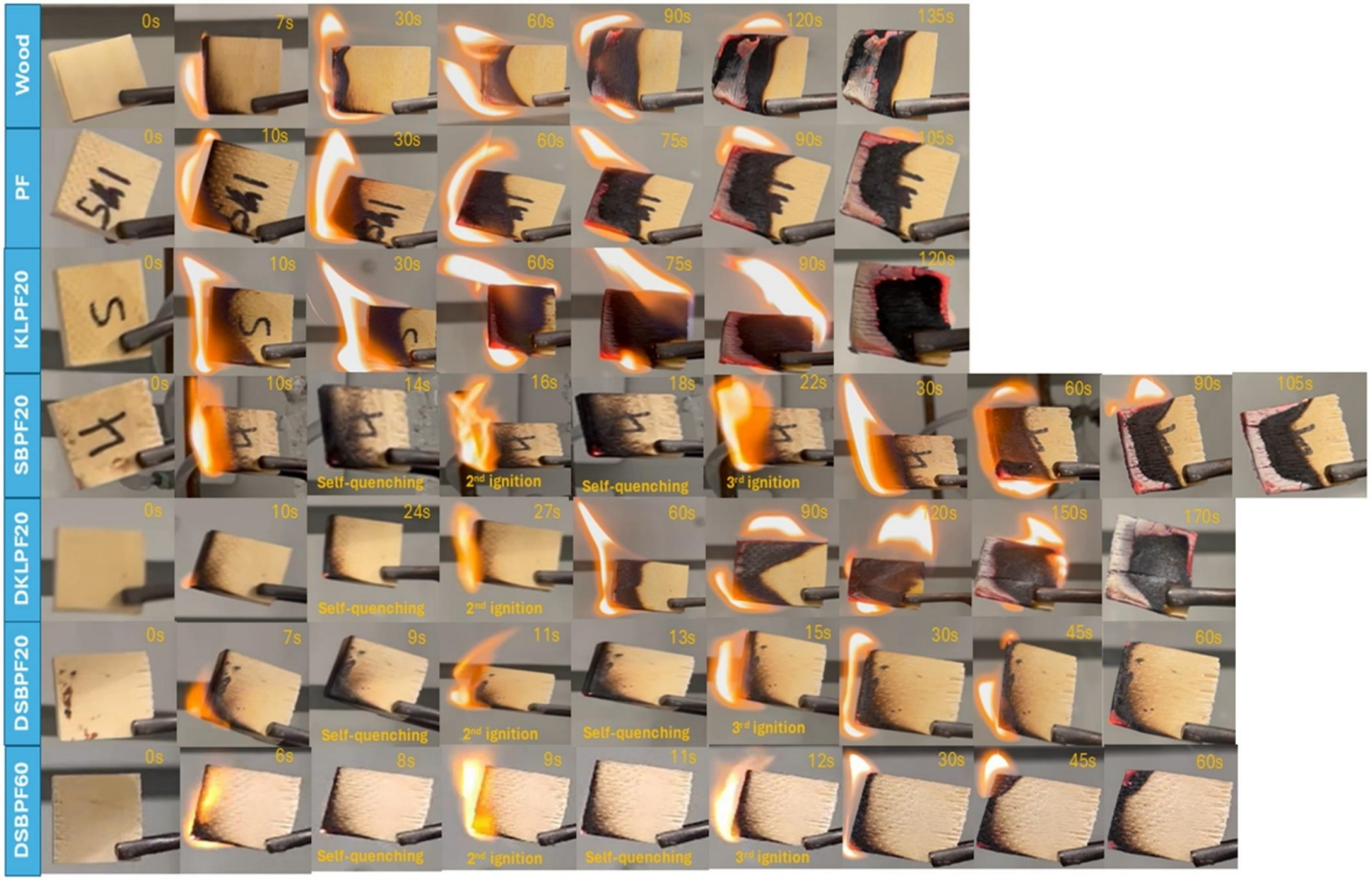

Figure 3-16: Flame test for lignin-PF and PF resins.

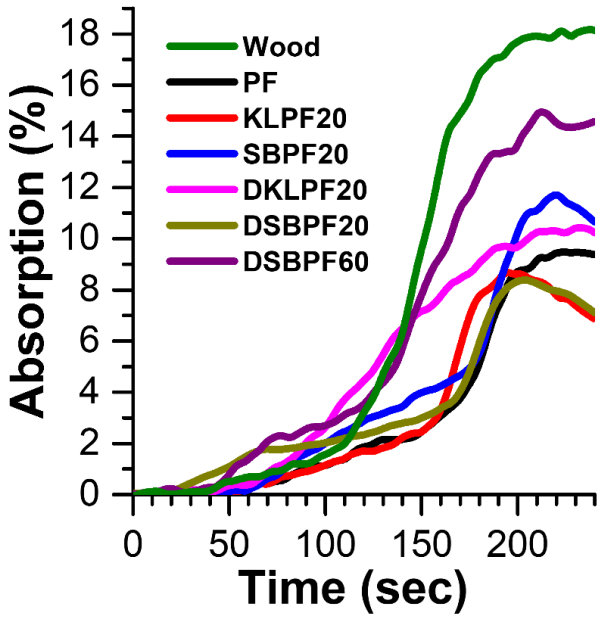

Figure 3-17: Light Absorption for lignin-PF and PF resins.

Table 3-8: Smoke Density for lignin-PF and PF resins.

Sample	Max Smoke Density (MSD), %	Average Smoke Density (ASD), %	Smoke Density Rate (SDR), %
Wood	19.47	7.28	7.26
PF	11.26	4.02	4.00
KLPF20	9.90	3.11	3.09
SBPF20	12.93	3.93	3.91
DKLPF20	11.28	4.86	4.83
DSBPF20	9.18	3.40	3.39
DSBPF60	15.81	6.18	6.15

3.4 Discussion

3.5 Impact of Sulfobutylation on resin properties

As observed by ^{1}H-NMR (Figure 3-8a), ^{13}C-NMR (Figure 3-8b), and HSQC NMR results (Figure 3-9), there was no major change in the molecular structure of SBPF20 compared to raw PF resin. The pH, non-volatile content, free formaldehyde content, and molecular weight (Table 3-4) of the SBPF20 resin were very similar to those of KLPF20. This similarity may be attributed to the minimal amount of sulfobutyl functional groups grafted onto the lignin as the objective of sulfobutylation was to graft the fewest possible SB groups to only mimic it water soluble. The increase in molecular weight of SBLPF20 was due to the larger molecular weight of SB compared to phenol in PF resin. The increased solubility (Table 3-2) results in a decreased viscosity (Table 3-4) for SBPF20 compared to PF and KLPF20 resin, leading to a decreased bonding strength (Figure 3-15). SBPF20 exhibited a weaker bonding strength compared to other resins, while its wet bonding strength was superior to PF, KLPF20, and DKLPF20 (Figure 3-15). This improved wet bonding strength was likely due to the cleavage of the sulfonate functional group at elevated curing temperatures, which reduced water solubility. Additionally, SBPF20 showed lower thermal stability than PF, KLPF20, and DKLPF20 (Figure 3-10a), and it demonstrated the lowest water absorption among all the resins. Furthermore, SBPF20 displayed fire-retardant properties, which were attributed to the charring characteristics of lignin, the self-quenching nature of sulfonate functional groups, and the influence of aliphatic chains (Figure 3-16). These effects could be attributed to the bulky aliphatic chain of the sulfobutyl functional group. The aliphatic chain may have introduced steric hindrance affecting crosslinking and leading to the decrease in bonding strength. At the same time, its presence enhanced hydrophobicity, contributing to improved wet bonding strength and reduced water absorption. However, aliphatic structures generally have lower thermal stability than aromatic ones due to their lower crosslinking density, which likely explains the reduced thermal stability observed in SBPF20. Additionally, aliphatic chains may have played a role in the resin's fire-retardant behavior, potentially influencing the combustion process alongside lignin's charring ability.

3.6 Impact of demethylation on resin properties

Similarly, SBPLPF, DSBPF20, and DSBPF60 had very similar molecular structures to raw PF resin (Figures 8, 9 and 10). The only difference was the reactive formaldehyde adducts that seem to increase with the substitution of DSB with DSBPF20 and DSBPF60 (Figure 3-10). The bonding strength increased by 19% with DSBPF20 and 25% with DSBPF60 compared to raw PF resin (Figure 3-15). The molecular weight of DSBPF20 was significantly larger than KLPF20, SBPF20, and DKLPF20 (Table 3-4). Following the same trend, the viscosity of DSBPF20 was also significantly higher than PF, KLPF20, SBPF20, and DKLPF20. Viscosity also increased significantly as molecular weight increased, following the trend of lignin substitution (Table 3-4). As lignin substitution increased, viscosity and molecular weight increased as well (Table 3-4). The thermal stability of DSBPF20 and DSBPF60 was lower than all other resin samples (Figure 3-10a). Water absorption was higher for DSBPF20 than DSBPF60, with both having the worst water absorption among the DLPF samples (Figure 3-11). The fire retardancy of DSBPF60 was higher than DSBPF20 (Figure 3-16). These effects were likely due to the larger molecular weight and dominant β-O-4 (possibly β-O-3) linkages of DSB, which influenced bonding strength, viscosity, thermal stability, water absorption, and fire retardancy. Bonding strength increased by 19% with DSBPF20 and 25% with DSBPF60 compared to raw PF resin (Figure 3-15). The wet bonding strength revealed a similar pattern of DSBPF60>DSBPF20 with all of the resins with DSB outperforming PF resin (Figure 3-15). However,

thermal stability decreased for DSBPF20 and DSBPF60. Water absorption was highest for DSBPF20 and DSBPF60. Fire retardancy was improved, with performance where DSBPF60 performed better than DSBPF20 (Figure 3-16). The changes observed in bonding strength (Figure 3-15), viscosity (Table 3-4), thermal stability (Figure 3-10a), water absorption (Figure 3-11), and fire retardancy (Figure 3-16) were primarily due to the increased molecular weight (Table 3-2) and dominant β-O-4 (possibly β-O-3) linkages in DSB (Table 3-1). Higher molecular weight and interunit linkages improved bonding strength but also increased viscosity (Figure 3-15, Table 3-4). As lignin substitution increased, viscosity rose due to the higher proportion of lignin (powder) and reduced phenol (liquid) content. However, the prevalence of β-O-4 linkages reduced thermal stability and increased water absorption due to their hydrophilic nature (Figure 3-10 and 3-11). At the same time, high viscosity and molecular weight led to reduced resin penetration into the veneer, forming a thicker bond line that improved fire retardancy, with additional contributions from sulfobutyl functional groups and the DSH reagent aliphatic chain promoting char formation.

As the substitution of lignin increased (DSBPF60), the free formaldehyde content increased while, the pH, and non-volatile content remained unchanged (Table 3-4). Molecular weight, viscosity, flame retardancy and bonding strength increased whereas thermal stability decreased with higher lignin substitution. DSBPF60 contained the highest free formaldehyde content at 3.18%, which was much higher the allowed 0.3% by the Chinese standard (GB/T 14074). It should be note that DSBPF20, KLPF20, SBPF20 and DKLPF20 contained 20 wt% lignin substitution. Compared to SBPF, DSBPF20 had similar free formaldehyde content, non-volatile content, and pH, but exhibited significantly higher viscosity and molecular weight. Both dry and wet bonding strength were improved compared to SBPF while thermal stability was lower due to condensation of DSB. Water absorption increased, and smoke density and fire resistance were enhanced.

3.7 Implications of the developed process

In Table 3-9, a comparison of the demethylated sulfobutylated PF resin can be seen against other lignin derivate PF resins that are reported in the literature. There is no standard PF resin synthesis, or hot-pressing procedure. All previous studies had different fabrication conditions, such as reaction, temperature, reaction time, formaldehyde/phenol mole ratio, steps of formaldehyde addition to resin, hot press time, temperature, and pressure for curing conditions. This inconsistency should be addressed for data to be reliably compared. Generally, bonding strength was decreased by up to 60% when lignin was added up to 50 wt%. Only two investigations have reported an improvement in performance with demethylation [16], [19]. Liu et al, reported an improvement in bonding strength of 70% (30 wt% kraft lignin substitution) and 52% (50 wt% kraft lignin), while keeping the free formaldehyde content under the 0.3% threshold [16]. They also had a lower F/P mol ratio than the current work. However, their best performing resin only contained 30 wt% lignin. At 70 wt% the performance of the lignin-PF resin was lower than PF resin. Additionally, their reagent curing consisted of a 2-step hot press process, which would increase production costs compared to the single stage hot press seen in most literature. Chen et al, reported an increase of 33 % in bonding strength with 20 wt% alkali lignin substitution, while maintaining the free formaldehyde around 0.12% [19]. With an increased lignin substitution (60%), the bonding strength was the same as raw PF with 0.28% free formaldehyde content [19]. This performance was maintained through the incorporation of urea, which forms a urea-formaldehyde (UF) resin and helped to improve strength and consume free formaldehyde. However, this study primarily focused on the emission of volatile organic compounds and did not characterize the resins or evaluate their performance under wet conditions, which is a notable drawback, particularly for UF resins.

Other modifications such as depolymerization, phenolation and hydroxymethylation have been reported a similar decrease in performance of up to 15% with 70 wt% lignin-oil can be seen. Typically, depolymerization has been seen to be the most consistent to improve performance with an increase from 8% to 58%. However, without the use of expensive catalyst, the yield of depolymerized lignin is typically low (15-56%) [9], [63]. This paper investigates the aqueous demethylation of lignin, offering a more sustainable and efficient alternative to petroleum-based methods. From an environmental standpoint, this water-based approach eliminates the need for hazardous organic solvents, reducing emissions and wastes. Process-wise, it simplifies reaction conditions, improves safety, and enhances scalability. The resulting resin outperforms many literature reports, showing a 20% increase in bonding strength at 20% lignin substitution and 25% at 60%, likely due to its higher molecular weight and viscosity. Flame retardancy was also superior to conventional phenol-formaldehyde (PF) resins, likely due to lignin's inherent charring ability and large molecular weight. Additionally, wet strength performance increased compared to PF resin. Advantages include sustainability, ease of processing, improved mechanical properties, and enhanced fire resistance. Unfortunately, the free formaldehyde content of the resins in this paper were too high. Only DSBPF20 was close to meeting the 0.3% free formaldehyde emission threshold with 0.35%. this should be able to be met by optimizing PF resin reaction. However, the unreacted formaldehyde adducts seen with ^{13}C-NMR (Figure 3-8b) and HSQC results (Figure 3-9) could potentially be reduced through reaction optimization and reducing the amount of formaldehyde used in resin synthesis.

Table 3-9: Comparison of lignin PF resins in literature to this paper's lignin-PF resin.

Modification	Lignin Type	Lignin Substitution, %	Bonding Strength, MPa	Bonding strength Percent Difference, %	Free Formaldehyde Content, %	References
Unmodified	White birch bark, white spruce bark	25, 50	WBB-LPF-50: 1.33 WSB-LPF-50: 1.78	-39 -46	0.54 [b] 0.45	[64]
	Kraft	50 + 5, 10, 15, 20, 30 furfural substitution	LFPF-10: 1.19 LFPF-15: 1.30 LFPF-20: 1.11	-6 2 -13	0.21 0.24 0.47	[55]
Depolymerization	Kraft	50, 60, 70	DLPF-olig-70: 15.2 DLPF-oil-70: 11.6	11 -15	N/A 0.9	[63]
	Organosolv	50, 75	OLPF-50: 2.3 DLPF-50: 2.0	28 11	1.0 0.5	[9]
	Wheat straw	20-100	LPF-40: 1.3 DLPF-40: 1.9	8 58	1.0 0.9	[65]
Demethylation	Wheat straw Akali	40	DLPF: 2.28 LPF: 1.13	-10 -56	0.22 0.65	[1]
	Wheat straw soda	50, 60, 65	DLPF-50: 1.52 DLPF-60: 1.35 DLPF-65: 1.09	----	----	[18]
	Alkali	50	DLPF-HI: 0.9 DLPF-Br: 0.6	-40 -60	0.47 [b] 0.49 [b]	[15]
	Alkali	50	DLPF: 1.07	-14	0.31 [b]	[14]
	Soda	30	Na_2SO_3 was the most effective sulfur containing reagent. DLPF-Na_2SO_3: 1.14	-9	0.56	[17]
	Alkali	10-60	DLPF-20: 1.6 DLPF-60: 1.2	33 0	0.12 0.28	[19]
	Kraft	10-70	DLPF-30: 2.43 DLPF-50: 2.18 DLPF-70: 1.34	70 52 -6	0.089 0.187 0.272	[16]
Phenolation	Organosolv	40	PLPF: 1.36[a]	-9	0.31	[11]
	Kraft, hydrolysis, wheat straw alkali	----	----	----	----	[66]
Hydroxymethylation	Softwood Kraft	----	----	----	----	[40]
	Kraft, sodium lignosulfonate	----	----	----	----	[10]
	Cornstalk	----	----	----	----	[12]
Nano	Alkali	10-60	LPF-40:1.11 NLPF-30: 1.59 NLPF-40: 1.30 NLPF-50: 1.10	14 64 34 13	3.20 0.12 0.28 0.53	[67]
	Hydrolysis	5, 10	NLPF-5: 9.58 MLPF-5: 10.92 NLPF-10: 8.10 MLPF-10: 5.90	10 26 -7 -32	----	[68]
	Alkali	----	----	----	----	[69]
Demethylation of sulfobutylated KL (this paper)	**Kraft**	**20, 60**	**SBPF20: 7.16** **DKLPF20: 6.88** **DSBPF20: 9.10** **DSBPF60: 9.51**	**-6** **-10** **20** **25**	**0.34** **0.36** **0.35** **3.18**	**This Paper**

a: Wet strength, b: mg/L

Commented [JP25]: Deleted 40

3.8 Conclusion

SB exhibited an increase in molecular weight and sulfonate group content, along with a decrease in methoxy and hydroxyl contents. These changes, coupled with improved solubility and charge density, indicated successful sulfobutylation. DSB exhibited a decrease in methoxy and sulfonate group content, a slight increase in hydroxyl groups, and an overall increase in molecular weight and β-O-4 inter-unit linkages. These changes suggest condensation, with β-O-4 serving as the dominant inter-unit linkage. DKL exhibited a decrease in hydroxyl content, an increase in molecular weight, and β-β as the dominant inter-unit linkage. These changes suggest condensation, with β-β linkages playing a major structural role. The main difference in DSB and DKL was associated with the solvent used for demethylation.

The molecular structure of SBPLPF20, DSBPF20, and DSBPF60 remained similar to raw PF resin, with increased reactive formaldehyde adducts as lignin substitution rose. Higher lignin content led to increased molecular weight and viscosity, following the trend of lignin substitution. Increased viscosity, due to reduced phenol content and higher lignin proportion, enhanced bonding but reduced resin penetration, leading to improved fire resistance. However, thermal stability decreased for DSBPF samples due to condensation. Bonding strength improved by 19% in DSBPF20 and 25% in DSBPF60 compared to PF resin. These changes were attributed to the higher molecular weight and dominant β-O-4 linkages in DSB, which influenced resin properties. Wet bonding strength followed a similar trend, with DSBPF resins outperforming PF resin. As lignin substitution increased, free formaldehyde content rose, reaching 3.18% in DSBPF60—far exceeding the 0.3% limit set by Chinese standards (GB/T 14074). Meanwhile, pH and non-volatile content remained stable. Water absorption of the resin increased, but smoke density and fire resistance were enhanced. Additionally, sulfobutyl functional groups and the DSH reagent contributed to char formation. Overall, DSB-modified PF resins demonstrated improved bonding and fire resistance but faced challenges with thermal stability, water absorption, and excessive free formaldehyde content at higher lignin substitution levels.

Table 3-10: List of abbreviations.

Abbreviations	Full name
PF	Phenol-formaldehyde
KL	Kraft lignin
LPF	Lignin-phenol-formaldehyde
LPFA	Lignin-phenol formaldehyde adhesive
ICH	iodocyclohexane
HBr	Hydrobromic acid
HI	Hydroiodic acid
DMF	Dimethylformamide
DSH	1-Dodecanethiol
SLS	static light scattering
NaOH	Sodium hydroxide
H_2SO_3	Sulfuric acid
BS	1,4-butane sultone
CDP	3–2-chloro-4,4,5,5-tetramethyl-1,3,2-dioxaphospholane
TMSP	3-(trimethylsilyl) propionic-2,2,3,3-d4 acid sodium salt
PDADMAC	poly (diallyldimethylammonium chloride)
NaMeO	Sodium methoxide
SB	Sulfobutylated lignin
SB-C	Sulfobutylated lignin control
DSB	Demethylated sulfobutylated lignin
DSB-C	Demethylated sulfobutylated lignin control
DKL	Demethylated kraft lignin
DKL-C	Demethylated kraft lignin control
NMR	Nuclear magnetic resonance
KLPF20	Kraft lignin-phenol-formaldehyde resin (20 wt% lignin)
SBPF20	Sulfobutylated kraft lignin-phenol-formaldehyde resin (20 wt% lignin)
DKLPF20	Demethylated kraft lignin-phenol-formaldehyde resin (20 wt% lignin)
DSBPF20	Demethylated sulfobutylated kraft lignin-phenol-formaldehyde resin (20 wt% lignin)
DSBPF60	Demethylated sulfobutylated kraft lignin-phenol-formaldehyde resin (60 wt% lignin)
TGA	Thermogravimetric analysis
DHR	Discovery hybrid rheometer
SEM	Scanning electron microscopy
EDS	Energy dispersive spectroscopy
EDX	Energy dispersive X-ray
SDR	Smoke density rating
FTIR	Fourier Transform Infrared spectroscopy
Al	Aliphatic
Ph	Phenolic
CHNSO	Carbon-hydrogen-nitrogen-sulfur-oxygen elemental analysis
DMSO-d_6	Deuterated dimethyl sulfoxide
G’	Storage modulus
G”	Loss modulus
BDE	Bond dissociation energy
MSD	Max smoke density
ASD	Average smoke density
SDR	Smoke density rate
UF	Urea-formaldehyde
WBB-LPF	Whie birch bark lignin-phenol-formaldehyde resin
WSB-LPF	Whie spruce bark lignin-phenol-formaldehyde resin
LFPF	Lignin-furfural-phenol-formaldehyde resin

DLPF	Depolymerized/demethylated-lignin-phenol-formaldehyde resin
PLPF	Phenolated lignin-phenol-formaldehyde
NLPF	Lignin nanoparticle-phenol-formaldehyde
MLPF	Lignin macroparticle-phenol-formaldehyde

3.9 Reference

[1] Y. Song, Z. Wang, N. Yan, R. Zhang, and J. Li, "Demethylation of wheat straw alkali lignin for application in phenol formaldehyde adhesives," Polymers (Basel), vol. 8, no. 6, May 2016, doi: 10.3390/polym8060209.

[2] Z. Peng, X. Jiang, C. Si, A. Joao Cárdenas-Oscanoa, and C. Huang, "Advances of Modified Lignin as Substitute to Develop Lignin-Based Phenol-Formaldehyde Resin Adhesives," Aug. 07, 2023, John Wiley and Sons Inc. doi: 10.1002/cssc.202300174.

[3] C. Xu and F. Ferdosian, "Lignin-Based Phenol–Formaldehyde (LPF) Resins/Adhesives," in Conversion of lignin into Bio-Based Chemicals and Materials, Springer, Berlin, Heidelberg, 2017, pp. 91–109. doi: 10.1007/978-3-662-54959-9_6.

[4] B. Zhu, X. Jiang, S. Li, and M. Zhu, "An Overview of Recycling Phenolic Resin," May 01, 2024, Multidisciplinary Digital Publishing Institute (MDPI). doi: 10.3390/polym16091255.

[5] P. Fatehi and J. Chen, "Extraction of Technical Lignins from Pulping Spent Liquors, Challenges and Opportunities," in Production of Biofuels and Chemicals from Lignin, Biofuels and Biorefineries, 6th ed., vol. 6, 2016, pp. 35–54. doi: 10.1007/978-981-10-1965-4_2.

[6] B. Ahvazi, É. Cloutier, O. Wojciechowicz, and T. D. Ngo, "Lignin Profiling: A Guide for Selecting Appropriate Lignins as Precursors in Biomaterials Development," Oct. 03, 2016, American Chemical Society. doi: 10.1021/acssuschemeng.6b00873.

[7] W. Gao and P. Fatehi, "Lignin for polymer and nanoparticle production: Current status and challenges," Canadian Journal of Chemical Engineering, vol. 97, no. 11, pp. 2827–2842, Nov. 2019, doi: 10.1002/cjce.23620.

[8] C. Huang, Z. Peng, J. Li, X. Li, X. Jiang, and Y. Dong, "Unlocking the role of lignin for preparing the lignin-based wood adhesive: A review," Nov. 01, 2022, Elsevier B.V. doi: 10.1016/j.indcrop.2022.115388.

[9] S. Cheng, Z. Yuan, M. Leitch, M. Anderson, and C. C. Xu, "Highly efficient de-polymerization of organosolv lignin using a catalytic hydrothermal process and production of phenolic resins/adhesives with the depolymerized lignin as a substitute for phenol at a high substitution ratio," Ind Crops Prod, vol. 44, pp. 315–322, Jan. 2013, doi: 10.1016/j.indcrop.2012.10.033.

[10] M. E. Taverna, F. Felissia, M. C. Area, D. A. Estenoz, and V. V. Nicolau, "Hydroxymethylation of technical lignins from South American sources with potential use in phenolic resins," J Appl Polym Sci, vol. 136, no. 26, Jul. 2019, doi: 10.1002/app.47712.

[11] B. Luo, Z. Jia, H. Jiang, S. Wang, and D. Min, "Improving the reactivity of sugarcane bagasse kraft lignin by a combination of fractionation and phenolation for phenol-formaldehyde adhesive applications," Polymers (Basel), vol. 12, no. 8, Aug. 2020, doi: 10.3390/POLYM12081825.

[12] S. Feng, T. Shui, H. Wang, X. Ai, T. Kuboki, and C. C. Xu, "Properties of phenolic adhesives formulated with activated organosolv lignin derived from cornstalk," Ind Crops Prod, vol. 161, Mar. 2021, doi: 10.1016/j.indcrop.2020.113225.

[13] L. Hu et al., “Chemical groups and structural characterization of lignin via thiol-mediated demethylation,” Journal of Wood Chemistry and Technology, vol. 34, no. 2, pp. 122–134, Jun. 2014, doi: 10.1080/02773813.2013.844165.

[14] J. Li, J. Zhang, S. Zhang, Q. Gao, J. Li, and W. Zhang, “Fast curing bio-based phenolic resins via lignin demethylated under mild reaction condition,” Polymers (Basel), vol. 9, no. 9, Sep. 2017, doi: 10.3390/polym9090428.

[15] H. Wang, T. L. Eberhardt, C. Wang, S. Gao, and H. Pan, “Demethylation of alkali lignin with halogen acids and its application to phenolic resins,” Polymers (Basel), vol. 11, no. 11, Nov. 2019, doi: 10.3390/polym11111771.

[16] Q. Liu, Y. Xu, F. Kong, H. Ren, and H. Zhai, “Synthesis of phenolic resins by substituting phenol with modified spruce kraft lignin,” Wood Sci Technol, vol. 56, no. 5, pp. 1527–1549, Sep. 2022, doi: 10.1007/s00226-022-01408-8.

[17] J. Li, W. Wang, S. Zhang, Q. Gao, W. Zhang, and J. Li, “Preparation and characterization of lignin demethylated at atmospheric pressure and its application in fast curing biobased phenolic resins,” RSC Adv, vol. 6, no. 71, pp. 67435–67443, 2016, doi: 10.1039/c6ra11966b.

[18] Wu Shubin and Zhan Huaiyu, “Characteristics of Demethylation wheat straw soda lignin and its utilization in ligin based phenolic formaldehyde resins,” Cellulose Chemistry Technology , vol. 35, no. 3–4, pp. 253–262, 2001.

[19] Y. Chen et al., “Demethylation of lignin with mild conditions and preparation of green adhesives to reduce formaldehyde emissions and health risks,” Int J Biol Macromol, vol. 242, Jul. 2023, doi: 10.1016/j.ijbiomac.2023.124462.

[20] D. Y. Hopa and P. Fatehi, “Using sulfobutylated and sulfomethylated lignin as dispersant for kaolin suspension,” Polymers (Basel), vol. 12, no. 9, Sep. 2020, doi: 10.3390/POLYM12092046.

[21] X. Meng et al., “Determination of hydroxyl groups in biorefinery resources via quantitative 31P NMR spectroscopy,” Nat Protoc, vol. 14, no. 9, pp. 2627–2647, Sep. 2019, doi: 10.1038/s41596-019-0191-1.

[22] M. K. R. Konduri and P. Fatehi, “Production of water-soluble hardwood kraft lignin via sulfomethylation using formaldehyde and sodium sulfite,” ACS Sustain Chem Eng, vol. 3, no. 6, pp. 1172–1182, Jun. 2015, doi: 10.1021/acssuschemeng.5b00098.

[23] A. Bacchus and P. Fatehi, “Structural changes of cationic grafted lignin at different drying temperatures,” Ind Crops Prod, vol. 222, Dec. 2024, doi: 10.1016/j.indcrop.2024.119837.

[24] S. Cheng et al., “Use of biocrude derived from woody biomass to substitute phenol at a high-substitution level for the production of biobased phenolic resol resins,” J Appl Polym Sci, vol. 121, no. 5, pp. 2743–2751, Sep. 2011, doi: 10.1002/app.33742.

[25] P. Phansamarng, A. Bacchus, F. Hassan Pour, C. Kongvarhodom, and P. Fatehi, “Cationic lignin incorporated polyvinyl alcohol films for packaging applications,” Ind Crops Prod, vol. 221, Dec. 2024, doi: 10.1016/j.indcrop.2024.119217.

[26] A. Moubarik, “Rheology study of sugar cane bagasse lignin-added phenol-formaldehyde adhesives,” Journal of Adhesion, vol. 91, no. 5, pp. 347–355, Jan. 2014, doi: 10.1080/00218464.2014.903803.

[27] S. Khodavandegar and P. Fatehi, “Phytic acid derivatized lignin as a thermally stable and flame retardant material,” Green Chemistry, vol. 26, no. 19, pp. 10070–10086, Sep. 2024, doi: 10.1039/D4GC03169E.

[28] B. Bemerw Kassaun and P. Fatehi, “Solvent-Free Lignin-Silsesquioxane wood coating formulation with superhydrophobic and Flame-Retardant functionalities,” Chemical Engineering Journal, vol. 493, Aug. 2024, doi: 10.1016/j.cej.2024.152582.

[29] W. He and P. Fatehi, “Preparation of sulfomethylated softwood kraft lignin as a dispersant for cement admixture,” RSC Adv, vol. 5, no. 58, pp. 47031–47039, 2015, doi: 10.1039/c5ra04526f.

[30] W. Gao, J. P. W. Inwood, and P. Fatehi, “Sulfonation of Phenolated Kraft Lignin to Produce Water Soluble Products,” Journal of Wood Chemistry and Technology, vol. 39, no. 4, pp. 225–241, Jul. 2019, doi: 10.1080/02773813.2019.1565866.

[31] S. Bandyopadhyay and A. Dey, “Convenient detection of the thiol functional group using H/D isotope sensitive Raman spectroscopy †,” 2014, doi: 10.1039/c3an02166a.

[32] K. Sawamura, Y. Tobimatsu, H. Kamitakahara, and T. Takano, “Lignin Functionalization through Chemical Demethylation: Preparation and Tannin-Like Properties of Demethylated Guaiacyl-Type Synthetic Lignins,” ACS Sustain Chem Eng, vol. 5, no. 6, pp. 5424–5431, Jun. 2017, doi: 10.1021/acssuschemeng.7b00748.

[33] H. E. Gottlieb, V. Kotlyar, and A. Nudelman, “NMR Chemical Shifts of Common Laboratory Solvents as Trace Impurities,” 1997.

[34] J. L. Wen, S. L. Sun, B. L. Xue, and R. C. Sun, “Recent advances in characterization of lignin polymer by solution-state nuclear magnetic resonance (NMR) methodology,” 2013. doi: 10.3390/ma6010359.

[35] M. Gorbounov, P. Halloran, and S. Masoudi Soltani, “Hydrophobic and hydrophilic functional groups and their impact on physical adsorption of CO2 in presence of H2O: A critical review,” Aug. 01, 2024, Elsevier Ltd. doi: 10.1016/j.jcou.2024.102908.

[36] M. Erfani Jazi et al., “Structure, chemistry and physicochemistry of lignin for material functionalization,” Sep. 01, 2019, Springer Nature. doi: 10.1007/s42452-019-1126-8.

[37] K. Takeno, T. Yokoyama, and Y. Matsumoto, “Beta-O-4 cleavage in lignin,” 2012.

[38] M. B. Smith, MARCH’S ADVANCED ORGANIC CHEMISTRY REACTIONS, MECHANISMS, AND STRUCTURE SIXTH EDITION. Wiley interscience , 2007. Accessed: Mar. 04, 2025. [Online]. Available: www.wiley.com.

[39] A. F. Voegele, C. S. Tautermann, T. Loerting, A. Hallbrucker, E. Mayer, and K. R. Liedl, “About the Stability of Sulfurous Acid (H2SO3) and Its Dimer,” Chemistry - A European journal, pp. 5644–5651, Dec. 2002, doi: 10.1002/1521-3765(20021216)8:24.

[40] H. Paananen, L. Alvila, and T. T. Pakkanen, “Hydroxymethylation of softwood kraft lignin and phenol with paraformaldehyde,” Sustain Chem Pharm, vol. 20, May 2021, doi: 10.1016/j.scp.2021.100376.

[41] T. Nemoto, I. Amir, and G. I. Konishi, “Synthesis of a formyl group-containing reactive novolac,” Polym J, vol. 41, no. 5, pp. 389–394, 2009, doi: 10.1295/polymj.PJ2008316.

[42] T. Zhang, X. Li, and L. Guo, “Initial Reactivity of Linkages and Monomer Rings in Lignin Pyrolysis Revealed by ReaxFF Molecular Dynamics,” Langmuir, vol. 33, no. 42, pp. 11646–11657, Oct. 2017, doi: 10.1021/acs.langmuir.7b02053.

[43] S. Bhattarai and S. Chen, “Adv Biotech & Micro Chemistry of Bond Cleavage in Lignin Degradation during Pretreatment of Lignocellulosic Biomass Lignocellulosic Biomass,” vol. 4, 2017, doi: 10.19080/AIBM.2017.04.555643.

[44] S. Kim et al., “Computational study of bond dissociation enthalpies for a large range of native and modified Lignins,” Journal of Physical Chemistry Letters, vol. 2, no. 22, pp. 2846–2852, Nov. 2011, doi: 10.1021/jz201182w.

[45] Y. Xu, L. Guo, H. Zhang, H. Zhai, and H. Ren, “Research status, industrial application demand and prospects of phenolic resin,” 2019, Royal Society of Chemistry. doi: 10.1039/c9ra06487g.

[46] E. Mansouri, N.-E. El Mansouri, Q. Yuan, and F. Huang, “Alkaline lignins for resins,” Bioresources, vol. 6, no. 3, pp. 2647–2662, 2011.

[47] A. Bacchus and F. Pedram, “Drying Temperature Effects on the Characteristics of Sulfoalkylated Kraft Lignin ,” Under publication , 2025.

[48] F. Cardona, “Modified PF Resins for Composite Structures with Improved Mechanical Properties,” 2010.

[49] M. Brebu and C. Vasile, “THERMAL DEGRADATION OF LIGNIN-A REVIEW,” 2010.

[50] M. M. Nassar and G. D. M. Mackay, “MECHANISM OF THERMAL DECOMPOSITION OF LIGNIN,” Wood and Fiber Science, vol. 3, no. 16, pp. 441–453, 1984.

[51] T. Imai, Y. Hisadomi, S. Sawamura, and Y. Taniguchi, “Uncovering the physical origin of the difference between aliphatic chain and aromatic ring in the ‘hydrophobic’ effects on partial molar volume,” Journal of Chemical Physics, vol. 128, no. 4, p. 54, Jan. 2008, doi: 10.1063/1.2828768/947051.

[52] J. C. Domínguez, M. Oliet, M. V. Alonso, E. Rojo, and F. Rodríguez, “Structural, thermal and rheological behavior of a bio-based phenolic resin in relation to a commercial resol resin,” Ind Crops Prod, vol. 42, no. 1, pp. 308–314, Mar. 2013, doi: 10.1016/j.indcrop.2012.06.004.

[53] M. Imani, K. Dimic-Misic, M. Tavakoli, O. J. Rojas, and P. A. C. Gane, “Coupled Effects of Fibril Width, Residual and Mechanically Liberated Lignin on the Flow, Viscoelasticity, and Dewatering of Cellulosic Nanomaterials,” Biomacromolecules, vol. 21, no. 10, pp. 4123–4134, Oct. 2020, doi: 10.1021/acs.biomac.0c00918.

[54] M. Patrick, “Rheology Principles and Applications,” youtube. Accessed: Feb. 03, 2025. [Online]. Available: https://www.youtube.com/watch?v=etR4ttjY4f0&ab_channel=AOCSAmericanOilChemists%27Society

[55] Y. Zhang et al., “Synthesis of high-water-resistance lignin-phenol resin adhesive with furfural as a crosslinking agent,” Polymers (Basel), vol. 12, no. 12, pp. 1–14, Dec. 2020, doi: 10.3390/polym12122805.

[56] L. Eshdat et al., “Flexibility vs rigidity of singly and doubly tethered biphenyls: Structure, dynamic stereochemistry, and resolution of tribenzo[a,c,f] cyclooctane, tetrabenzo[a,de,h,kl]bicyclo[6.6.0]tetradecane, and their alkyl derivatives,” Journal of Organic Chemistry, vol. 64, no. 10, pp. 3532–3537, 1999, doi: 10.1021/jo990090u.

[57] M. Foston, G. A. Nunnery, X. Meng, Q. Sun, F. S. Baker, and A. Ragauskas, “NMR a critical tool to study the production of carbon fiber from lignin,” Carbon N Y, vol. 52, pp. 65–73, Feb. 2013, doi: 10.1016/j.carbon.2012.09.006.

[58] A. Shukla, V. Sharma, S. Basak, and S. W. Ali, “Sodium lignin sulfonate: a bio-macromolecule for making fire retardant cotton fabric,” Cellulose, vol. 26, no. 13–14, pp. 8191–8208, Sep. 2019, doi: 10.1007/s10570-019-02668-7.

[59] F. R. Vieira et al., “Bio-Based Polyurethane Foams from Kraft Lignin with Improved Fire Resistance,” Polymers (Basel), vol. 15, no. 5, Mar. 2023, doi: 10.3390/polym15051074.

[60] N. M. Abumounshar, S. Ibrahim, and A. Raj, “A detailed reaction mechanism for elemental sulphur combustion in the furnace of sulphuric acid plants,” Canadian Journal of Chemical Engineering, vol. 99, no. 11, pp. 2441–2451, Nov. 2021, doi: 10.1002/cjce.24185.

[61] A. Makwana, S. Iyer, M. Linevsky, R. Santoro, T. Litzinger, and J. O’Connor, “Effects of Fuel Molecular Weight on Emissions in a Jet Flame and a Model Gas Turbine Combustor,” J Eng Gas Turbine Power, vol. 140, no. 3, Mar. 2018, doi: 10.1115/1.4037928.

[62] H. Zhang et al., “Study on the synthesis and thermal stability of silicone resins reinforced by Si-O-Ph cross-linking,” RSC Adv, vol. 11, no. 49, pp. 30971–30979, Sep. 2021, doi: 10.1039/d1ra05524k.

[63] P. Solt, B. Rößiger, J. Konnerth, and H. W. G. van Herwijnen, “Lignin phenol formaldehyde resoles using base-catalysed depolymerized kraft lignin,” Polymers (Basel), vol. 10, no. 10, 2018, doi: 10.3390/polym10101162.

[64] S. Feng, Z. Yuan, M. Leitch, and C. C. Xu, “Adhesives formulated from bark bio-crude and phenol formaldehyde resole,” Ind Crops Prod, vol. 76, pp. 258–268, Dec. 2015, doi: 10.1016/j.indcrop.2015.06.056.

[65] B. Di et al., “Phenol-enriched hydroxy depolymerized lignin by microwave alkali catalysis to prepare high-adhesive biomass composites,” Polym Eng Sci, vol. 61, no. 5, pp. 1463–1475, May 2021, doi: 10.1002/pen.25664.

[66] S. Yang, J. L. Wen, T. Q. Yuan, and R. C. Sun, “Characterization and phenolation of biorefinery technical lignins for lignin-phenol-formaldehyde resin adhesive synthesis,” RSC Adv, vol. 4, no. 101, pp. 57996–58004, 2014, doi: 10.1039/c4ra09595b.

[67] Y. Chen, X. Gong, G. Yang, Q. Li, and N. Zhou, “Preparation and characterization of a nanolignin phenol formaldehyde resin by replacing phenol partially with lignin nanoparticles,” RSC Adv, vol. 9, no. 50, pp. 29255–29262, 2019, doi: 10.1039/c9ra04827h.

[68] W. Yang et al., “Preparation and properties of adhesives based on phenolic resin containing lignin micro and nanoparticles: A comparative study,” Mater Des, vol. 161, pp. 55–63, Jan. 2019, doi: 10.1016/j.matdes.2018.11.032.

[69] I. A. Gilca, R. E. Ghitescu, A. C. Puitel, and V. I. Popa, “Preparation of lignin nanoparticles by chemical modification,” Iranian Polymer Journal (English Edition), vol. 23, no. 5, pp. 355–363, 2014, doi: 10.1007/s13726-014-0232-0.

Chapter 4: Conclusion and future work

This thesis investigated the use of lignin as a sustainable alternative in adhesive formulations, focusing on its role in phenol-formaldehyde (PF) resins. Chapter 1 provided a comprehensive literature review on lignin-based adhesives, including PF, UF, MF, epoxy, polyurethane, lignin-tannin, lignin-soy protein, lignin-PEI, and lignin-furfural resins. Despite its abundance and potential as a bio-based adhesive component, lignin presents challenges, such as low reactivity, structural heterogeneity, and reduced bonding strength. Various modification techniques, including demethylation, hydroxymethylation, and phenolation, have been explored to improve lignin's reactivity, but widespread industrial adoption remains limited due to performance trade-offs and processing challenges.

The experimental results confirmed that the sulfobutylation showed increased molecular weight and sulfonate content, with reduced methoxy and hydroxyl groups, leading to better solubility and charge density, confirming successful sulfobutylation. Sulfobutylation improved lignin solubility, enabling demethylation in an aqueous medium. DSB had higher molecular weight, more β-O-4 linkages, and reduced methoxy and sulfonate content, indicating condensation, with β-O-4 as the dominant inter-unit linkage. DKL exhibited β-β linkages as the primary structure, with increased molecular weight and reduced hydroxyl content, highlighting the impact of different demethylation solvents. SBPLPF20, DSBPF20, and DSBPF60 retained PF resin's molecular structure but had more reactive formaldehyde adducts. Higher lignin content raised molecular weight and viscosity, improving bonding but reducing penetration and thermal stability. The β-O-4 linkages in DSB contributed to enhanced resin properties, increasing bonding strength (19% in DSBPF20, 25% in DSBPF60), but free formaldehyde exceeded safety limits. While pH and non-volatile content remained stable, water absorption increased. Despite improved adhesion and fire resistance, challenges with thermal stability, water absorption, and formaldehyde emissions require further optimization. Overall, the study demonstrated that sulfobutylation followed by demethylation effectively enhanced lignin's reactivity in PF adhesives, improving bonding strength and fire resistance. However, challenges such as increased viscosity, reduced thermal stability, and excessive formaldehyde emissions must be addressed for industrial viability.

Future research should focus on establishing standardized hot-pressing (curing) conditions and resin synthesis methods. Currently, significant variations in synthesis and curing parameters across the literature hinder direct comparisons. A standardized approach would enable a clearer understanding of the effects of different modifications and formulations. Additionally, resin synthesis in this study should be optimized to minimize emissions while maintaining adhesive performance. This can be achieved by reducing excess formaldehyde in the formulation, as indicated by its emissions in DSBPF resins. Optimizing the NaOH catalyst amount, reaction temperature, and reaction time for resin synthesis is also crucial for enhancing resin performance. Furthermore, curing conditions, including hot-pressing temperature and time, should be examined as they significantly impact adhesive properties. Finally, the potential use of enhancers such as melamine, urea, or furfural should be investigated. These additives could help reduce formaldehyde content while maintaining or even improving adhesive performance, ultimately further decreasing reliance on petroleum-based materials. This work contributes to advancing lignin-based adhesives, offering a potential pathway toward more sustainable and high-performance bio-based adhesives.

Appendix 3A: Supplementary Information

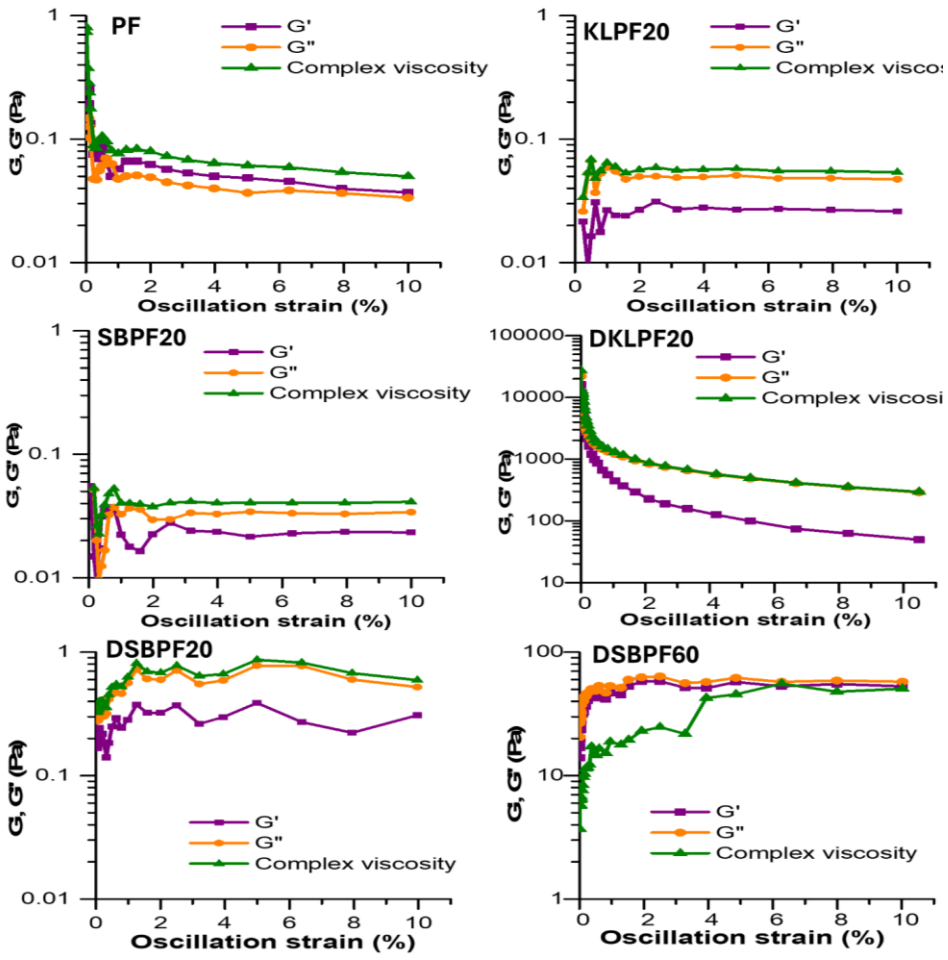

Figure S1: Amplitude sweep for lignin-PF and PF resins.

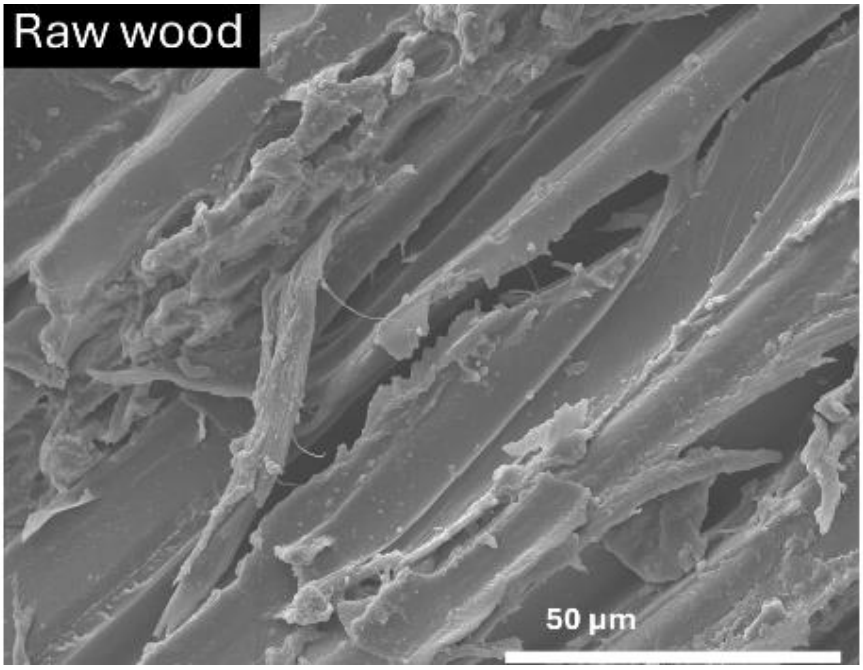

Figure S2: SEM image for raw wood

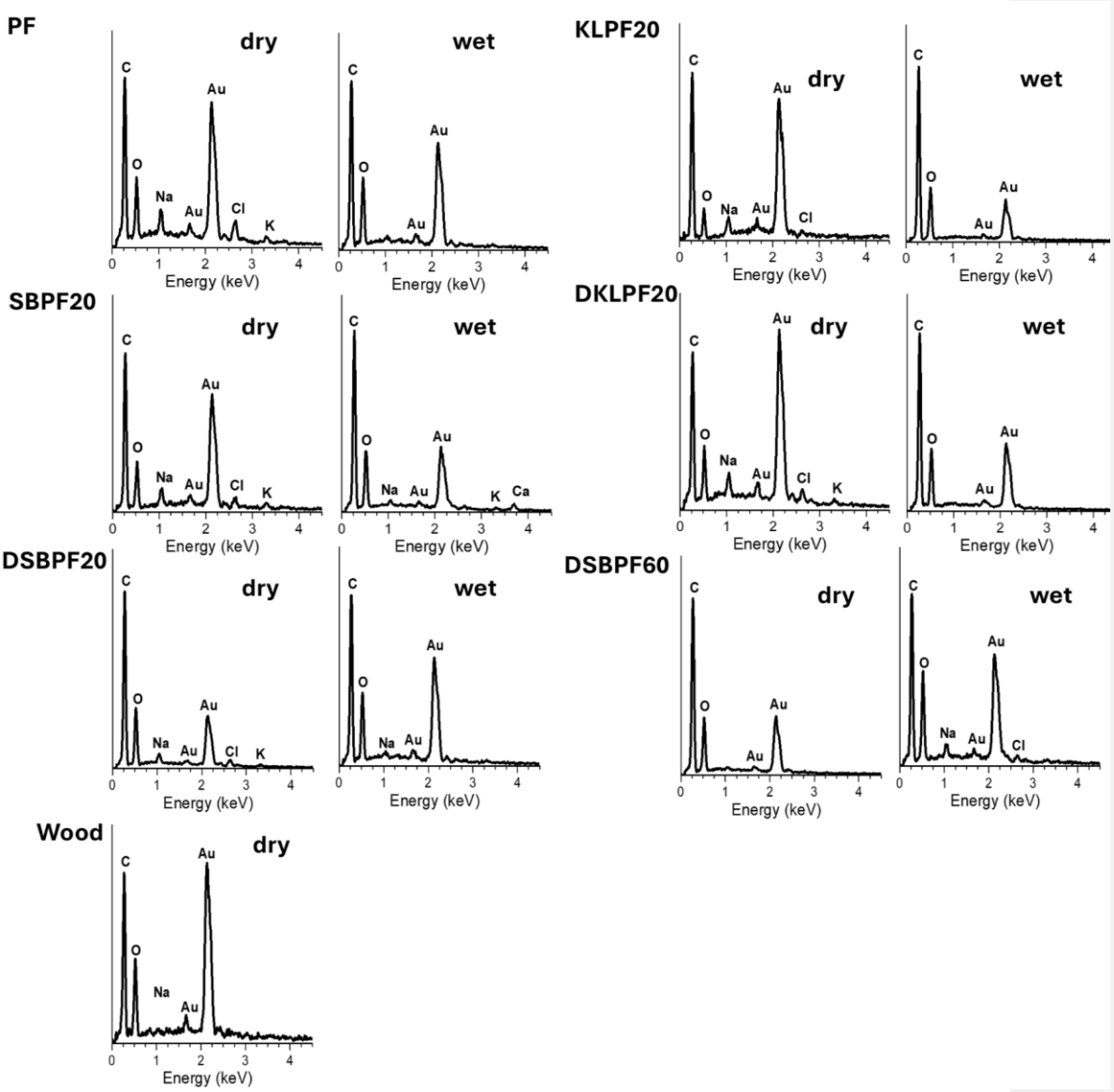

Figure S3: EDX/EDS spectra for lignin-PF and PF resins